

TETRAHEDRON REPORT NUMBER 137

GAS PHASE ANALOGUES OF SOLVOLYSIS REACTIONS*

THOMAS HELLMAN MORTON

Department of Chemistry, University of California, Riverside, CA 92521, U.S.A.

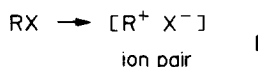
(Received in the U.S.A. 29 January 1982)

CONTENTS

Introduction	3195
1. Gas Phase Quasi-heterolysis	3196
Vicinal elimination from alkyl halides	3197
Distal eliminations	3199
2. Mass Spectrometric Hydrogen Rearrangements	3202
The conventional mechanism	3203
Glyme vs methyl cellosolve	3207
Vinculoselective hidden hydrogen rearrangements	3208
3. Ion-Molecule Complexes in Gaseous Bimolecular Reactions	3209
Anion-Molecule reactions	3210
Cation-molecule reactions	3212
4. Experimental Methods	3215
Neutral products from reactions of gaseous ions	3216
Field ionization kinetics	3220
Metastable ion studies	3221
5. Gas Phase Solvolyses	3222
Phenyl ethers	3224
"Onium" ions	3231
Leaving group effects	3235
Prospects	3240

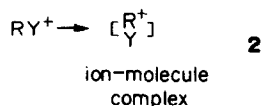
INTRODUCTION

Transformation of a covalent bond into an ionic (or electrostatic) bond is an elementary chemical reaction. The best known case is represented by reaction (1) and the most common milieu is in solution. This transformation is the rate-determining step in many well studied examples, especially solvolysis reactions. Solvolyses are familiar, and it seems appropriate to refer to any covalent→electrostatic transformation as an analogue to solvolysis



Can this reaction take place in the absence of solvent? Does it occur in the gas phase? Since the late 1950's this possibility has been given serious consideration, originally as the rate determining step in thermal eliminations of HX from alkyl halides. This proposal offers a simple basis for predicting the outcome of gas phase eliminations from solvolysis experiments (and *vice versa*). It unifies a large body of seemingly disparate data and permits an assessment of solvent properties in terms of the difference between a gaseous reaction and its solution phase counterpart.

Alas, few gas phase reactions can be described so simply in terms of a model in which reaction (1) is the rate-determining step. The original picture has been subject to alterations (which will be discussed in Part I), and some of the objectives listed in the preceding paragraph have been more closely met by studies of gaseous ions than by studies of gaseous ion pairs



*Dedicated to Prof. F. H. Westheimer on the occasion of his seventieth birthday.

Recently, this type of mechanistic pathway has become recognized in the unimolecular decompositions of gaseous cations, as represented by reaction (2). Electrostatic attraction binds an ion and a neutral (rather than a two oppositely charged ions) to form an ion-molecule complex (rather than an ion pair), and the energetics of binding are of the appropriate magnitude (several kcal mol⁻¹). It has not yet been possible to distinguish an ion-molecule complex from its covalent precursor by spectroscopic methods. But when the complex decomposes, it yields products that resemble the products of solvolytic elimination.

In this report, the term "gas phase solvolysis" will be used to designate a sequence of steps inaugurated by reaction (2). What is the justification for this terminology? As techniques for examining gaseous molecular aggregates develop, the view emerges that there is a continuity of chemical mechanism connecting reaction pathways in bulk solvent with those in small clusters. The limiting case is reaction (2), where RY^+ is an isolated ion. At this limit, the association of the cation (R^+) with the leaving group (Y) is the aspect of solvolysis that is preserved.

What kind of evidence exists for reaction (2) at the unimolecular limit? First of all, it is physically plausible. Secondly, experiments have ruled out reasonable alternatives. Third, there are precedents from bimolecular reactions. Finally, experimental tests provide confirmation.

Accordingly, this report has five parts. Part 1 discusses the physical arguments, with particular attention to reaction (1). Although there is no conclusive evidence that any neutral molecule actually reacts via this "quasi-heterolytic" pathway, the evolution of the notion of quasi-heterolysis provides a useful background. Part 2 presents conventional mechanisms for ion decomposition. These examples do not proceed via reaction (2). The purpose of discussing them is to describe the reasonable alternatives that have to be ruled out in cases where gas phase solvolysis is believed to occur. Part 3 summarizes the chemistry of electrostatically bound complexes that arise from ion-molecule reactions. Part 4 describes experimental techniques by which gas phase solvolyses have been examined. Finally, Part 5 presents several instances where reaction (2) has been shown to take place.

1. GAS PHASE QUASIHETEROLYSIS

Dissociation of neutral molecules in the gas phase to form free ions is rarely observed (except for alkali halides¹), and for good reason. The reaction is very endothermic and, even in alkali halides, homolysis is energetically favored. For fragmentation of NaCl to free Na^+ and Cl^- , ΔH is approximately +130 Kcal mol (550 kJ mol),² while ΔH for the corresponding homolysis to sodium and chlorine atoms is slightly less than 100 Kcal mol.

Heterolysis in the gas phase should become less endothermic if the ions are not required to achieve infinite separation from one another. If the Na^+ and Cl^- ions have to get only 9 Å apart, ΔH for the heterolysis is about the same as ΔH for the homolysis.¹ This leads to the following picture as the metal-halogen bond is stretched well beyond its equilibrium distance, the molecule loses covalent character and acquires ionic character. Although the energetically favored dissociation limit is not ionic, the molecule in an intermediate range of internuclear separation may be qualitatively described as an electrostatically bound ion pair.

It is not obvious how one might detect the transitory ionic character of a dissociating diatomic. However, a comparable situation can be discussed for triatomic molecules. One approach has been to describe dissociation pathways in terms of coupling between molecular vibrations, and a qualitative description of nitrosyl fluoride, FNO, has been presented by Jones and Ryan.³ Thermodynamically, homolytic dissociation to NO and a fluorine atom is 56 Kcal mol endothermic, while the heterolytic dissociation to NO^+ and F^- is 135 Kcal/mol more endothermic than the homolytic pathway. From classical electrostatics, one can estimate that, at separations >2.5 Å between the centers of charge, the heat of formation of noninteracting atoms is lower than that of an ion pair. Since the N-F bond distance in the ground state molecule is 1.52 Å, thermodynamics alone provides a limited basis for inferring transitory ionic character for the transition state.

However, other arguments may be brought to bear on this question. Nitrosyl fluoride has been closely scrutinized spectroscopically, and its response to distortion is what would be expected if ionic character develops during dissociation. The molecule is bent, as shown at the left in Fig. 1, and the interaction displacement coordinates $(l)_k$ have been calculated from its vibrational spectrum.⁴ The value of $(l)_k$ is the displacement of coordinate l that results from a small displacement of coordinate k . For every picometer (= 0.01 Å) that the NF bond is stretched, the NO bond shortens by 0.16 picometer and

the FNO bond angle decreases by 0.05° . The force constant for the NO bond becomes stiffer, and the molecule begins to resemble that valence-bond structure shown at center.

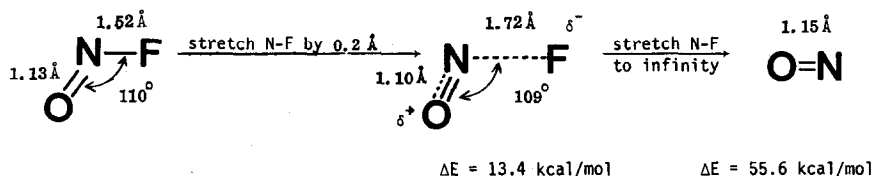


Fig. 1. Response of the FNO molecule to stretching the N-F bond. The center structure shows the bond angle and N-O bondlength that minimizes the potential energy after the N-F bond is stretched 0.2 \AA .⁴

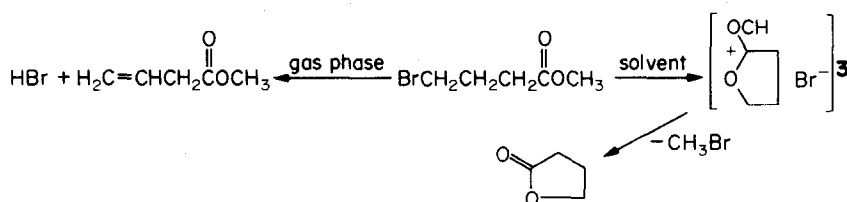
Jones and Ryan³ have pointed out that the force constant for the bond in nitric oxide is virtually the same as the force constant for the NO stretch in FNO, and the bond distance in nitric oxide is longer (1.15 \AA) than that of FNO. On the other hand, the force constant of NO^+ is much greater than that of NO and the bond distance is much shorter, 1.06 \AA . Therefore, as the NF bond of FNO is stretched, the molecule does not start to resemble the ultimate product of dissociation, neutral NO. Instead, the molecule begins to look like an ion pair, although at sufficiently large NF displacements, this trend must reverse.

Can the same arguments be applied to organic compounds? At present, the vibrational structure of few organic molecules are known with sufficient detail to permit a determination of the interaction displacement coordinates, and it seems unlikely that we shall soon be able to dissect reaction coordinates with the precision that Jones and Ryan³ have done for triatomics. Nonetheless, experimental criteria can be established for discussing reaction 1 as a pathway for unimolecular reactions. One basis for discussion is the activation energy.

Vicinal elimination from alkyl halides

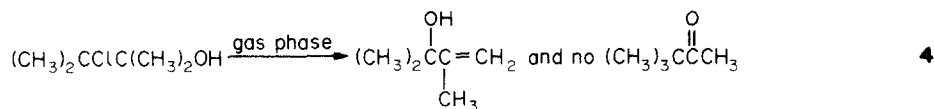
An extensive review of thermal eliminations of HX from alkyl halides was presented in 1969 by Allan Maccoll. He noted that activation energies correlate well with heterolytic bond dissociation energies, but poorly with homolytic bond dissociation energies.⁵ In 1958, Maccoll had made a simple calculation for the activation barrier to elimination of HBr from bromoethane.⁶ Taking ΔH for $\text{C}_2\text{H}_5\text{Br} \rightarrow \text{C}_2\text{H}_5^\cdot + \text{Br}^-$ to be 184 Kcal/mol (the currently accepted value, based on recently determined heat of formation⁷ and ionization potential⁸ of the ethyl radical, is $1\text{--}2 \text{ Kcal/mol}$ higher), Maccoll concluded that if reaction 1 were the rate determining step for $\text{C}_2\text{H}_5\text{Br} \rightarrow \text{C}_2\text{H}_4 + \text{HBr}$, the activation barrier for the elimination could be estimated by subtracting the coulombic attraction of the ion pair from the heterolytic dissociation energy. He assumed that the critical distance for the C-Br extension was equal to the sum of the ionic radius of positively charged carbon (which he estimated to be 0.55 \AA) and the ionic radius of Br^- (1.95 \AA). At this critical extension of 2.5 \AA , the coulombic energy would be $\approx 130 \text{ Kcal/mol}$, and the activation barrier for HBr elimination should be approximately $185 - 130 = 55 \text{ Kcal/mol}$. The currently accepted value for E_a is 54 Kcal/mol .⁹

The accuracy of Maccoll's calculation is impressive and gave strong impetus to the development of the quasi-heterolytic model (namely, reaction 1 as the rate determining step). One expectation was that, in an ion pair, the directed valence of the C-X bond would be lost, and optically active halides would racemize if reaction (1) were reversible. Maccoll found, however, that D-(+)-2-chlorooctane does not racemize under thermolytic conditions (where the half life for HCl elimination is approximately 90 min).



Another expectation was that an ion pair would be intercepted (or its formation accelerated) by a suitable internal nucleophile. Kwart and Waroblak¹¹ tested this by heating methyl 4-bromobutyrate under various conditions. Thermolysis in a variety of solvents (including 1,3-dimethyl-4-ethyladamantane) led

to formation of butyrolactone, while in the gas phase HBr elimination (and no lactonization) was observed (reaction 3). Moreover, this elimination reaction is no faster than HBr elimination from 1-bromobutane. A third test of the quasiheterolytic model is to probe for characteristic rearrangement of cationic intermediates. The pinacol rearrangement is a familiar example from solution chemistry, but it does not occur in the thermolysis shown in reaction 4.¹²



In the decade since his review, Maccoll's group has continued to examine thermal eliminations from alkyl halides. Recently they have published a study of ³⁵Cl/³⁷Cl isotope effects on thermolyses of isopropyl chloride and *tert*-butyl chloride.¹³ A calculation from the quasi-heterolytic pathway assumes a C-Cl bond extension from 1.81 Å in *tert*-butyl chloride to 2.43 Å in the transition state (corresponding to a bond order of 0.09). Using calculations for different models, Maccoll found that the heavy atom isotope effects are best fit by a transition state in which the C-Cl bond is stretched only 0.054 Å. Structural features of this transition state are shown in Fig. 2.

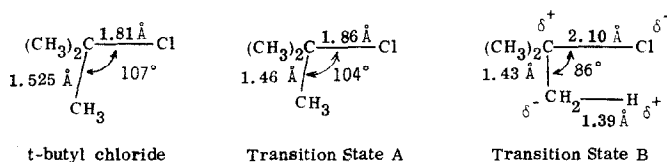


Fig. 2. Structural features of *t*-butyl chloride¹⁴ and transition states for HCl elimination. Transition state A is the model that best fits the experimental work of Maccoll *et al.*³ Transition state B is the modified semi-ion pair model of Tschuikow-Roux *et al.*^{9,15}

The present picture of thermal eliminations is quite different from that represented by reaction 1. Tschuikow-Roux *et al.* have elaborated a semi-ion pair model that accounts for the activation barriers of a large number of 4-center vicinal eliminations from alcohols and alkyl halides.¹⁵ This model portrays the transition state as developing a partial formal charge separation, δ , as shown in transition state B in Fig. 2. The values of δ is taken to be the same for both breaking bonds and is determined using empirical factors (e.g. for *tert*-butyl chloride, $\delta = 0.178$). In these reactions, three single bonds convert to one double and one single bond. Generalized bond order conservation requires that the sum of the charge separations (2δ) and the orders of the partial bonds in the transition state be equal to 3. Bond lengths in the transition state are calculated by assuming that the two breaking bonds have the same partial bond order, that the developing H-Cl bond has a bond order of 0.5, and that the developing C=C bond has a bond order of 1.5. The geometry of the transition state is specified by assuming that the four atomic centers are coplanar and that the shortest distance between two breaking bonds is at a maximum. The energy of the transition state is computed by adding the energies of the partial bonds to the energy of attraction of the partial charges, and the calculated activation energy, 48.4 Kcal/mol, is ≈ 3 Kcal/mol higher than the literature value for HCl elimination from *tert*-butyl chloride.⁹

Chuchani *et al.* have reported a number of studies of thermal eliminations from bifunctional halides in an effort to validate reaction 1 by demonstrating anchimeric assistance.¹⁶ In most instances, thermochemical data on the reactants and products are insufficient to permit an estimate of the activation barrier for a 4-center elimination by the semi-ion pair model. In another series of investigations, Chuchani's group has concluded that neighboring double bonds also provide assistance via a 3-member cyclic transition state, as shown by structure a in Fig. 3.¹⁷ Their inference is based on the observation of lower activation energies for elimination from homoallylic chlorides than from saturated analogues, but they have not tested this hypothesis by comparing the observed E_a with the value anticipated on the basis of the semi-ion pair model, b, which does not include neighboring group assistance. As shall be shown below, weakening of the allylic bonds suffices to account for the experimental data without requiring any additional participation of the double bond in the transition state.

In order to make model calculations for the E_a , values for bond dissociation energies and heats of formation must be known or estimated. We shall assume that all of the pertinent single bond distances in 1-chloro-3-butene are the same as in saturated analogues and that the only new homolytic bond

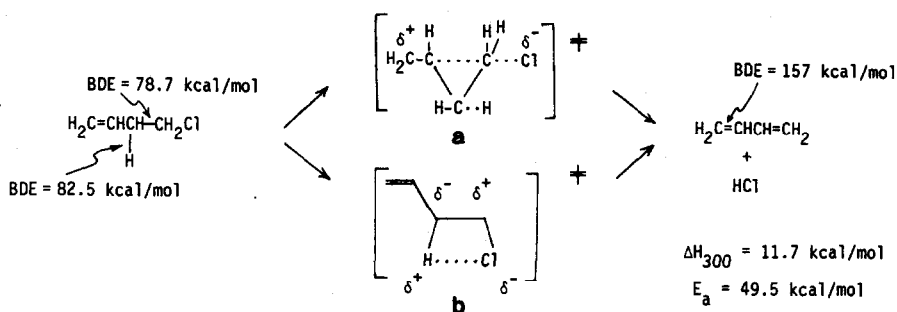
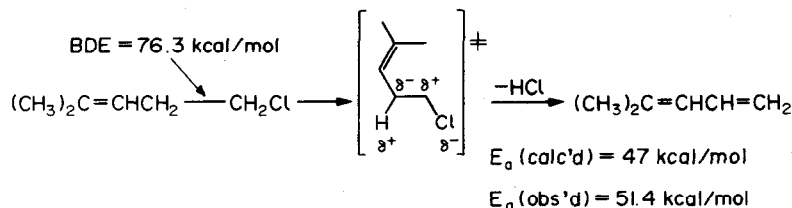


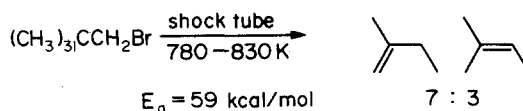
Fig. 3. Two alternative transition states for elimination of HCl from 1-chloro-3-butene.

dissociation energies (BDE's) that need to be estimated are for the allylic C-H and the C₁-C₂ bond of the reactant and for one of the double bonds of butadiene. The former carbon-carbon BDE is estimated by adding 3.7 Kcal mol⁻¹ to the BDE of the C₃-C₄ bond of 1-butene.^{7,19} The latter carbon-carbon BDE is equal to the ΔH for converting 1,3-butadiene to triplet methylene plus triplet vinylcarbene, and the heat of formation of the latter (relative to cyclopropene) has been estimated by generalized valence bond calculations.²⁰ The BDE of the allylic C-H bond is taken to be the same as the value reported for the lowest C-H bond dissociation energy of 1-butene.²¹

The charge separation for a 4-center transition state, is calculated to be $\delta = 0.239$. By using the same C-C-Cl bond angle that Tschuikow-Roux computes for 30 out of 31 alkyl chloride eliminations,⁹ we find that the geometry shown for transition state b in Fig. 3 corresponds to an E_a that is 5.5 Kcal mol lower than is calculated for HCl elimination from 1-chlorobutane.⁹ Chuchani *et al.* report an experimental E_a for elimination from 1-chloro-3-butene that is 1.7 Kcal mol lower than the experimental E_a for 1-chlorobutane.



Chuchani *et al.* also report that the dimethylhomoallyl chloride shown in reaction 5 has an E_a for elimination 2.1 Kcal mol lower than that for elimination from 1-chloro-3-butene. If, for the purpose of a semi-ion pair model calculation, we assume that the only difference between the two reactants is a decreased C₁-C₂ BDE (attributable to the 2.4 Kcal mol greater resonance stabilization reported for the dimethylallyl radical),²² then we calculate a value of δ for 4-center transition state equal to 0.210. The corresponding value for the E_a is 2.5 Kcal mol lower than for elimination from 1-chloro-3-butene. The semi-ion-pair model seems to overestimate the energetic effects of allylic bond weakening. But there seems to be no justification for inferring transition states like a in pyrolyses of homoallylic halides.



Distal eliminations

Although it evolved from the quasi-heterolysis concept, the semi-ion-pair model does not represent a gas phase analogue of solvolysis. Vicinal HX eliminations do not proceed via discrete ion pairs. Recently, careful examinations of neopentyl halide eliminations have been reported²³ that show evidence for cationic rearrangements that are more nearly consistent with a mechanism like reaction 1. A 4-center transition state is impossible for these eliminations, and the values of E_a are substantially higher than for

vicinal eliminations. A major obstacle in these studies has been a persistently high level of surface catalysis, as well as lability of the reaction products under reaction conditions. A single pulse shock tube study, however, avoids these complications and gives the product distribution shown in reaction 6. It is interesting to note that the product ratio (in which the thermodynamically less favored product predominates) is virtually the same as has been reported from deprotonation of free *tert*-amyl cations by triethylamine in the gas phase.²⁴

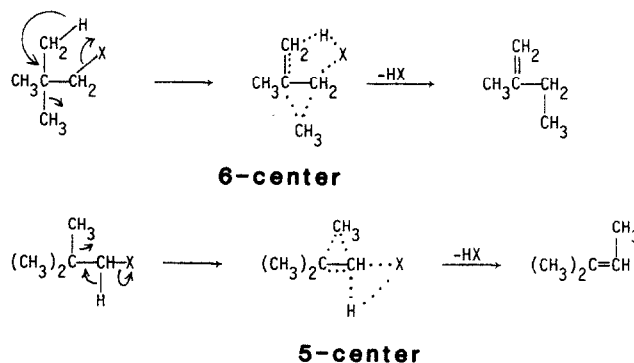


Fig. 4. Cyclic transition states for concerted HX elimination from neopentyl halides to yield 2-methylbutenes.

Reaction 1 represents the alternative to a cyclic transition state. Maccoll's 1958 calculation is physically plausible, but an available β -hydrogen can transfer to the leaving group before an ion pair develops. Transfer is less facile from the γ -position in the absence of β -hydrogens (as in the neopentyl halides), and the activation barrier for a cyclic transition state increases. A contrast between reactions 4 and 6 is pertinent. In solution, pinacol rearrangements are rapid, even when sterically hindered quaternary carbons (e.g. a triisopropylmethyl group²⁵) are generated. This kind of alkyl shift does not occur in the gas phase because a 4-center elimination is more favorable. Methyl shift does occur in reaction 6. Two mechanisms can be proposed. The competing 5- and 6-center cyclic transition states depicted in Fig. 4 represent one alternative. The other explanation is that in the absence of β -hydrogens an ion pair intermediate is preferable to cyclic transition states.

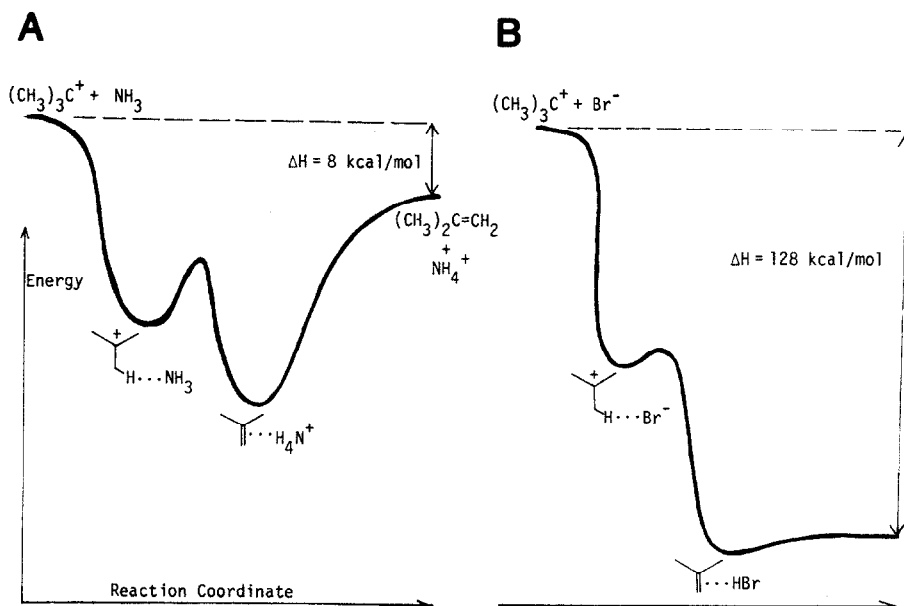


Fig. 5. Qualitative potential energy profiles for gas phase proton transfer. Scheme at left is for the ion-molecule reaction of *tert*-butyl cation with ammonia. Scheme at right is for the cation-anion reaction of *tert*-butyl cation with bromide.

What should the potential energy surface look like for a reaction that proceeds via an ion pair? First consider an ion-molecule reaction. Suppose that a *tert*-butyl cation encounters a neutral base such as NH_3 in the gas phase. The preferred picture for the proton transfer portrays the reaction coordinate passing through a "saddle point transition state".²⁶ Figure 5A depicts a potential energy curve based on the work of Jasinski and Brauman.²⁷ At large separations, the ion and neutral experience a pure attractive potential leading to a local minimum in which there is a hydrogen bond between a $\text{C}^+-\text{C}-\text{H}$ and NH_3 . Most hydrogen bonds lie in double-minimum potential wells, and an energy barrier for shifting to a hydrogen bond between $\text{C}=\text{C}$ and H_4N^+ is expected. Separating the products is endothermic; in the absence of collisions, however, the hydrogen bonded complex has sufficient energy to overcome that purely thermodynamic barrier, since the proton transfer is 8 Kcal/mol exothermic and since no energy is lost from the system (i.e. the two molecules are presumed to interact adiabatically in a vacuum).

Now consider proton transfer in an ion pair. If this occurs via the same type of reaction coordinate, then it will be skewed in the fashion shown for $(\text{CH}_3)_3\text{C}^+ + \text{Br}^-$ in Fig. 5B because the reaction is 128 Kcal/mol exothermic. The first energy minimum corresponds to a hydrogen bond between $\text{C}^+-\text{C}-\text{H}$ and Br^- and the second, very shallow minimum to a hydrogen bond between $\text{C}=\text{C}$ and HBr (a van der Waals complex). The energy barrier between these two minima may be so low as to be only an inflection point.

A potential energy profile for a neopentyl halide elimination via an intermediate ion pair is depicted in Fig. 6. We surmise that the reaction coordinate at first follows the curve for heterolysis of the C-Br

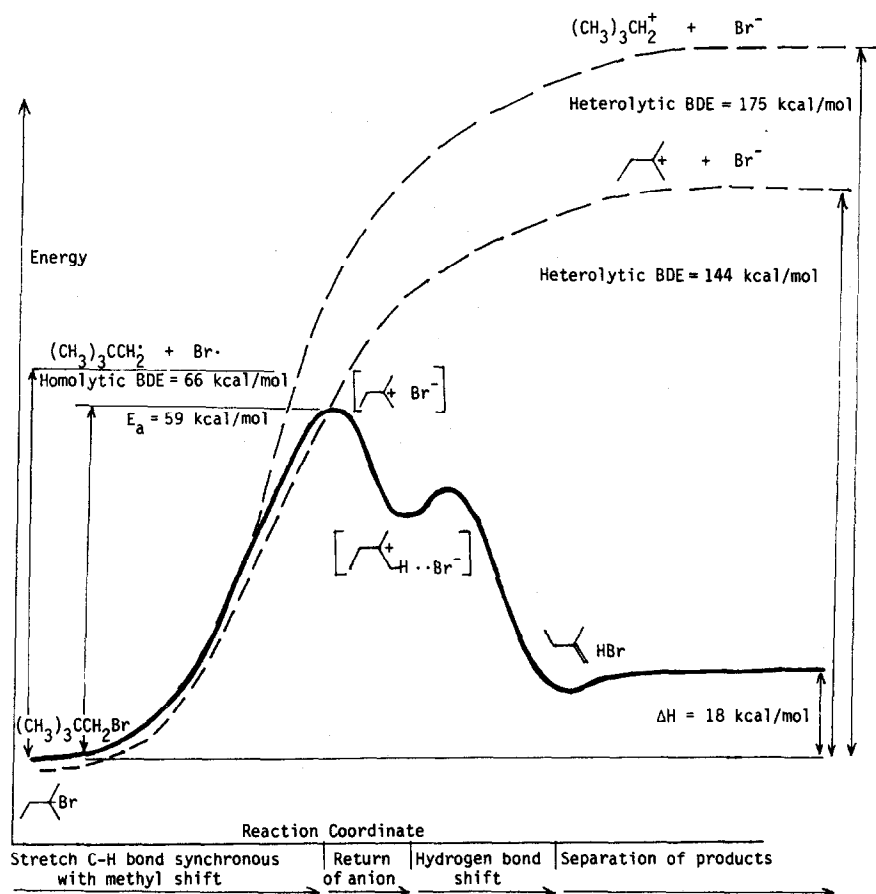


Fig. 6. Hypothetical potential energy profile for HBr elimination from neopentyl bromide via an ion pair. The dashed curves represent heterolytic dissociation curves for *tert*-amyl (lower) and neopentyl (upper) bromides (these two isomeric bromides have heats of formation with 0.5 kcal/mol of one another). Energies are based on Refs. 2, 19 and 28.

bond, which rises monotonically and is represented by the upper dashed curve. As the C-Br bond distance increases and charge separation develops, the emerging neopentyl cation begins to rearrange to its much more stable isomer, the *tert*-amyl cation. In Fig. 6, this is depicted by a crossing from the upper

dotted curve to the lower dotted curve, which represents the monotonically increasing potential energy for heterolysis of the C-Br bond in *tert*-amyl bromide. We presume that motion of the methyl group is synchronous with elongation of the C-Br bond. The transition state corresponds to the completion of the methyl shift at the maximum separation of the ion pair. The experimental activation barrier for elimination is quite high and corresponds to the energy of a >4.5 Å separation of Br^- from the center of charge of a *tert*-amyl cation. The reaction coordinate after the transition state corresponds to shortening the distance between the two ions to form, at a local minimum, a hydrogen bonded complex. There is then a second, low energy barrier for a very exothermic hydrogen bond shift, and the neutral products then separate.

What experimental distinction can be made between the concerted mechanism shown in Fig. 4 and the ion-pair mechanism represented by the potential energy curve in Fig. 6? Figure 7 depicts the products expected from an isotopically labelled neopentyl bromide with 3 chiral centers. On the one hand, as shown, concerted expulsion of DBr would yield two isomers of ^{13}C -labelled 1-tritio-3-deuterio-2-methyl-1-butene that are, in principle, distinguishable. In the *trans*-isomer, the ^{13}C label is in position 4; in the *cis*-isomer, the ^{13}C label is in the other methyl group, at position 2'. If, on the other hand, an ion-pair were to intervene in the gas phase elimination of DBr , rotation about the $\text{C}_2\text{-C}_3$ bond of the intermediate *tert*-amyl cation would lead to production of two additional isomers, the *cis*-4- ^{13}C and the *trans*-2'- ^{13}C , for a total of 4 isomers. In any event, the configuration at C_3 of the product should be the same as shown in Fig. 7, regardless of the mechanism.

From a practical standpoint, Fig. 7 represents merely a thought-experiment. Not only would the preparation of the starting material and characterization of the product constitute a formidable problem, but collecting products from a rigorously homogenous gas-phase thermolysis of neopentyl bromide also presents enormous obstacles. For that reason, the question whether reaction 1 intervenes in any gas phase elimination remains unanswered.

If, instead of being an anion, the leaving group is neutral, the situation becomes different. Complete separation of the carbocation and the leaving group requires much less energy; it is less than half as endothermic as the heterolyses indicated by the dashed curves in Fig. 6. Reaction 2 has been experimentally validated even in eliminations from reactants with β -hydrogens. However, because the reactants are themselves charged, they have been examined by mass spectrometry and allied techniques. Therefore, it is appropriate to review some aspects of ion chemistry.

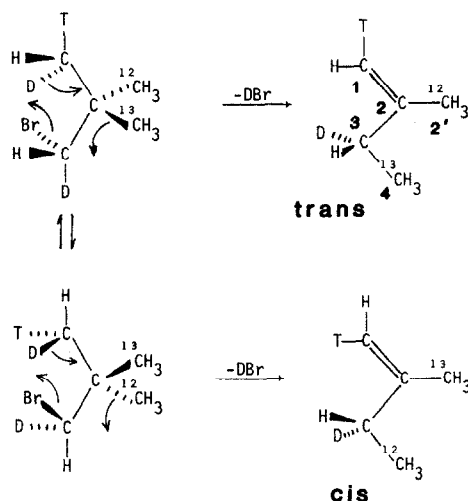
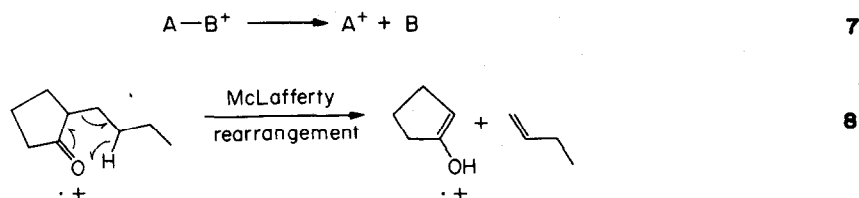


Fig. 7. Thought experiment: major products expected from concerted elimination of DBr from an isotopically labelled neopentyl bromide with 3 chiral centers.

2. MASS SPECTROMETRIC HYDROGEN REARRANGEMENTS

Ionization of gaseous polyatomic molecules often leads to decomposition, and the range of imputed mechanisms is quite vast. A large proportion of peaks in most mass spectra can be rationalized in terms of simple bond fissions, as represented by reaction 7. Of the remaining peaks, some must surely result from deep seated rearrangements (such as the virtually ubiquitous C_3H_3^+ ion), while many others are

produced by hydrogen rearrangements. The McLafferty rearrangement shown in reaction 8 is an example of the latter.



The mechanisms that have been conventionally proposed for hydrogen rearrangements are the converse of gas phase solvolysis. In gas phase solvolysis, a bond breaking step precedes bond forming steps. In conventional mechanisms, bond forming steps precede bond breaking steps. In Part I of this report, mechanisms for thermal elimination from neutrals were discussed. This part will present examples of conventional mass spectrometric elimination mechanisms that begin with the steps shown in Fig. 8. The reactions in Parts I and II will be contrasted with gas phase solvolytic eliminations in Part V.

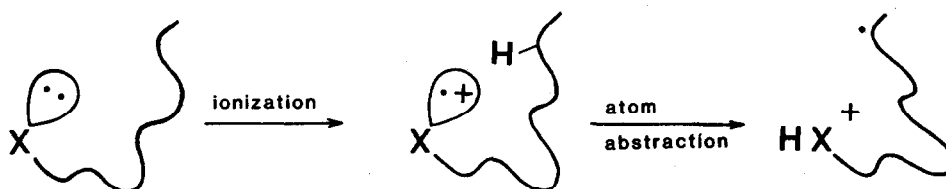


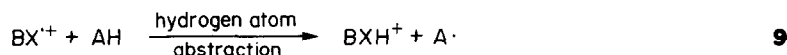
Fig. 8. Conventional picture of a mass spectrometric hydrogen rearrangement. Electron vacancy is viewed as being localized on the functional group of the molecular ion.

The conventional mechanism

Since it is a radical cation, an ionized functional group can behave as a radical or as a cation. As a radical it is able to abstract a hydrogen from elsewhere in the molecule—for instance, from a methylene chain. This is shown in Fig. 8. Following hydrogen transfer, expulsion of neutral HX or of HX^+ is frequently observed. The choice between these two alternatives is usually consistent with Stevenson's rule, that the charge is retained by the fragment with the lowest ionization potential.³⁰ Often, the charged fragment rearranges to the most stable structure.

Figure 8 depicts what we call the conventional mechanism. Such hydrogen rearrangements are often regiospecific. The McLafferty rearrangement is a good example, for the itinerant hydrogen comes exclusively from the γ -position.³¹ Some are even stereospecific—this subject has been recently reviewed by Mark Green in these reports,³² and he has demonstrated extensive similarities between the reaction in Fig. 8 and intramolecular reactions of radicals and radical cations in solution.

What sorts of constraints are imposed by the conventional mechanism? The internal atom abstraction step has to be exothermic (unless the parent ion is in a vibrationally or electronically excited state). The ΔH for this tautomerization is not easy to measure, but it can be estimated by considering the bimolecular analogue, reaction 9, whose ΔH is the difference between the dissociation energy of the severed bond and the hydrogen atom affinity (HA) of the abstracting center.



Hydrogen atom affinities (HA) of ionized functional groups can be calculated from the proton affinity (PA) and ionization potential (IP) of the unionized functional group via the Born-Haber cycle shown in Fig. 9.²⁸ A typical calculation is given for bromomethane, whose ionization potential is 243 Kcal/mol and whose proton affinity is 163 Kcal/mol.³³ The hydrogen atom affinity of CH_3Br^{++} is equal to the ionization potential of CH_3Br minus the ionization potential of atomic hydrogen (313 Kcal/mol) plus the proton affinity of CH_3Br . The result is $HA(CH_3Br^{++}) = 93$ Kcal/mol. The same calculation for CH_3CH_2Br also gives a value of 93 Kcal/mol.³³ In general, the HA is characteristic of the functional group and is relatively insensitive to the nature of alkyl groups bound to it.^{28,33}

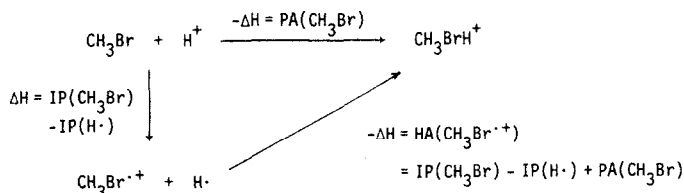
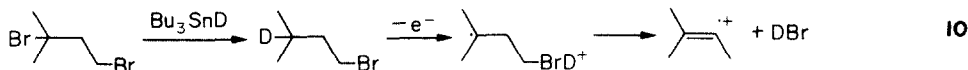
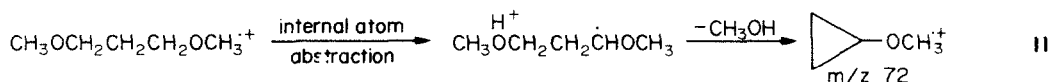


Fig. 9. Born-Haber cycle for calculating the hydrogen atom affinity (HA) of bromomethane.

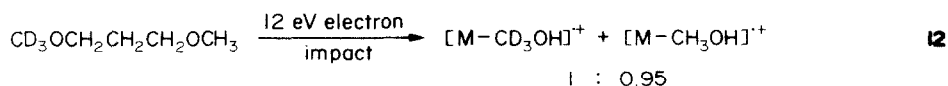


In the case of alkyl bromides, the HA is less than most primary and secondary C-H bond dissociation energies in saturated alkanes, but it is greater than tertiary C-H BDE's.⁷ In other words, for X = Br, reaction 9 is endothermic unless the abstracted hydrogen is bound to a tertiary carbon. We have tested the relevance of this calculation to intramolecular hydrogen rearrangements. A few years ago, we discovered that tributyltin hydride will reduce tertiary bromides in the presence of primary bromides. We used this procedure to prepare the specifically deuterated isoamyl bromide shown in reaction 10. When it is ionized, isoamyl bromide exhibits a prominent peak in its mass spectrum corresponding to HBr expulsion from the molecular ion. When the γ -position is labelled, virtually exclusive elimination of DBr is observed.²⁴ Thus, the prediction based on analogy between reaction 9 and Fig. 8 is borne out: a nominal 1,3-elimination occurs in preference to an accessible vicinal elimination.

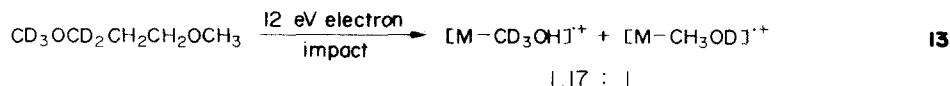
The contrast between elimination from a molecular ion and from a neutral alkyl halide is marked and illustrates the significance of the mechanistic difference between the two reactions. Figure 8 depicts the former as an internal radical abstraction. This model is useful, but it is not perfect. For instance, a typical primary deuterium kinetic isotope effect for intermolecular hydrogen abstraction by a neutral radical is quite large, $k_{\text{H}}/k_{\text{D}} = 4$ for $\text{HO}\cdot$ on butane vs butane- d_{10} at 300 K,³⁴ a reaction that is 20–24 Kcal/mol exothermic. One anticipates that the primary kinetic isotope effect for a less exothermic hydrogen abstraction will be greater.³⁵



We have studied isotope effects in molecular ion hydrogen rearrangements. Although effects of deuterium substitution are widely observed in mass spectrometry, it is often difficult to determine $k_{\text{H}}/k_{\text{D}}$ values, since observed ion abundances generally represent the effects of both competing and sequential pathways. For instance, a ratio of deuterated to undeuterated fragment ion abundances may reflect kinetic isotope effects on further decompositions of the fragments as well as on their rates of production. A ratio of peak intensities can most rigorously be equated to a $k_{\text{H}}/k_{\text{D}}$ value when a single deuterated precursor gives only two peaks in its mass spectrum.



We have reported that compounds of the general formula $\text{CH}_3\text{OCH}_2(\text{CH}_2)_m\text{CH}_2\text{OCH}_3$ do not exhibit molecular ions for $m > 0$ even at low ionizing energies.³⁶ 1,3-Dimethoxypropane ($m = 1$) shows only one peak in its mass spectrum from ≤ 12 volt electron impact. This peak results from the hydrogen rearrangement shown in reaction 11. The regiospecificity of the abstraction was determined from deuterium labelling studies, and the structure of the m/z 72 fragment ion was inferred from ion-molecule reactions of the fragments from various deuterated analogues.³⁶



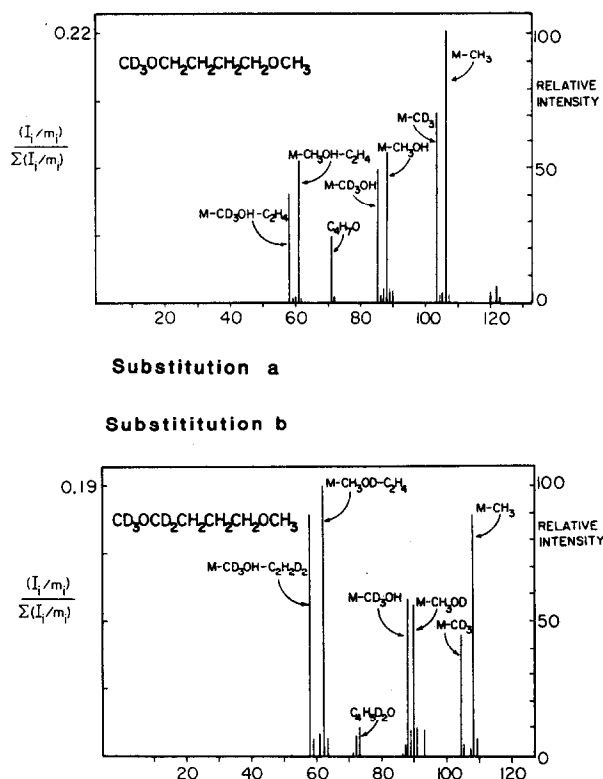
The ratio of the two peaks seen in the low energy mass spectrum of the monomethyl- d_3 compound in reaction 12 is close to unity. That is, a small inverse secondary isotope effect is seen for the hydrogen rearrangement. When additional deuterium is incorporated at an α -methylene group, as shown in reaction 13, there is a normal primary isotope effect of somewhat greater magnitude. Multiplying $[M-CH_3OH]/[M-CD_3OH]$ from reaction 12 times $[M-CD_3OH]/[M-CH_3OD]$ from reaction 13 gives the isotope effect from methylene substitution alone (i.e. the contributions from methyl substitution cancel). The resulting value of k_H/k_D is 1.12, very much smaller than for bimolecular atom abstraction by a neutral radical.³⁷

Table 1. Deuterium isotope effects on methanol expulsion from ions generated by 12 volt electron impact on $CH_3OCH_2(CH_2)_mCH_2OCD_3$ (substitution a) and $CH_3OCH_2(CH_2)_mCD_2OCD_3$ (substitution b)³⁷

<i>m</i>	$[M-CH_3OH]/[M-CD_3OH]$ from substitution a	$[M-CD_3OH]/[M-CH_3OC]$ from substitution b	Product of ratios in columns 2 and 3
1	0.95 ± 0.02	1.17 ± 0.02	1.12
2	1.21 ± 0.03	1.01 ± 0.02	1.22
3	0.97 ± 0.02	1.22 ± 0.02	1.18

Isotope effects of comparable magnitude are seen for the hydrogen rearrangements of the homologous compound whose mass spectra are shown in Figs. 10 and 11. Although the equation of peak intensity ratio to k_H/k_D values is less rigorous in these cases, the isotope effect from methylene substitution, shown in the fourth column of Table 1, is about the same for all three chainlengths studied. This uniformity persists despite variations in the secondary isotope effect from methyl substitution.

The ΔH of hydrogen abstraction from a methylene by an ionized methoxy group is approximately -10 to -15 Kcal mol, based on an HA for dialkyl ether molecular ions of 103–105 Kcal mol.²⁸ This is less exothermic than for neutral HO^\bullet abstractions, yet the k_H/k_D values are much greater for hydroxyl. This issue has been discussed extensively by Green,³² who has shown that isotope effects of the same magnitude are seen in hydrogen rearrangements of radical cations in solution as in the gas phase. In



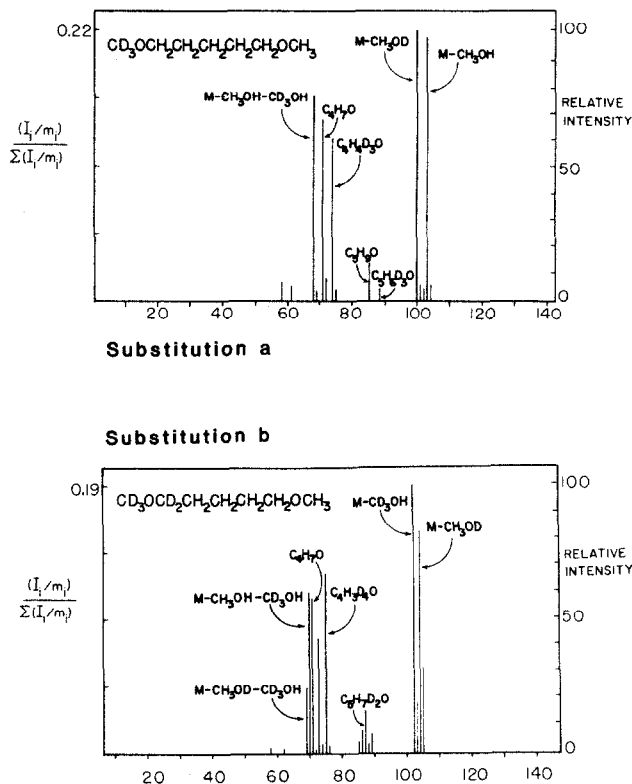


Fig. 11. 12 eV ICR mass spectra (drift mode; no ion-molecule reactions) of deuterated analogues of 1,5-dimethoxypentane. Peak intensities are normalized by mass (I_i/m_i) in order to give proper ion intensities.

general, k_H/k_D values for hydrogen rearrangements are ≤ 1.5 , a magnitude more typical of intermolecular proton transfers²⁷ than of atom abstractions. What interpretation can be given to this apparent mechanistic ambiguity?

Since intuition and experiment support the analogy between intramolecular hydrogen transfer and bimolecular atom abstraction, we shall discuss this question in terms of reaction 9. We surmise that the potential energy curve for the bimolecular reaction is represented by Fig. 12. Let us suppose that the ionization potential of BX is lower than that of AH. Obviously, electron transfer from AH to BX^{+} is endothermic, but as the ion and neutral approach one another there is a monotonic decrease of potential energy due to the ion-dipole attraction. Two curves are shown in Fig. 12. The lower, solid one is for approach of AH and BX^{+} ; the upper, dashed curve is for AH^{+} and BX. Classically, bringing a point charge towards a spherical polarizable neutral liberates energy equal to $(e^2\alpha/2r^4)$, where r is the distance between the centers of charge, e the unit of electronic charge, and α the molecular polarizability. The

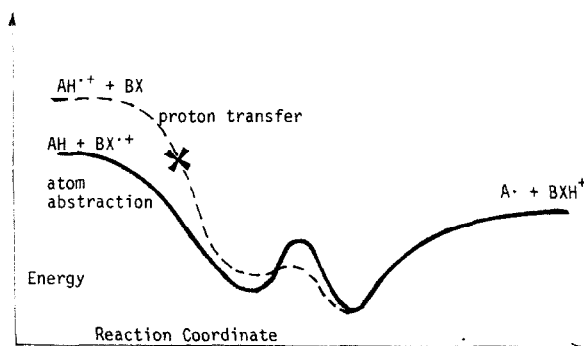


Fig. 12. Hypothetical potential energy curves for atom abstraction and proton transfer. The curves cross just before the transition state for shift of the hydrogen from the donor to the acceptor.

value of α is essentially equal to the molecular volume. A value of $\alpha = 10 \text{ \AA}^3$ is reasonable for a small organic molecule, and approach from infinite distance to $r = 4 \text{ \AA}$ liberates 13 Kcal mol. This computation represents a lower bound, since most molecules have nonspherical charge distributions (and many have permanent dipole moments) that increase this exothermicity. It is reasonable to expect that, at close distances, the dashed curve dips past a point (marked by an X) where charge transfer is thermodynamically accessible.

We speculate that the activation barrier for a formal atom abstraction is higher than for a formal proton transfer. That is, that the local maximum of the dashed curve is lower than that of the solid curve in Fig. 12. Very exothermic hydrogen atom abstractions by neutral radicals (e.g. at 300 K HO^\bullet on methane, for which $\Delta H = -14$ Kcal mol, has an $E_a \approx 4$ Kcal mol³⁸) have energy barriers that are about the same as estimated for thermoneutral bimolecular proton transfers in the gas phase.²⁷ Therefore, the barrier for a very exothermic proton transfer (from AH^{++} to BX) should be lower than that for a less exothermic atom abstraction (from AH by BX^{++}), and the curves should cross, as shown. If the reaction pathway adheres to a minimum potential energy, the transition state will resemble that for proton transfer.

This curve-crossing model characterizes hydrogen transfer to an ionized functionality as a hybrid of proton transfer and atom abstraction. Experimentally, these hydrogen transfers (both inter- and intramolecular) tend to be regiospecific and, where examined, stereospecific. To illustrate the scope of the conventional mechanism, two more examples will be presented. First, the contrast between glyme and methyl cellosolve will be treated. Despite the similarity of the two compounds, the low energy mass spectra show interesting (and explicable) differences. The second example is a case of hidden hydrogen transfer in the mass spectra of 1,4-dimethoxybutane and its deuterated analogues shown in Fig. 10.

Glyme vs methyl cellosolve

Both of these bifunctional ethers are widely used solvents. The fragment ions observed in their low energy mass spectra are summarized in Fig. 13, and the most salient difference between the two compounds is in the identities of the most prominent fragments. The base peak from glyme is an odd-electron species, ion **c**, that results from loss of formaldehyde from the molecular ion. Methyl cellosolve exhibits an even-electron species, ion **d**, that results from expulsion of formyl radical from the molecular ion.³⁶ $[\text{M}-\text{CHO}^\bullet]$ is not seen from glyme; neither is $[\text{M}-\text{CH}_2\text{O}]$ seen from methyl cellosolve.

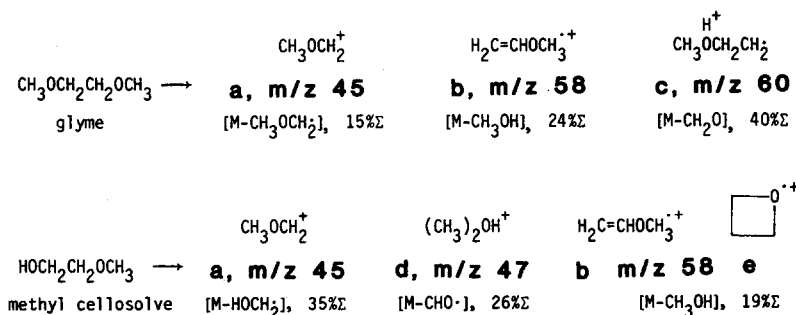
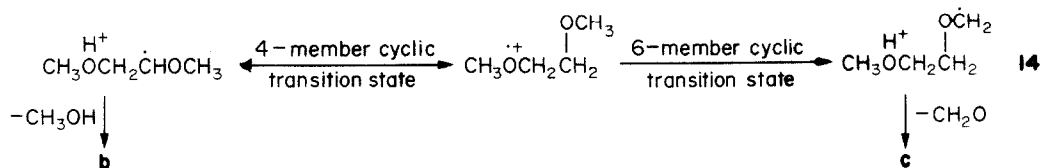
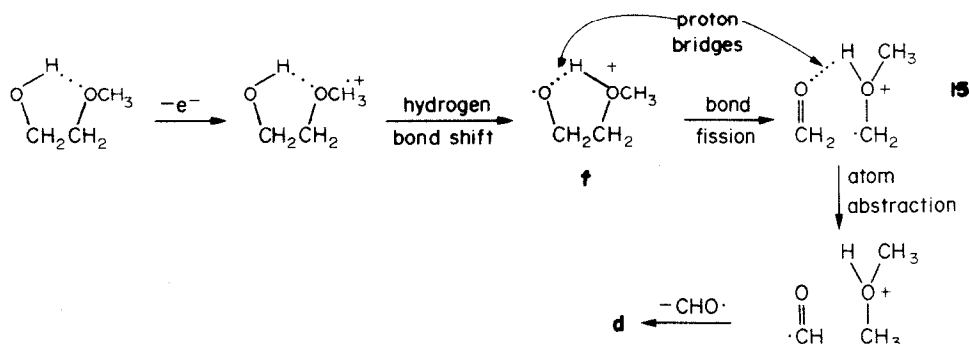


Fig. 13. Fragment ions seen from 12 eV electron impact on glyme and methyl cellosolve. The remainder of the total ionization (Σ) in both cases is the molecular ion.³⁶

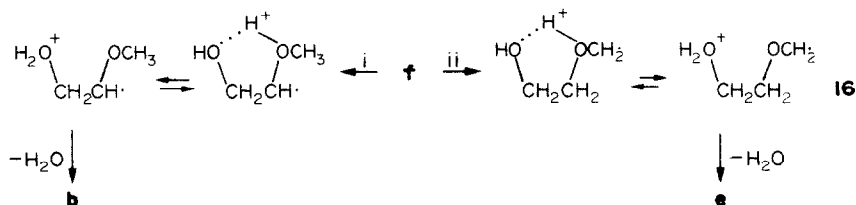
The structures shown in Fig. 13 have been deduced from deuterium labelling studies, ion-molecule reactions, and collisional activation mass spectra. Low energy ionization of $\text{CH}_3\text{OCD}_2\text{CD}_2\text{OCH}_3$ in the ICR yields two odd-electron daughters. The ion corresponding to **b** contains just 3 deuteria, while the ion corresponding to **c** has 4 deuteria. At sufficiently high pressures, **c** transfers a proton to glyme in an ion-molecule reaction. The d_4 analogue of **c** transfers only protons and no deuterons,³⁶ and it reacts with nitriles by displacement of CH_3OH to transfer $\text{C}_2\text{D}_4^{++}$.⁴⁰ Therefore **c** has the structure shown in Fig. 13 instead of the tautomeric structure $\text{CH}_3\text{CH}_2\text{OCH}_3^{++}$.³⁶ The conventional mechanism provides a straightforward interpretation, as shown in reaction 14: an ionized methoxy group abstracts hydrogen either via a 4-member or (more likely) via a 6-member cyclic transition state. The former route leads to an intermediate that readily loses methanol, the latter to an intermediate that more rapidly expels formaldehyde.



Neutral methyl cellosolve exists almost entirely as an internally hydrogen bonded structure in the gas phase.⁴¹ We believe that, upon ionization, the hydrogen bond shifts, as shown in reaction 15, to form a proton bridge (an intramolecular strong hydrogen bond⁴²). This tautomer of the molecular ion, f, can do one of three things. One, a C-C bond can break to yield formaldehyde and $\text{CH}_3\text{OCH}_2^+$, with the two fragments still held together by a proton bridge. We estimate the HA of the radical cation to be the same as that of its conjugate base, $\text{CH}_3\text{OCH}_2^+$, which is 93 Kcal mol.²¹ This is greater than the BDE of a formaldehyde C-H, and an exothermic atom transfer takes place in the proton-bridged bimolecular complex. Expulsion of CHO^\cdot follows, producing ion d. The structure is confirmed by ICR collisional induced decomposition (CID), which shows that d is indeed protonated dimethyl ether. The CID of d and of authentic $(\text{CH}_3)_2\text{OH}^+$ both yield the same two product ions, CH_3^+ and CH_3O^+ , while the CID of the isomeric ion, $\text{CH}_3\text{CH}_2\text{OH}_2^+$, yields only CH_3CH_2^+ .³⁹ By contrast, when the molecular ion of glyme expels CH_2O (reaction 14), the aldehyde oxygen is not complexed by a proton, and the CH_2O does not remain in the vicinity of ion c long enough to undergo exothermic hydrogen atom abstraction.



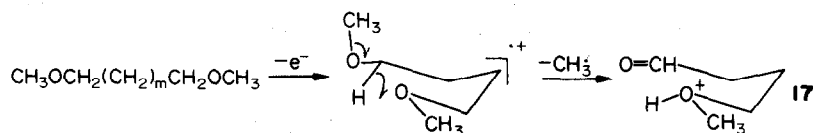
The other two possible unimolecular reactions of f are both hydrogen atom abstractions by the oxy radical, via either a 4-member (i) or 6-member (ii) cyclic transition state. As reaction 16 shows, this yields carbon-centered radicals and a hydroxy group. Because the methoxy oxygen is protonated, CH_2O expulsion cannot occur after step ii. Subsequent proton transfer back to the hydroxy group in both cases leads to expulsion of water, and two isomeric m/z 58 ions are formed, b and e, as revealed by their collisional activation mass spectra.⁴³



Vinculoselective hidden hydrogen rearrangements

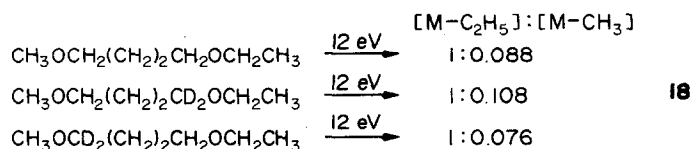
In 1971, Djerassi *et al.* introduced the notion of a hidden hydrogen rearrangement in radical eliminations from molecular ions.⁴⁴ (This subject has been recently reviewed.⁴⁵) In 1975, we reported that a hydrogen transfer could be concerted with a C-O bond cleavage.³⁶ The focus of our attention was the expulsion of CH_3^\cdot from 1,4-dimethoxybutane, for which we proposed the pathway shown in reaction 17. We noted that none of the other α,ω -dimethoxyalkanes exhibit $[\text{M}-\text{CH}_3]^\cdot$ ions at any electron energy, whereas $[\text{M}-\text{CH}_3]^\cdot$ not only is prominent at 70 eV,⁴⁶ but also becomes the base peak in the low energy mass spectrum,³⁶ constituting over half of the total ionization from 11 eV electron impact. Since simple

C-O bond cleavage is implausible at low ionizing energies, we proposed that a concomitant exothermic hydrogen transfer must be occurring via the 6-member cyclic transition state shown in reaction 17.



At ionizing energies within a few eV of threshold, all of the α,ω -dimethoxyalkanes from $m = 0$ to $m = 4$, with the exception of $m = 2$, fragment exclusively via expulsion of oxygen-bearing moieties to produce, primarily, odd-electron daughter ions. The anomaly in the $m = 2$ case led to our introduction of the term *vinculoselection* (from the Latin *vinculum*, chain) to designate a reaction of a polyfunctional molecule in which a specific chainlength or spatial separation between functional groups is requisite for the reaction to occur.³⁶

In reaction 17, thermochemical requirements demand that hydrogen transfer occur before or during methyl radical expulsion. But hydrogen transfers such as those shown in reaction 14 occur for all of the dimethoxyalkanes, and in every other homologue they lead only to CH_3OH or CH_2O expulsion. Therefore, the *vinculoselectivity* of reaction 17 seems to require that the hydrogen transfer occur simultaneously with $\text{CH}_3\cdot$ expulsion. We tested this hypothesis by probing deuterium isotope effects in the mass spectra shown in Fig. 10. In $\text{CD}_3\text{OCH}_2(\text{CH}_2)_2\text{CH}_2\text{OCH}_3$, the ratio $[\text{M}-\text{CD}_3]/[\text{M}-\text{CH}_3]$ is 0.71. In $\text{CD}_3\text{OCD}_2(\text{CH}_2)_2\text{CH}_2\text{OCH}_3$, the ratio $[\text{M}-\text{CH}_3]/[\text{M}-\text{CD}_3]$ is 2.02. Multiplication of these two ratios cancels the isotope effect from methyl deuteration. This gives a value of $k_{\text{H}}/k_{\text{D}}$ for methylene deuteration alone of 1.44. This isotope effect is even larger than the primary isotope effects summarized in Table 1, and it is consistent with a hydrogen rearrangement synchronous with expulsion of the methyl radical.³⁹



As we should expect, *vinculoselective* alkyl radical expulsion also occurs for $m = 2$ in the homologous series $\text{CH}_3\text{OCH}_2(\text{CH}_2)_m\text{CH}_2\text{OH}$ and $\text{CH}_3\text{OCH}_2(\text{CH}_2)_m\text{CH}_2\text{OCH}_2\text{CH}_3$.³⁶ In the latter case, ethyl radical expulsion provides the base peak for $m = 2$ at low ionizing energies. We have examined the deuterium isotope effects on the compounds shown in reaction 18. As tabulated, deuteration of an α or ω methylene decreases expulsion of the corresponding alkyl radical.³⁷ Again this result is consistent with a hydrogen transfer synchronous with a C-O bond cleavage.

As a mechanistic tool, examination of *vinculoselective* reactions has applications throughout chemistry. Although *vinculoselection* is widely observed in the mass spectrometry of bifunctional compounds, it is also observed in solution phase studies, for instance in Cr(VI) oxidations of dihydroxy acids.⁴⁷ In the present case, this phenomenon illustrates the strong influence of 6-member cyclic transition states in mass spectrometric hydrogen rearrangements.

3. ION-MOLECULE COMPLEXES IN GASEOUS BIMOLECULAR REACTIONS

In the gas phase, two neutral species are considered either to be covalently bound (or hydrogen bonded) or else to be completely free to escape from one another. It is conventionally accepted that neutral molecules experience *collisions*, but not *encounters* in the gas phase. This convention was widely adopted by mass spectrometrists. It assumed that if an ion and a neutral are not covalently (or hydrogen) bonded, then they would fly apart, and that geminate encounters would be exceedingly rare. For that reason, conventional mechanisms impose two requirements for rearrangements of acyclic ions: (1) bond-forming steps precede bond-breaking steps, and (2) bond-forming steps take place via cyclic transition states.

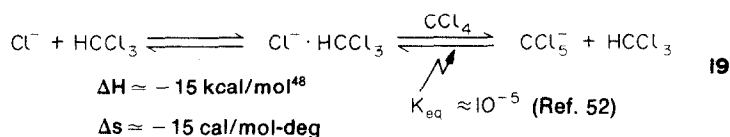
As we have pointed out in discussing Fig. 12, ion-dipole attractions are actually much greater than kT at distances where covalent bonds are usually thought to be broken. Encounters between charged and neutral species take place in reactions of gaseous ions, even those that obey first-order kinetics. The qualitative picture for such "unconventional" mechanisms is much the same as for the quasi-heterolyses discussed in Part I, and steps like reaction 2 can occur prior to bond-forming steps.

Binding energies of gaseous ion-molecule complexes had been measured long before their mechanistic importance was recognized by organic chemists. By 1977, Paul Kebarle *et al.* at Alberta had examined the thermodynamics of a number of ion clusters that are stabilized by numerous collisions with a bath gas in a high pressure mass spectrometer.⁴⁸

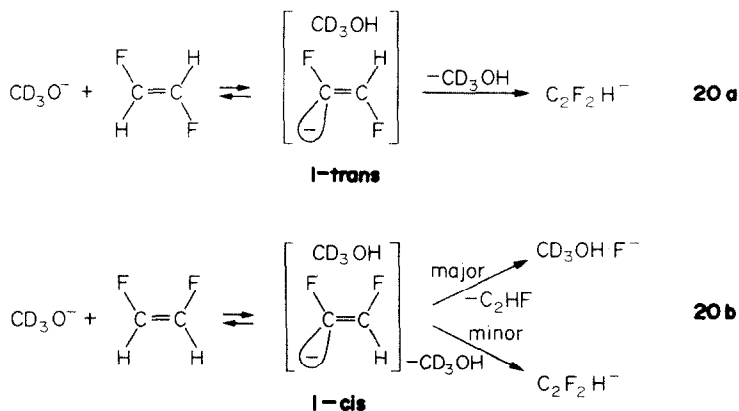
In that year, researchers at Caltech⁴⁹ and at Colorado⁵⁰ published discussions of bimolecular reactions that involve ion-molecule complexes as transient intermediates. A year or two later the significance of reaction 2 in unimolecular reactions was proposed and demonstrated. It seems historically appropriate to describe ion-molecule complexes first in the context of intermediates in ion-molecule reactions.

Anion-molecule reactions

Many of the stable ion clusters studied by Kebarle's group, such as $\text{NH}_4^+(\text{H}_2\text{O})_n$, can be viewed as being held together by hydrogen bonds. But it is impossible to view stable aggregates like XeCl^- ⁵¹ and CCl_5^- ⁵² in this way. From the equilibria shown in reaction 19 for the chloride-chloroform complex, it is clear that ion-permanent dipole attraction contributes to binding stability, but that ion-induced dipole forces are also substantial.

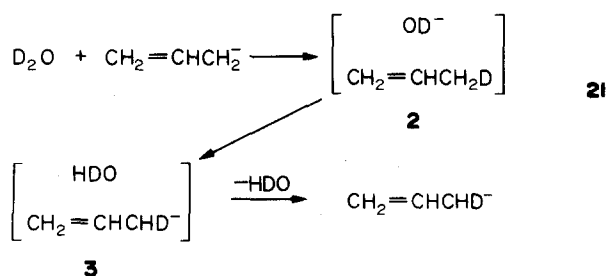


How long does an ion-molecule complex live in the absence of stabilizing collisions? Using ion cyclotron resonance (ICR) techniques, Sullivan and Beauchamp observed reactions 20a and b. Methoxide ion reacts with *trans*-1,2-difluoroethylene exclusively by deprotonation, and C_2HF_2^- is the only product observed. With the *cis* isomer, extensive HF elimination is seen as well. It seemed impossible to explain this difference except by proposing a long-lived collision complex. The Caltech group did not draw explicit diagrams of this complex, but one possibility is shown by structure 1. If we assume that the sp^2 anions are configurationally stable, then the carbanions drawn in 1-*trans* and 1-*cis* remain different. If elimination requires an *anti* geometry, the difference in reactivities of the two isomers becomes apparent. Complex 1-*trans* has enough internal energy to fragment to C_2HF_2^- but lives long enough for its component to rotate freely with respect to one another. Close approach of methanol to the fluorine *anti* to the negative charge is probable, and the stereoelectronically favorable elimination takes place.



The mechanism proposed in reaction 20 illustrates the most important aspect of ion-molecule complexes. Covalent and hydrogen bonds are examples of directed valence. The bond may permit free rotation about its axis, but not in other directions. For an electrostatically bound pair, relative rotation is unrestricted in all directions.

At the ASMS meeting in May 1976, the Colorado group reported that a variety of gaseous carbanions exchange hydrogens with D_2O on single collisions.⁵³ Their mechanism for exchange between allyl anion and D_2O is shown in reaction 21. Species 2 and 3 are ion-molecule complexes. Since propene and water have approximately the same gas phase acidities,⁵⁴ allyl anion is not quenched by collisions with D_2O .



Complex **2** can revert to reactants, but in doing so isotopic label is scrambled. In principle, conversion of **2** to **3** could lead to incorporation of 2 deuteria into the carbanion if the ion-molecule complex lives long enough. Experimentally, on subsequent collisions with D_2O allyl anion exchanges a maximum of 4 of its 5 hydrogens.

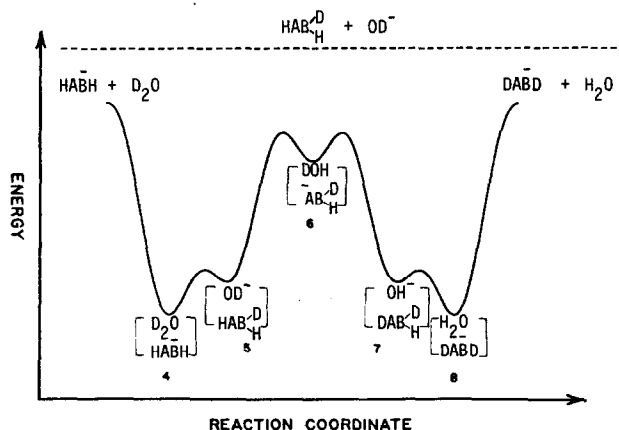
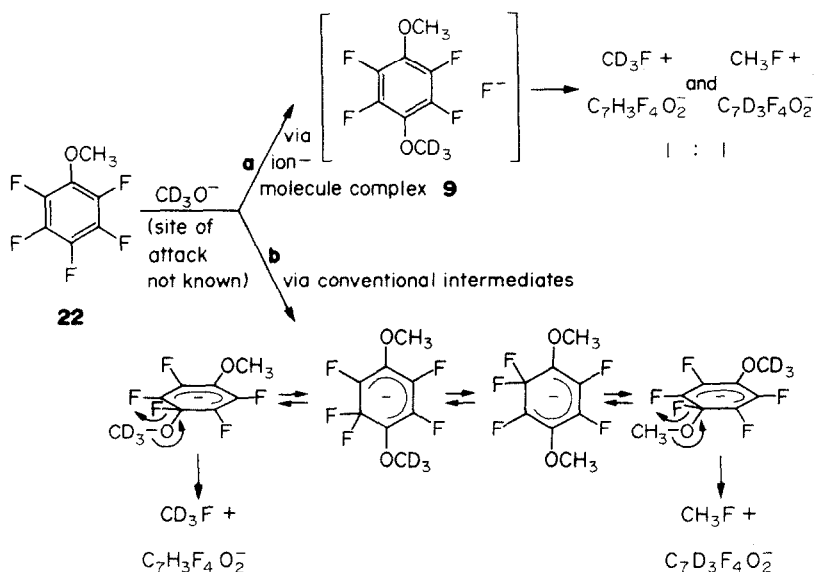


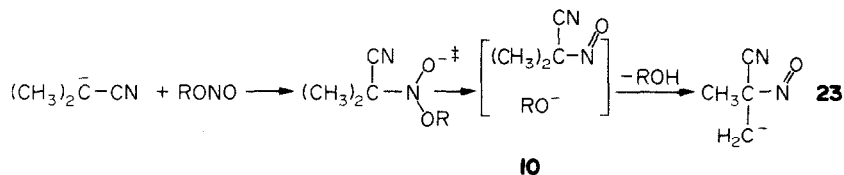
Fig. 14. Reaction coordinate for two H-D exchanges in a carbanion, HABH , with two different types of hydrogen. Both exchanges result from a single encounter with D_2O . Dashed line shows the relative energy of the isolated products of a net proton transfer.

Recently, Squires, DePuy, and Bierbaum have reported that both hydrogens of D_2O can exchange with all the hydrogens in 2-phenylallyl anions on a single collision. A qualitative potential energy curve is shown in Fig. 14 (adapted from Ref. 55) for exchange of two different types of hydrogen in a carbanion, HABH , with D_2O . The dashed line is added to indicate that net proton transfer is endothermic. Aggregation of the carbanion with D_2O is exothermic, however, and enough vibrational energy is liberated by formation of complex **4** for proton transfers to become thermodynamically accessible *so long as ion and neutral remain electrostatically bound*. Thus there is enough kinetic energy in the ion-molecule complex for it to travel uphill to complex **5** or even to complex **6**. In order to decompose, the complex must travel downhill again, likely as not via complexes **7** and **8**, which complete the incorporation of two deuteria into the carbanion. In order for this scrambling to take place, the energies of all the intermediate complexes *and of the transition states between them* must lie below the energy of the separated reactants.⁵⁵

These hydrogen-deuterium exchange reactions have become recognized as a useful technique for assigning structures of gaseous anions, not only in the flowing afterglow apparatus used by the Colorado group,⁵⁶ but also in negative chemical ionization⁵⁷ and ICR^{58,59} studies. Intermediacy of ion-molecule complexes is now a generally accepted mechanistic option in bimolecular gas phase reactions. In a recent study, Ingemann and Nibbering have demonstrated such an intermediate in nucleophilic attack on pentafluoroanisole, as represented in reaction 22.⁶⁰ A nucleophile, X^- , initially displaces fluoride from the ring to yield an ion-molecule complex of F^- and $\text{CH}_3\text{OC}_6\text{F}_4\text{X}$. In many cases, F^- then attacks the methyl group to displace free $\text{C}_6\text{F}_4\text{XO}^-$ and yield neutral CH_3F . The site of the initial attack by X^- is not known—in reaction 22 it has been arbitrarily depicted as *para* for the nucleophile CD_3O^- . As path **a** shows, intermediacy of ion-molecule complex **9** demands that the CD_3 and CH_3 groups become equivalent (regardless of the site of nucleophilic attack), and the proportions of CD_3F and CH_3F expelled



should be the same (assuming that the isotope effect is negligible). This is the experimental result. If, on the other hand, only conventional intermediates intervene, as shown in path **b**, then several isomeric σ -complexes must interconvert in order to render both methyl groups equivalent. This interconversion would have to take place much faster than the expulsion of fluoromethane, or else CD_3F expulsion would have been preferred. Since suprafacial 1,2-sigmatropic shifts in a cyclohexadienide anion are thermally forbidden, path **b** seems improbable.



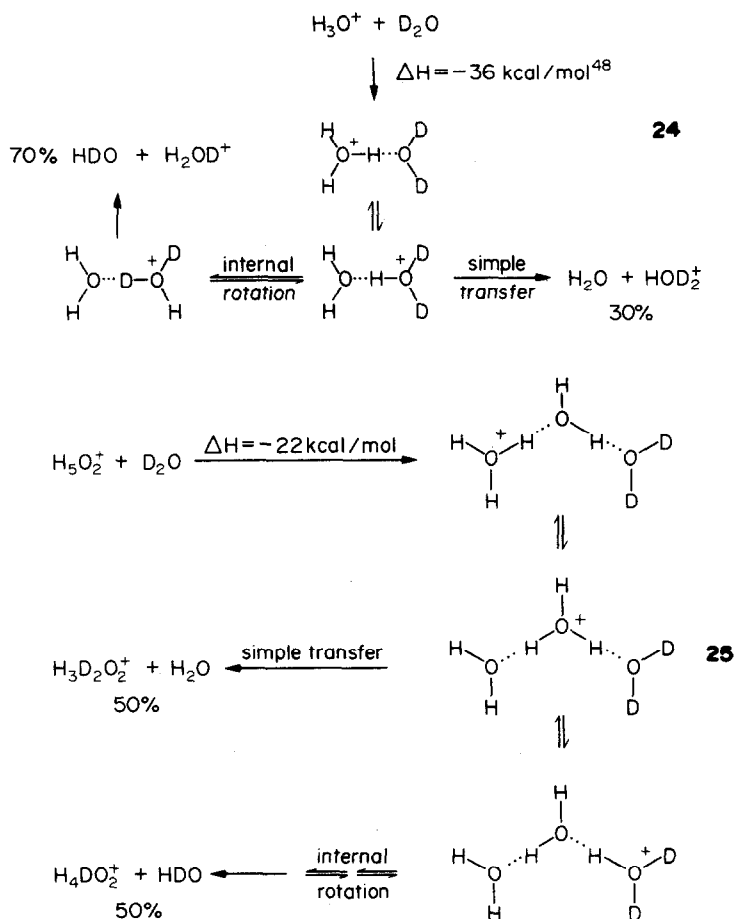
Noest and Nibbering have invoked ion-molecule complex **10** in reaction 23,⁵⁸ in preference to a conventional mechanism that they had originally proposed.⁶¹ The anion from isobutyronitrile attacks an alkyl nitrite to produce, initially, the product of nucleophilic addition to nitrogen. This covalently bound adduct is vibrationally excited, as symbolized by the double-dagger (\ddagger) superscript. It fragments to form an ion-molecule complex (**10**) of alkoxide plus 2-nitrosoisobutyronitrile. In the next step, the alkoxide anion abstracts a proton to yield the observed product, which is homoconjugatively stabilized (similar to the acyclic anions derived from pivaldehyde or *t*-butylnitrone⁵⁹). The Colorado group has proposed the same mechanism for the substitution of H by NO in $\text{CH}_3\text{COCH}_2^-$ when it reacts with alkyl nitrites.⁶²

Cation-molecule reactions

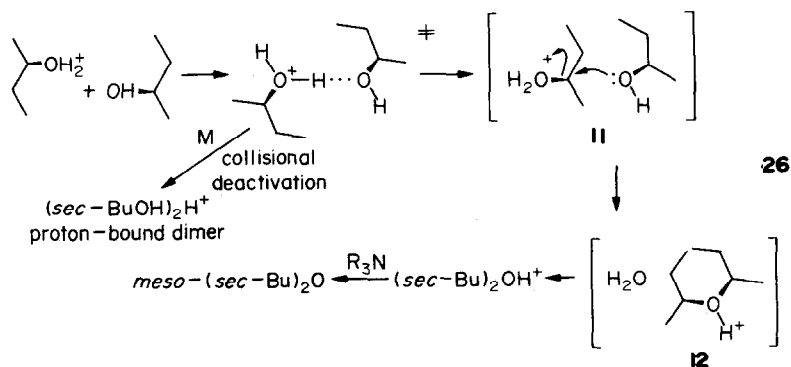
An ion-molecule complex is held together by an electrostatic bond. This implies low barriers in all directions for rotation of the ion with respect to its neutral partner. It also means that the ion can undergo internal rearrangements independently of the rest of the complex. This latter feature is especially important in discussing cation-molecule complexes. First, let us consider hydrogen-bonded complexes.

In positive ion-molecule reactions, hydrogen-bonded complexes exhibit remarkable lability. Reactions 24 and 25 would be expected to give only the products of simple transfer shown to the right if internal rotation were restricted. Experimentally, the observed product distributions indicate that all hydrogens become thoroughly scrambled in the course of reaction.⁶³ A hydronium ion apparently turns easily within the conventional intermediate, undergoing many revolutions in each of the equilibrating structures before the complex dissociates.

How well does this picture apply to other reactions? Protonated alcohols are well known to react with their neutral precursors via nucleophilic displacement of water; the reaction of 2-butanol with its

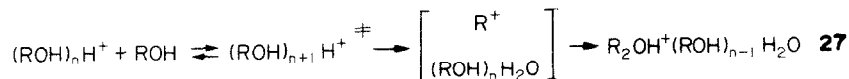


protonated parent ion is a good example.⁶⁴ Reaction 26 shows a mechanism for this reaction that is similar to reaction 24. A vibrationally excited proton-bridged species (drawn with a ‡ superscript) is initially formed. Internal rotation leads to ion-molecule complex 11. S_N2 displacement of an alkyl group forms ion-molecule complex 12, which then dissociates to the observed product, protonated *sec*-butyl ether. Species 11 and 12 need not correspond to energy minima, but we suppose that the principal energy barrier for the overall reaction lies between these two ion-molecule complexes.



We have examined reaction 26 by collecting the neutral *sec*-butyl ether that results from deprotonating its product with gaseous amine bases. Our technique and apparatus will be described more fully in the next section. Briefly, an experiment consists of running a gaseous ionic reaction at low pressures ($< 10^{-3}$ Torr) and condensing the neutral products in a cold trap. When optically pure 2-butanol is used, we find inversion of configuration of the migrating center in reaction 26. The *meso* predominates, as would be expected from backside displacement.⁶⁵

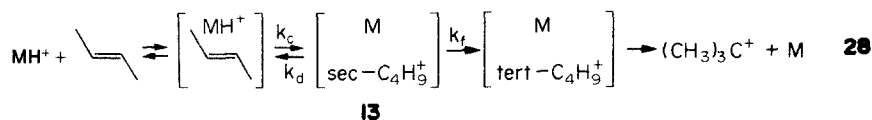
The vibrationally excited proton-bridged intermediate in reaction 26 also undergoes other reactions, including collision with neutral molecules (M) to become deactivated. Stable proton-bound dimers are observed to a much greater extent than R_2OH^+ at pressures $\geq 10^{-5}$ Torr, and they aggregate further with other neutrals, with a substantial liberation of enthalpy each time a new molecule is added to the cluster.⁷² Excess internal energy may be carried away by subsequent collisions, and proton-bound trimers are formed and observed on the millisecond timescale at pressures $\geq 10^{-4}$ Torr.⁶⁴



These growing clusters can be thought of as tiny droplets of solution that are suddenly (and violently) heated each time a new molecule joins the cluster. The behavior of these higher-order clusters will not necessarily conform to reactions 25 or 26, since an S_N1 pathway becomes available as the cluster grows. As symbolized in reaction 27, alkyl cations are increasingly stabilized in ion-molecule complexes as the number of neutral partners increases. We infer this type of intermediate, in which the cation is free to rotate, for the case $R = \text{sec-butyl}$ because of the effect of varying the added amine base on the yield of neutral diastereomers. When strongly basic amines are present (such as tri-*n*-propylamine), oxygen-protonated species (even proton-bound dimers) are quenched on virtually every collision. Cluster formation is intercepted at an early stage, and the recovered R_2O is largely the product of reaction 26. When only a weaker base (e.g. NH_3) is present, proton-bound oligomers are not quenched. They persist and grow, and the S_N1 pathway predominates. A mixture of diastereomers of *sec*-butyl ether (*meso* and *d,l* in roughly equal proportions) is produced when there is no added base stronger than ammonia. Reaction 27 affords most of the R_2OH , and the recovered neutral ether comes from condensation of the clusters with ammonia in the cold trap.

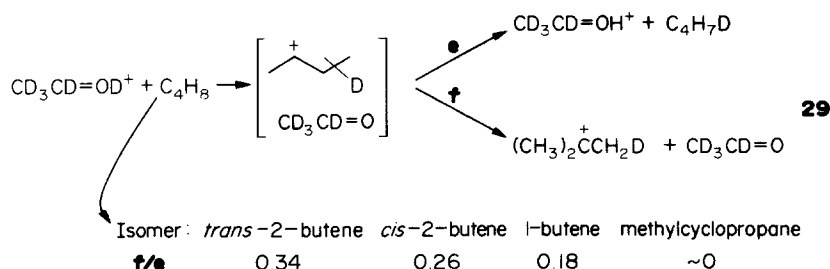
Gas phase nucleophilic displacements can thus be tuned along the S_N2 - S_N1 mechanistic continuum by changing the number of neutrals in the reactive cluster. For $R = \text{sec-butyl}$, the reaction is stereospecific (S_N2) when vibrationally excited $(ROH)_2H^+$ expels water. For larger clusters, ion-molecule complexes containing R^+ are energetically more accessible, and the reaction becomes stereorandom (S_N1). For $R = \text{tert-butyl}$, the S_N1 pathway may occur even for all cluster sizes because of the stability of the *t*-butyl cation. In any event, the reaction $ROH_2^+ + ROH \rightarrow R_2OH^+ + H_2O$ goes at about the same rate for $R = \text{sec-butyl}$ and for $R = \text{tert-butyl}$.⁶⁶

Rearrangement of *sec*-butyl cation to *tert*-butyl cation occurs if the ion-molecule complex is formed with enough internal energy. This isomerization is 15 Kcal/mol exothermic,⁶⁷ but there is a substantial energy barrier ($E_a \approx 18$ Kcal/mol in solution⁶⁸), and no rearrangement is detected in the products of reaction 26 or 27. But under different conditions, rearrangement does occur. Lias, Shold, and Ausloos at the National Bureau of Standards report that gaseous acids (MH^+) transfer protons efficiently to *trans*-2-butene even when the olefin is 5–8 Kcal less basic than the conjugate base M.⁶⁷ The product of these proton transfer reactions is *tert*-butyl cation, as revealed by its subsequent ion-molecule reactions. The NBS group has closely studied several related reactions, including isomerization of *sec*-butyl to *tert*-butyl cation induced by collisions with neutral M, and they conclude that skeletal isomerization of $C_4H_9^+$ within intermediate ion-molecule complexes, as represented in reaction 28, renders the net proton transfer exothermic.



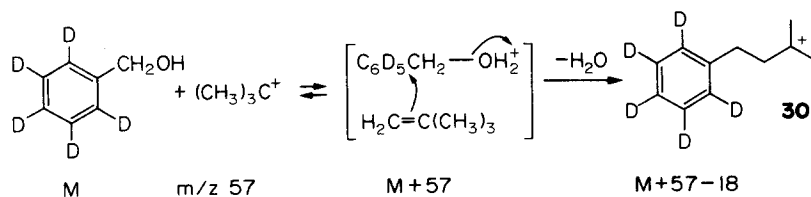
Reaction 28 is more efficient for $M = CH_3CN$ than for CH_3SH , even though the former is a stronger gas phase base (i.e. $CH_3C\equiv NH$ is a weaker acid than $CH_3SH_2^+$). The dipole moment of acetonitrile is greater (3.8D vs 1.3D for methyl mercaptan), and the attractive forces in the ion-molecule complex are stronger. The energetics of forming the intermediate electrostatic complex are important, for as internal energy liberated by forming the complex becomes greater, the rate with which the $C_4H_9^+$ surmounts the barrier to skeletal rearrangement becomes more rapid. Although the proton transfer to form complex 13 is about 1 Kcal/mol more endothermic for $M = CH_3CN$ than for CH_3SH , the greater ion-dipole attraction

in the former case more than compensates. If we assume that the reaction efficiency is proportional to the value of the rate constant expression $k_c/(1 + k_d/k_f)$, the efficiency increases as the denominator gets smaller. With acetonitrile, complex 13 lies in a deeper well and k_d/k_f should be less than for methyl mercaptan. From measurements of the rate constants for hydrogen scrambling vs deuterium transfer from $\text{CD}_3\text{C}\equiv\text{ND}^+$, the ratio k_d/k_f is ≥ 3 for acetonitrile.



The dipole moment effect is not simply a consequence of increasing the energy content of 13. In a recent study, Hunter and Lias have varied the internal energy of the complex by changing the reactants. Four C_4H_8 isomers yield the same complex when they react with $\text{CD}_3\text{CD}=\text{OD}^+$ via reaction 29. Formation of the complex becomes increasingly exothermic as the starting material is changed from the most stable (*trans*-2-butene) to the least stable (methylcyclopropane) structure. In all cases, simple isotope exchange (e) predominates. The neutral product from this reaction cannot be isobutene, since that olefin is 7 kcal/mol more basic than acetaldehyde. The efficiency of the isomerization reaction (f) decreases relative to step e as the initial ion-molecule complex is produced with increasing energy.⁶⁹ This is fully consistent with the expectation that increasing the dipole moment of the neutral partner in the ion-molecule complex lowers the barrier to isomerization of the cation relative to dissociation of the complex.

The final example of an ion-molecule complex from a cation-molecule reaction is taken from the literature on chemical ionization, a mass spectrometric technique in which a neutral substrate acquires electrical charge via an ion-molecule reaction. A widely used gas phase acid for chemical ionization is *tert*-butyl cation (generated by electron impact on isobutane reagent gas). The initial chemical ionization step is either proton transfer (a Brønsted acid-base reaction) or electrophilic attack (a Lewis acid-base reaction), with the neutral substrate acting as base. The initially formed ionic products may be vibrationally excited and often decompose to lighter fragment ions.



A recent study of chemical ionization of benzyl alcohol reports that the principal ion corresponds to loss of water from the $(\text{M} + 57)^+$ ion. Isotopic labelling of the ring (as shown in reaction 30) or of the methylene reveals that both hydrogens in the expelled water come from the reagent gas and the hydroxyl. This result excludes most conventional intermediates, and the $[\text{M} + 57]$ ion-molecule complex depicted in reaction 30 has been proposed. Proton transfer yields an ion-molecule complex between the $\text{M} + 1$ ion and neutral isobutene, followed by nucleophilic displacement of H_2O by the olefin. The structure of the final ionic product is confirmed by comparing its collisional activation mass spectra with that of an authentic sample from another source.⁷⁰

4. EXPERIMENTAL METHODS

Ion decompositions that obey first-order kinetics have been studied by a variety of methods, several of which differ from those described in the previous section. Whereas many ion-molecule reactions appear to have zero activation barriers, most fragmentations are endothermic and have energy barriers

that are at least as great as the thermodynamic threshold. Appearance potential measurements have been used extensively to map potential energy surfaces for unimolecular rearrangements and dissociations. Though it seems a straightforward notion to vary ionizing energy and look for onset of a reaction, a great deal of ingenuity has been required to develop reliable and accurate methods of measurement. Both electron impact and photoionization techniques are in wide use, but these are not routine procedures. In most commercial mass spectrometers, nominally low energy electron beams have a very broad energy distribution owing to electric fields needed for ion optics. Even when an electron beam can be produced with a narrow energy spread, ionization efficiency increases only gradually with electron energy, and great care is needed in interpreting IP's and AP's.

Photoionization mass spectrometry (PIMS) is most familiar in the context of ionization potential measurements. When a molecule absorbs a photon whose energy is greater than the IP, a fraction of the excited molecules eject an electron. There is usually a sudden onset of ionization as a function of photon energy, and typical quantum yields for photoionization lie in the range 0.05–0.6, the values reported for benzene in the photon energy range from 9.25 eV (the IP) to 11.7 eV.⁷¹ PIMS can also be used to probe reaction pathways with fixed frequency light sources. We have discussed the advantages of using low energy ionization for mass spectrometric experiments in Part 2, and PIMS provides an excellent method for studying mass spectrometric hydrogen rearrangements. Various types of resonance lamps provide intense photon sources for PIMS experiments above threshold, and extraneous short wavelength photons can be excluded by use of appropriate filters.

Three other techniques have provided important data for understanding gas phase solvolyses: examination of neutral products, field ionization kinetics (FIK), and metastable ion studies. These will first be presented in the context of conventional mechanisms.

Neutral products from reactions of gaseous ions

Mass spectrometry is limited to examining electrically charged species. Reactions that transform one ion to another are ordinarily accompanied by neutrals, either as reaction partners or as products (or both), but only ions can be observed. Neutral products are never seen (unless they are subsequently ionized). Their identities are usually inferred from the difference between the masses of reactant and product ions, sometimes with the aid of isotopic labelling, thermochemical estimates, and chemical intuition. In many cases, there is little question regarding the structures of neutral products. It seems unlikely, for instance, that reaction 8 produces any neutral product other than 1-butene. But no one had examined this directly.

In 1972–1974 we designed and built the first apparatus for collecting neutrals under conditions corresponding to the ionizers of most mass spectrometers (namely ≤ 100 eV electron impact). The problem was to get enough product from bombarding low pressure samples ($\leq 10^{-3}$ Torr) with mono-energetic electrons. We decided to use a long (60–130 cm) reaction vessel contained in a solenoid electromagnet (3–9 cm i.d.). Gaseous sample flows the length of the reaction vessel while electrons, focussed by the magnetic field, are beamed down its axis. Products (and unreacted starting material) are collected in a liquid nitrogen cooled trap at the end of the reaction vessel. We have built more than one version of this system, and a typical schematic is shown in Fig. 15.

Reaction 8 was one of the first subjects of study. A sample of pure 2-*n*-butylcyclopentanone at 2.5×10^{-4} Torr was bombarded with 3–4 microamperes of 70 volt electrons for 6 hr. The total throughput of substrate was 10^{-4} moles, and approximately 4×10^{-7} moles of C_2 – C_4 hydrocarbons were recovered from the radiolysis. As expected, 1-butene was the major product⁷³ (40% of the hydrocarbon yield), with propene (20%), acetylene (10%), 1,3-butadiene (7%), and ethylene (6%) constituting the bulk of the remainder. If we consider the electrons as the limiting reagent, a normalized yield is calculated by dividing the micromoles of each product by the integrated electron current in ampere-seconds (or coulombs). A normalized yield of 1 micromole per ampere-second corresponds to an efficiency of 1 molecule produced for every 10 electrons. The yield of 1-butene was slightly greater than $2 \mu\text{mol/A-s}$, and other C_4H_8 isomers were barely detectable; the only ones observed in measurable quantities were *cis*-(0.06 $\mu\text{mol/A-s}$) and *trans*-(0.07 $\mu\text{mol/A-s}$) 2-butenes and isobutene (0.02 $\mu\text{mol/A-s}$). Neither cyclobutane nor methylcyclopropane was detected.⁷⁴

What is the significance of this experiment? We demonstrated that we could collect analyzable quantities of products in our EBFlow (short for Electron Bombardment Flow) reactor. How did our

ELECTRON BOMBARDMENT FLOW REACTOR

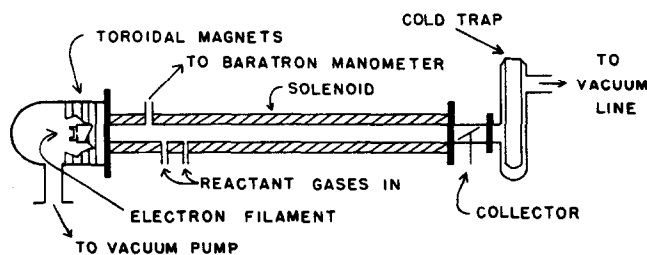


Fig. 15. EBFlow reactor, schematic diagram. Electron filament is a directly heated thoria-coated iridium ribbon immersed in a blank of 500 gauss toroidal permanent magnets (axial field). Products of EBFlow radiolysis are transferred from the cold trap after completion of the radiolysis and are sealed in a glass tube *in vacuo* for subsequent analysis by gas chromatography.

yield compare with the theoretical yield? The mean free path of 70 eV electrons (with respect to ionizing collisions) under our reaction conditions was approximately the same as the length of the reaction vessel. Therefore, we recovered approximately 1 molecule of 1-butene for every 3–4 ionizations. Reaction 8 contributes the base peak (approximately 25% of the total ionization, Σ) from 70 eV electron impact on 2-*n*-butylcyclopentanone (related fragmentations that produce $C_4H_8^{+}$, m/z 56, constitute the next most abundant peak, 10% Σ).⁷⁵ If all the 1-butene came from ion fragmentations, our recovery was virtually quantitative.






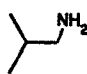
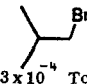
However, there is no assurance that all of the 1-butene did come from positive ion fragmentations. Although negative ion formation can be dismissed as having too low a cross section, electron impact can excite molecules electronically or vibrationally without ionizing them. Electronically excited 2-*n*-butylcyclopentanone could have expelled 1-butene via a Norrish Type I cleavage. Vibrational excitation might have led to butyl radicals, which could have reacted with other radicals to produce 1-butene. But there is no way for reaction 8 to be distinguished from these sources in an EBFlow experiment.

This points up an important limitation of neutral product studies; ionization cannot necessarily be assumed to be the source of the recovered products. Therefore, EBFlow experiments are designed so that positively charged intermediates form neutral products that cannot result from excited neutrals. Our studies of a number of such reactions lead us to conclude that the bulk of the recovered products (even from 2-*n*-butylcyclopentanone) come from gaseous cations.

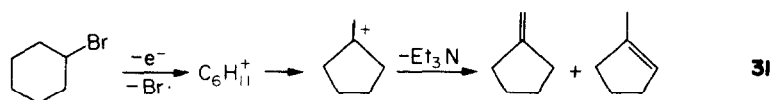
Formation of free $C_4H_9^{+}$ in the EBFlow reactor leads to a product distribution very different from reaction 8. As summarized in Table 2, 70 volt electron bombardment of *n*-butyl bromide and isobutyl bromide both lead to isomers that could not have arisen from excited neutrals. For instance, there is no way that the 2-butenes could have come from either starting material except via cationic rearrangements, which are well preceded both in the gas phase⁷⁹ and in solution.⁷⁶ For comparison, the isomer distribution from generation of $C_4H_9^{+}$ in liquid chloroform by diazotation of isobutylamine⁷⁶ is included in Table 2. The similarity between the relative C_4H_8 yields in nonpolar solvent and in the gas phase corroborates our conclusion that most of the neutral products in these experiments come from deprotonation of carbocations. Just as in solution, added base affects the observed yield. When diethyl ether (proton affinity = 198 Kcal/mol) is added to the EBFlow radiolysis of 1-bromobutane (proton affinity = 190 Kcal/mol), the mix of isomers changes. This difference represents the contribution of the gas phase deprotonation of *free sec*-butyl cation with ether to give, predominantly, *trans*-2-butene.⁷⁸

We have performed a more rigorous study of the products of deprotonation of *tert*-alkyl cations. Bombardment of bromocyclohexane with 70 volt electrons yields a C_6H_{10} mixture, in which methylenecyclopentane and 1-methylcyclopentane are the principal isomers. The latter is thermodynamically more stable, having a $\Delta H_{f,300}^\circ$ that is 3.9 Kcal/mol less than that of the former. Adding a gas phase base to the EBFlow reaction vessel affects the isomer ratio. (Isomer ratios discussed below will always refer to the yield of the thermodynamically less stable isomer divided by that of the thermodynamically more stable isomer.) When triethylamine is used, the ratio increases (i.e. shifts in the direction of the thermodynamically less favored isomer) with increasing base concentration. This result is interpreted as

Table 2. C₄H₈ isomer distributions from butyl cations under various conditions, relative to the olefin from vicinal elimination (=1) in each case. No cyclobutane is observed in any of these reactions

						Ref.
 $\xrightarrow[\text{HOAc, CHCl}_3]{\text{C}_3\text{H}_7\text{ONO}}$	1	0.10	0.025	0.06	0.20	76
 $\xrightarrow[3 \times 10^{-4} \text{ Torr}]{70 \text{ eV electron impact}}$	1	0.13	0.06	0.10	0.12	77
$\text{CH}_3\text{CH}_2\text{CH}_2\text{CH}_2\text{Br} \xrightarrow[4 \times 10^{-4} \text{ Torr}]{70 \text{ eV electron impact}}$	0.4	1	0.3	0.2	0.2	78
$\text{CH}_3\text{CH}_2\text{CH}_2\text{CH}_2\text{Br} + \text{Et}_3\text{O} (3:1) \xrightarrow[4 \times 10^{-4} \text{ Torr}]{70 \text{ eV electron impact}}$	0.8	1	0.4	1.4	0.4	78

follows: the C₆H₁₁⁺ cation is the most abundant ion in the 70 eV mass spectrum of bromocyclohexane. It rearranges to the most stable structure, methylcyclopentyl cation, and when it collides with a triethylamine molecule, it is deprotonated, as shown in reaction 31.

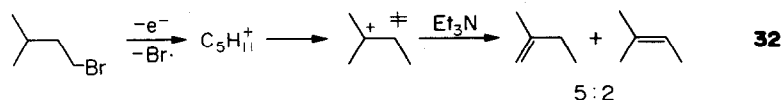


But there is another possible source of olefinic products. In the EBFlow reactor, all charged species ultimately strike electrically grounded metal surfaces. A charge collector, mounted at the end of the reaction vessel, insures that all ions are neutralized before any products are condensed in the cold trap. The current measured at the collector is usually negative and represents the difference between the number of electrons and the number of positive ions leaving the reaction vessel. Perhaps a portion of the recovered neutral products come from surface neutralization instead of ion-molecule reactions. We can be sure that when the product distribution changes as a result of adding a gas phase base, the difference is a consequence of a gas phase proton transfer. When addition of triethylamine shifts the product distribution in the direction of the thermodynamically less favored isomer, that means that the isomer ratio from the gas phase deprotonation is greater than (or equal to) the ratio of recovered neutrals.

In order to quantify isomer ratios from gas phase deprotonation (instead of measuring their lower bound), it is necessary to assess contributions from surface neutralization. One way of doing so is to vary the magnetic field strength of the solenoid electromagnet that surrounds the reaction vessel. Two forces restrain positive ions from hitting the reaction vessel wall, magnetic deflection and attraction to the electron beam. Deflection by the axial magnetic field forces electrical charges to travel spiral paths down the axis. In general, the radius of the spiral is less than the diameter of the tube, and charged particles do not travel to the wall unless they are jogged there by collisions with neutrals. Electrons are more effectively contained by the magnetic field than positive ions since they are so much less massive (the momentum of a 70 eV electron is about the same as that of a thermal proton at room temperature). Focussing the electron beam down the central axis of the reaction vessel provides another force for positive ion containment, space-charge focussing by attraction to the negative beam.⁸⁰ As the magnetic field is made stronger, the electron beam becomes less diffuse, and positive ions are held more tightly to the axis. The rate of migration to the wall (from ion-molecule collisions) becomes slower.

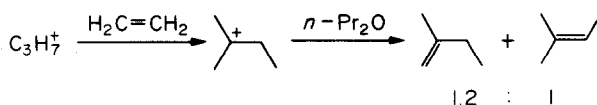
For cations in the EBFlow reactor, reaction with molecules of gaseous base competes with unreactive collisions (with neutral starting material) that bump ions towards the wall. As the axial magnetic field is increased, the rate of quenching by the wall decreases. At sufficiently high field strengths, contributions from wall collision become negligible, and further increasing the field does not affect product yields. The isomer ratio in reaction 31 increases with field strength until it levels off at about 150 Gauss. Thus, it reaches a plateau both with increasing field strength and with increasing base concentration at a value of methylenecyclopentane:1-methylcyclopentene = 0.83.²⁴

We can distinguish different ionic sources in the EBFlow reactor. One technique is the method of base variation, as described in the previous section for differentiation of reaction 26 from reaction 27. Another technique is isotopic labelling. Enough product can be recovered from EBFlow radiolyses to be purified and collected by preparative gas chromatography for subsequent mass spectrometric analysis. GC-MS is not suitable for precise work, since isotopic fractionation requires that the peak be collected and analyzed in its entirety.



Bombardment of isoamyl bromide, $(\text{CH}_3)_2\text{CHCH}_2\text{CH}_2\text{Br}$, with 70 volt electrons yields 2-methylbutenes, as shown in reaction 32. When triethylamine is present, the thermodynamically less stable isomer is the major C_5H_{10} product, and the normalized yields of 2-methyl-1-butene and 2-methyl-2-butene are 2.3 and 2.0 $\mu\text{mole/A-s}$, respectively. There are two ionic precursors to these products. The principal ion in the 70 eV mass spectrum of $(\text{CH}_3)_2\text{CHCH}_2\text{CH}_2\text{Br}$ is $\text{C}_5\text{H}_{11}^+$. In the EBFlow reactor, it rearranges to the most stable structure to give vibrationally excited *tert*-amyl cation, which is then deprotonated to give both products, as shown in reaction 35. From solution NMR studies, it is known that *tert*-amyl cation scrambles all of its hydrogens with an activation barrier $E_a = 19 \text{ kcal mole}^{-1}$.⁶⁸ A deuterium label will therefore be completely randomized in a sufficiently activated gaseous cation. Since we presume that $\text{C}_5\text{H}_{11}^+$ is initially produced as a primary cation from 70 eV electron impact on $(\text{CH}_3)_2\text{CHCH}_2\text{CH}_2\text{Br}$, the *tert*-amyl cation that results from rearrangement ought to have an internal energy $\geq 30 \text{ kcal mol}^{-1}$. RRKM calculations indicate that hydrogen scrambling in such a cation will be complete within a few microseconds.⁸¹ Therefore, the *tert*-amyl cation from $(\text{CH}_3)_2\text{CDCH}_2\text{CH}_2\text{Br}$ should have a random distribution of deuterium, and both of the 2-methylbutenes from its deprotonation ought to be at least 90%- d_1 . The ratio 2-methyl-1-butene- d_1 :2-methyl-2-butene- d_1 from EBFlow radiolysis of $(\text{CH}_3)_2\text{CDCH}_2\text{CH}_2\text{Br}$ in the presence of triethylamine is approximately 2.6.²⁴ From this, we infer that the isomer ratio from reaction 35 is on the order of 5:2.

A large fraction of the $(\text{CH}_3)_2\text{C}=\text{CHCH}_3$ from $(\text{CH}_3)_2\text{CDCH}_2\text{CH}_2\text{Br}$ radiolysis contains no deuterium. We calibrated our analysis of deuterium content by examining the relative peak intensities in the mass spectra of the neutral products from 70 eV EBFlow radiolysis of $(\text{CH}_3)_2\text{CHCH}_2\text{CH}_2\text{Br}$. The 2-methylbutenes from both d_1 bromides gave essentially the same mass spectra. But the 2-methyl-2-butene from $(\text{CH}_3)_2\text{CDCH}_2\text{CH}_2\text{Br}$ was substantially depleted in deuterium. We ascribe the d_0 product to neutralization of the C_5H_{10} ion from reaction 10, and it is on this basis that we draw the ion as having the most stable structure, as shown. We observe that the intensity of the peak from reaction 10 is about half that of the M-Br peak in the mass spectrum of $(\text{CH}_3)_2\text{CDCH}_2\text{CH}_2\text{Br}$. Since the yield of $(\text{CH}_3)_2\text{C}=\text{CHCH}_3$ in the EBFlow experiment is approximately 25% of the 2-methylbutene yield from the Brønsted acid-base reaction of $\text{C}_5\text{H}_{10}\text{D}^+$ with triethylamine, we conclude that about half of the odd-electron ions were neutralized to give C_5H_{10} .



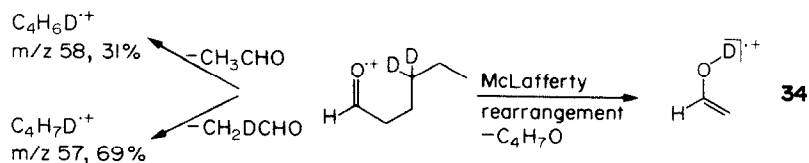
We note that the isomer ratios from reactions 31 and 32, 0.83 and 2.5, are close to the simple statistical ratios of the two types of nonequivalent acidic protons in the respective cations. The ratio of acidic methyl to methylene hydrogens in methylcyclopentyl cation is 3:4, while the ratio in *tert*-amyl cation is 6:2. But this is true only when vibrationally excited cations are deprotonated by a strong gas phase base like triethylamine. We have looked at these reactions with weaker bases and find that the isomer ratio decreases.⁸¹ For instance, when isopropyl cation adds to ethylene in the EBFlow reactor to produce, ultimately, *tert*-amyl cation (as represented in reaction 33), deprotonation by *n*-propyl ether yields an isomer ratio of 1.2.²⁴ The reaction is run in a large excess of ethylene (with *n*-propyl ether also serving as the source of isopropyl cation via 70 eV electron impact), and the *tert*-amyl cation is very likely to be vibrationally deactivated by nonreactive collisions with ethylene. The normalized yield of 2-methylbutenes is only 0.17 μ moles A-s, a low value that is consistent with RRKM calculations of the efficiency of bimolecular electrophilic addition to ethylene at 10^{-3} Torr.⁸¹

The implication of these studies is clear: deprotonation by a strong base like triethylamine (proton affinity = 232 kcal mole)²⁸ is almost statistical, while an increasing preference for the thermodynamically favored isomer is seen with a weaker base like diisopropyl ether (proton affinity = 203 kcal mole).²⁸ These results illustrate the scope of EBFlow techniques for identifying ion structures and for looking at reactions that exhibit second (or higher) order kinetics. We have also devoted considerable effort to investigating the neutral products from ion decompositions that obey first-order kinetics. Our results provide the best direct evidence for gas phase solvolyses, but before discussing them, we shall briefly describe mass spectrometric techniques for studying the kinetics of ion decompositions.

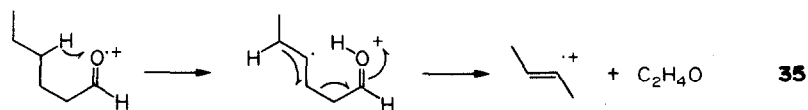
Field ionization kinetics

Field ionization kinetics (FIK) offers a method for directly measuring rates of unimolecular ion decompositions. Field ionization refers to removal of electrons from molecules by very strong electric fields. Typically, the ionizer is a razor blade that is biased several kilovolts positive of a nearby cathode slit, which is electrically grounded. Within a nanometer or so of the sharp edge of the blade, the electric field is strong enough to pull electrons out of molecules. Ionization occurs in a spatially well defined region, and the positive ion is repelled by the razor blade emitter. The ion accelerates toward the slit, and after passing through the slit it has a known translational kinetic energy. If the ion beam is mass analyzed (momentum analyzed, to be precise) by deflection in a magnetic field, some peaks appear to be broadened and shifted from their proper positions. These are ions that have undergone decompositions en route from the emitter to the slit. They have changed mass while falling through an electric potential and are deficient in kinetic energy relative to ions of the same mass that were formed at the emitter. The kinetic energy of each ion is defined by its distance from the emitter (and, hence, its position in the accelerating field) when the change of mass occurs.⁸²

From the translational kinetic energy of an ion and the m/z value of its precursor, the position in space where the decomposition took place (and, consequently, the time lapse between ionization and decomposition) can be calculated. In a double focussing mass spectrometer, ions are sorted by kinetic energy (in an electric sector analyzer) before they are mass analyzed. The kinetic energy distribution of an ion beam can be measured by scanning the electric sector while monitoring a given ion mass. Alternatively, the electric sector can be set to a fixed energy bandpass and the voltage on the emitter varied. This is the FIK technique for looking at the 0.01–1 nanosecond timescale. FIK can be used to study longer timescales by examining ions that decompose after passing through the cathode slit. The current of fragment ions at a single mass observed at a given setting corresponds to the rate with which those fragments are produced at a specific time after ionization. Therefore, FIK data are reported as graphs of ion decomposition rate vs time.⁸³ A standard form for presenting those data is as a normalized rate, namely the rate of decomposition at a given time divided by the measured molecular ion current⁸⁴ (e.g. the current measured at the mass of the molecular ion when the emitter voltage is at its lowest setting, 8 kV).



The McLafferty rearrangement shown in reaction 34 has been studied by FIK. This is by far the fastest rearrangement of the hexanal molecular ion, having a normalized rate $\geq 5 \times 10^9 \text{ sec}^{-1}$ at the shortest decomposition times. The rate decreases monotonically with an increasing delay between ionization and decomposition.³¹ The reaction is regiospecific, as indicated.⁸⁵ As mentioned in Part 2, Stevenson's rule dictates that the charge remains with the fragment having the lower ionization potential.³⁰ In the fragments from hexanal, 1-butene has an IP of 9.6 eV,² while vinyl alcohol has an IP ≤ 9.14 eV (based on studies of $\text{C}_2\text{H}_4\text{O}$ from pyrolyses of cyclobutanol).⁸⁶ Thus Stevenson's rule is obeyed here (although it would not have been if the ion had the acetaldehyde structure, since the IP of CH_3CHO is 10.2 eV).² Indeed, one of the driving forces of this McLafferty rearrangement is that the molecular ion of vinyl alcohol has a heat of formation approximately 15 Kcal mol lower than its keto tautomer.⁸⁷



A related rearrangement of hexanal, which produces $\text{C}_4\text{H}_8^{++}$, occurs with a slower rate. This rate reaches a maximum value with increasing delay time between ionization and decomposition and then falls off.³¹ The hydrogen rearrangement is not regioselective and the hexanal-4,4- d_2 gives m/z 57 and m/z 58 from nominal 15 eV electron impact in the proportions shown in reaction 34.⁸⁵ The shape of the rate vs time curve from FIK is consistent with a two step rearrangement in which the second step is slower than the first. A mechanism involving a second hydrogen rearrangement has been proposed⁸⁸ as shown in reaction 35, and there seems to be general agreement that the $\text{C}_4\text{H}_8^{++}$ ion has, predominantly, the most stable structure, namely that of a 2-butene.^{31,89} The ionization potential of *trans*-2-butene (9.12 eV)² is sufficiently low that Stevenson's rule is not disobeyed, regardless of the structure of the $\text{C}_2\text{H}_4\text{O}$ neutral fragment, but there has been some debate whether this neutral is vinyl alcohol³¹ or acetaldehyde.⁸⁹ Conventional mechanisms for production of neutral CH_3CHO have contorted transition states, but it is possible that the reaction occurs via a gas phase solvolysis. This interpretation will be presented in the last section of this report, but, first, reactions will be discussed for which there is firm evidence of this type of mechanism.

Metastable ion studies

Metastable ion studies offer a direct method for examining the energetics of ion decompositions. Whereas FIK examines ions that decompose while being accelerated in an electric field, the term "metastable" is ordinarily applied to ions that decompose in field-free regions of the mass spectrometer. Ion decompositions in both regions lead to broadened peaks in a single-focussing magnetic sector instrument. In a field ionization experiment, the broadening is largely due to the distribution of delay times (and, hence, fragment ion kinetic energies) between ionization and fragmentation, and the peak is usually shifted only a fraction of an amu away from its actual m/z value. A metastable ion is typically shifted very far away from its actual m/z value, and the general expression for the position of the peak maximum is m^2/M (where m is the m/z value of the daughter ion and M the m/z value of its parent), regardless of where the decomposition took place in the field-free region. The broadening is largely attributable to conversion of internal energy of the parent ion into translational kinetic energy of the daughter ion during decomposition. The center of mass of the parent travels at a constant velocity before and after the fragmentation, but the breakup of the parent can take place with any orientation relative to the direction of motion. If the neutral is expelled in the direction of motion, the daughter ion will move more slowly than the center of mass. If the neutral is expelled in the opposite direction, the daughter will move faster than the center of mass. These two extremes are less likely than expulsion perpendicular to the direction of motion, in which case the daughter ion moves towards the magnetic sector at the same speed as the center of mass.

There are several ways of determining the amount of translational kinetic energy release. Most involve measuring the width of a metastable peak using a double focussing mass spectrometer, and one technique is to use an electrostatic energy selector prior to mass analysis. In ion kinetic energy (IKE) spectroscopy, all ions are given the same kinetic energy by falling through a potential drop of several kilovolts, and are then admitted into a field-free region. Any ion that decomposes in this first field-free

region will be deficient in kinetic energy, because its mass has decreased without a compensating increase in its speed.⁹⁰

After the first field-free region, ions are energy analyzed by an electrostatic sector. The internal energy of the parent that is converted into translation in the fragmentation (usually abbreviated T) can be determined from the energy spread of the metastable ion beam that comes out of the electrostatic sector (assuming that the masses of parent and daughter are known). The activation barriers for an endothermic decomposition will almost always be greater than T, and a large fraction of the energy difference between the transition state and the products sometimes appears as translational kinetic energy. For instance, ΔH for the reaction $\text{H}_2\text{C}=\text{OH}^+ \rightarrow \text{HC}\equiv\text{O}^+ + \text{H}_2$ is 28 Kcal, while the activation barrier E_0 is 80 Kcal. Of the 52 Kcal energy difference between transition state and products, 33 Kcal appears in the form of translational energy release.⁹¹

For simple bond fissions, it is usually assumed that there is no activation barrier above the endothermicity of the cleavage. For ions that have internal energy E^* in excess of the thermodynamic barrier, the average translational energy release is about what is expected if the excess energy is partitioned between the 3 new translational degrees of freedom and the remaining vibrations of the products (assuming complete randomization of internal energy within the present ion).⁹² To a good approximation, the translational energy release is given by the naive expression $(1/\alpha)(E^*/N)$, where N is the number of internal degrees of freedom in the parent ion and $(1/\alpha)$ is empirically determined. In a study of eight simple cleavages of molecular ions, $(1/\alpha)$ was found to be between 1.8 and 2.5.⁹³

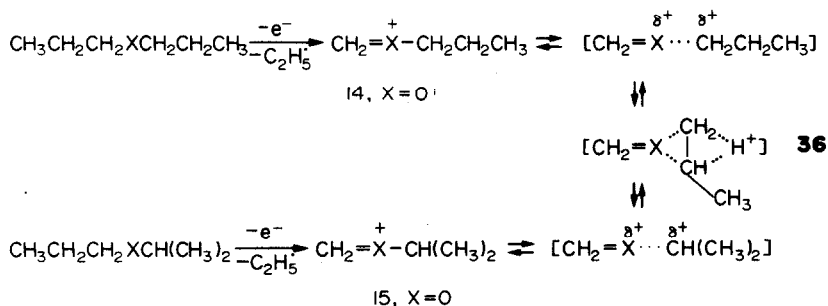
Metastable ion intensity decreases relative to molecular ion intensity as N, the number of internal degrees of freedom in the parent ion, gets larger. In the homologous series of linear 2-alkanones, the metastable from the $\text{M}^+ \rightarrow \text{H}_2\text{C}=\text{CHOHCH}_3^{++}$ decomposition becomes less intense relative to M^{++} with increasing molecular weight. The functional form of the dependence on N has been shown to be consistent with complete energy randomization in the molecular ion prior to fragmentation.⁹⁴

The relationship between the value of T and the reverse activation energy (i.e. the energy difference between the transition state and the products) has been studied for a variety of McLafferty rearrangements. Calculations based on the assumption of complete internal energy randomization suggest that T represents only a small fraction of the reverse activation energy for these reactions. The ΔH for McLafferty rearrangement of a 2-alkanone is approximately +15 Kcal mol.^{87,89} For a reverse activation energy of 9 Kcal mol, a 2-pentanone molecular ion with about 4 Kcal mol internal energy in excess of the activation barrier is calculated to give an average translational kinetic energy release, T_{av} , of only 0.7 Kcal mol. This calculation is based on a cyclic transition state and corresponds to products with a total energy content (E^*) of about 13 Kcal mol. For the relation $T_{\text{av}} = (1/\alpha)(E^*/N)$, this calculation corresponds to a value of $(1/\alpha) = 2.1$. If different values for the reverse activation barrier (and for E^*) are used in the calculation, $(1/\alpha)$ changes from 2.8 for $E^* = 4$ Kcal mol to 1.5 for $E^* = 39$ Kcal mol. The experimental value of T_{av} is 0.735 Kcal mol. If the reported difference between the ionization potential of 2-pentanone and the appearance potential of the $\text{H}_2\text{C}=\text{CHOHCH}_3^{++}$ ion (0.9 eV) was a correct measure of the average energy content of the molecular ions giving the metastable in this experiment, the value of E^* was approximately 6 Kcal mol. Thus the experimental $T_{\text{av}} = 5.1 E^*/N$, and the translational energy release is somewhat greater than predicted by calculations. There are not sufficient thermochemical data to allow us to estimate the value of the empirical coefficient $(1/\alpha)$ for the other rearrangements for which T_{av} has been reported (T_{av} is on the order of 1 Kcal mol or less for a half dozen other ketones and carboxylic esters whose McLafferty rearrangements were studied, but no metastable peaks were observed for ten other carbonyl compounds investigated).⁹⁵ For ion decompositions that are not simple bond fissions, Ref. 93 (which used time-of-flight rather than metastable measurements) reports values of $(1/\alpha)$ in the range of 2–7. In the absence of further experimental data, we feel justified in guessing that $N/2$ times the value of the translational kinetic energy release is $\geq E^*$ for a fragmentation that is not a simple cleavage. This gives an upper bound for the reverse activation energy (which is always less than E^*).

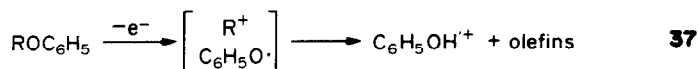
5. GAS PHASE SOLVOLYSES

It is clear from Part 3 that ion-molecule complexes are now widely accepted intermediates in the gas phase. The decomposition of the vibrationally excited adduct in reaction 23 represents a unimolecular dissociation via an ion-molecule complex, the anionic counterpart of reaction 2. Yet ion-molecule complexes were, at first, put forth very cautiously in explaining reactions that obey first-order kinetics in the mass spectrometer. The initial investigations concerned fragmentations of ions derived from sample

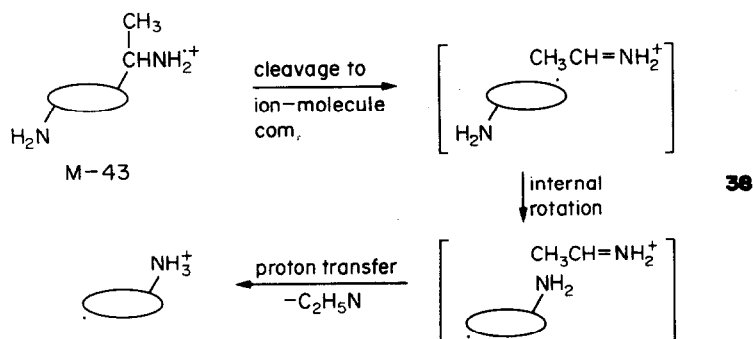
ethers. In 1978, a communication from the University Chemical Laboratory at Cambridge appeared that discussed the reactions of "weakly co-ordinated carbonium ions in the mass spectrometer".¹¹ In this paper, Bowen, Stapleton, and Williams described decompositions of the oxonium ions **14** and **15**, which come from fragmentations of propyl ethers.⁹⁶ Using metastable ion techniques and appearance potential (AP) measurements, Bowen and Williams had mapped the $C_4H_9O^+$ potential energy surface.⁹⁷ They concluded that **14** and **15** must equilibrate, since both ions exhibit the same energy threshold for CH_2O expulsion, and the AP is too low for the remaining ion to have any structure but isopropyl. The Cambridge group proposed the ion-dipole complexes drawn in reaction 36 to account for this.



At the same time, we were studying another class of ethers using neutral product analysis. We had reported the olefin isomer distribution from electron bombardment of alkyl phenyl ethers⁷³ and were developing the mechanism shown in reaction 37 to explain the production of $C_6H_5OH^+$ from the molecular ions. After a tedious examination (and rejection) of every reasonable conventional alternative, I presented evidence for the mechanism shown in reaction 37 at the East Coast ICR Symposium in March, 1979



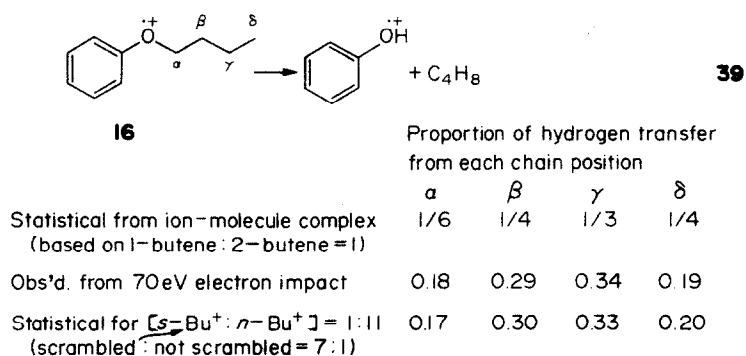
Subsequently, other investigators independently proposed comparable pathways for mass spectrometric fragmentations. Longevialle and Botter explained apparent "long distance" hydrogen transfers in rigid steroidal diamines by invoking the ion-molecule complex shown in reaction 38 (in which the steroid skeleton is symbolized by an ellipse). Simple α -cleavage forms a protonated imine, which transfers a proton to the neutral amine-containing radical in the ion molecule complex to yield the observed M-43 fragment ion.⁹⁸



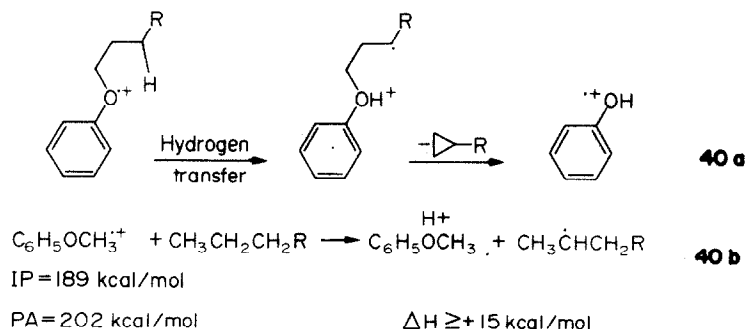
Ion-molecule complexes are stipulated for these reactions because directed valence must be lost without complete dissociation. In reaction 38, rotation of the neutral radical within the complex brings together two functional groups that are 10 Å apart in the neutral precursor. In reactions 36 and 37, the energetics require that alkyl groups undergo structural rearrangements that are well preceded in free cations, but which would seem bizarre for groups that are covalently bound. Our investigation of reaction 37 has provided direct evidence for the gas phase solvolytic mechanism. The Cambridge group's investigations of reaction 36 and its homologues has provided the best characterization of the kinetics and energetics of this pathway.

Phenyl ethers

The decomposition of alkyl aryl ethers has been a widely studied problem in organic mass spectrometry. Prior to our demonstration of a gas phase solvolytic pathway, more than a dozen published studies between 1966–1976 dealt with the mechanism of formation of $C_6H_5O^+$ from phenoxyalkanes where the alkyl is a saturated group with ≥ 2 carbons.^{73,90,99–109} Although there was some disagreement regarding the structure of $C_6H_5O^+$ (whether it is the keto or enol tautomer), all investigators accepted a conventional mechanism that invoked competition among several cyclic transition states of different ring sizes. Why did this reaction attract such attention? First of all, the decomposition represents a huge base peak in the mass spectra, representing at least one third of the total ionization at 70 eV and increasing in intensity as the ionizing energy is lowered. Secondly, as discovered by MacLeod and Djerassi in 1966 in the first study of reaction 37, a non-specific hydrogen rearrangement takes place. In phenyl butyl ether, one hydrogen is transferred from the alkyl chain to the fragment ion, and specific deuterium labelling showed that this hydrogen can come from any of the chain positions. Although the proportions from each position vary somewhat with the energy content of the parent ion, the values for rapidly decomposing ions (rate $> 10^6 \text{ sec}^{-1}$) at 70 eV are typical and are summarized in reaction 39. These values are based on the $[m/z \ 95]/[m/z \ 94 + m/z \ 95]$ ratio from four deuterated analogues and assume that the deuterium isotope effect is the same for each one.⁹⁹ Studies of the effects of ionizing energy showed that these results could not be explained by complete hydrogen randomization in the chain prior to decomposition.¹⁰⁵



Let us review why the conventional mechanism becomes untenable. As discussed in Part 2 (see reaction 10), an intramolecular hydrogen transfer tends to operate under the same thermochemical constraints as its bimolecular analogue. The most probable first step of a conventional mechanism for reaction 39 would have to be step i of reaction 40a (because γ -transfer predominates,⁹⁹ and the experimental data strongly support the $C_6H_5OH^+$ structure for the daughter ion).^{102–109} A thermochemical estimate is made by comparing this step to reaction 40b. The hydrogen atom affinity (HA) of ethers is independent of the saturated alkyl group attached to oxygen, so the value for anisole is pertinent. The proton affinity of anisole is known, although it probably represents ring protonation. From this value (202 Kcal/mol)¹¹⁰ and the ionization potential of anisole (189 Kcal/mol),² we calculate an $HA = 78 \text{ Kcal/mol}$. This means that hydrogen abstraction from a CH_2 is endothermic by $> 15 \text{ Kcal/mol}$! Furthermore, since the oxygen of anisole is not as basic as the ring, this value of ΔH represents a lower bound if we stipulate atom abstraction by oxygen in reaction 40b.



Of course, the comparison in reaction 40 may not be germane. The molecular ion **16** must be excited to begin with, since ΔH for C_4H_8 expulsion is at least +20 Kcal (based on an adiabatic IP for phenyl butyl ether of 185 Kcal mol).⁷³ Even so, it seems surprising that such an endothermic hydrogen transfer should show such little discrimination (<2 to 1) between a methylene and a remote methyl group. Moreover, in studies of phenyl *n*-propyl ether ($R = H$ in reaction 40a), deuterium labelling shows that the γ -position (which is a methyl group) contribution *increases* to 0.40–0.50.^{108,109}

The conventional mechanism does not clearly predict an identity for the expelled neutral. Expulsion of methylcyclopropane was originally entertained,⁹⁹ as shown in step ii of reaction 40a. This suggestion prompted us to run an EBFlow study of phenyl butyl ether, which we performed at 2.5×10^{-4} Torr over a range of electron energies. Our results are summarized in Fig. 16: 1-butene and the two geometric

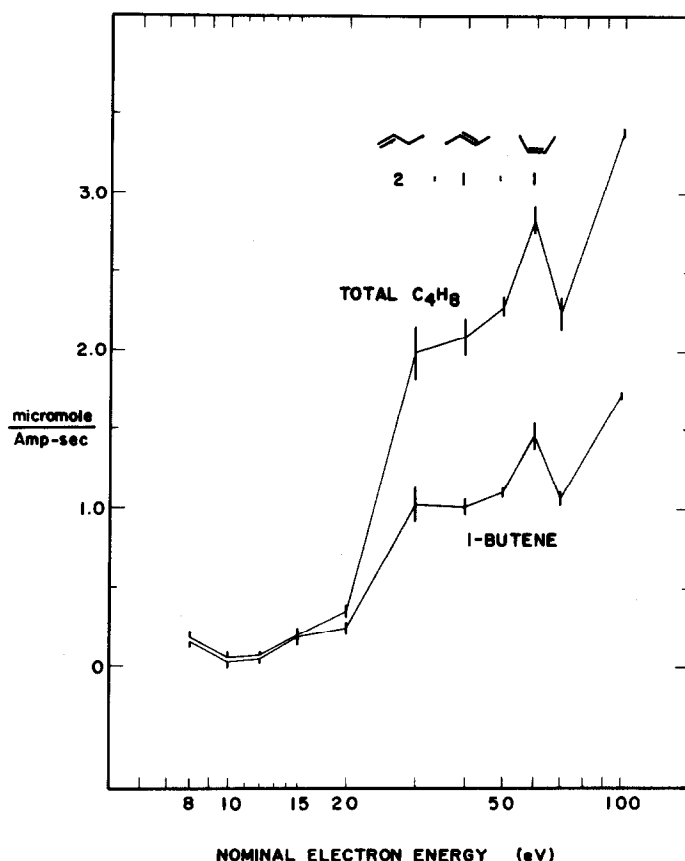


Fig. 16. Neutral product yields from 70 eV electron bombardment of *n*-butyl phenyl ether at 2.5×10^{-4} Torr. Isomer yield as indicated at all electron energies ≥ 30 eV.

isomers of 2-butene are recovered in a 2:1:1 ratio at all electron energies from 30 to 100 eV.⁷³ Yields of other C_4H_8 isomers are virtually nil. Two questions immediately present themselves: (1) Could the true product have isomerized or been destroyed under the reaction conditions? (2) Could reactions of free butyl cations account for the results? We can provide firm negative answers. (1) Our EBFlow study of reaction 8 gave only 1-butene, so significant isomerization does not occur under the reaction conditions. Bombardment of methylcyclopropane at $4\text{--}6 \times 10^{-4}$ Torr with 70 eV electrons produces only ppm levels of products, so this product is obviously not being destroyed under the reaction conditions. (2) A glance at Table 2 shows that the isomer distribution from free $C_4H_9^+$ is very different from what we observed from *n*-butyl phenyl ether.

More complicated questions can also be asked. Could the products have come from nonionic sources? Not likely, since an exhaustive set of controls (pyrolysis and photolysis of phenyl butyl ether) showed no production of 2-butenes from excited neutrals. Or, granted that positive ions are the source of the recovered C_4H_8 , could the recovered products come from ion-molecule or surface reactions? The abundance of other fragments is so low that only the reactions of **16** and $C_6H_5OH^{++}$ need to be

considered. Nibbering observed the reaction of $\text{C}_6\text{H}_5\text{OH}^{++}$ with amine bases and noted that proton transfer takes place rapidly from the oxygen.¹⁰⁶ We examined the ion-molecule reaction of $\text{C}_6\text{H}_5\text{OH}^{++}$ with 2×10^{-4} Torr of phenyl-*n*-butyl ether by ICR and observed a fast ion-molecule reaction. It was important to examine this reaction in the pressure range of our EBFlow experiments (rather than using pulsed ICR techniques at lower pressures), even though collisional broadening made it impossible to resolve ion **16** (m/z 150) from the protonated parent ion (m/z 151). Electron and proton transfer from $\text{C}_6\text{H}_5\text{OH}^{++}$ to the neutral ether are both exothermic, the former by about 11 Kcal/mol and the latter by 9 Kcal/mol (since the hydrogen atom affinity of **16**—assumed equal to that of ionized anisole—is 2 Kcal/mol less than the bond dissociation energy of phenol).¹¹¹ We decided that the product is ion **16** on the basis of the ICR double resonance spectrum reproduced in Fig. 17. Using ion ejection, the ratio of

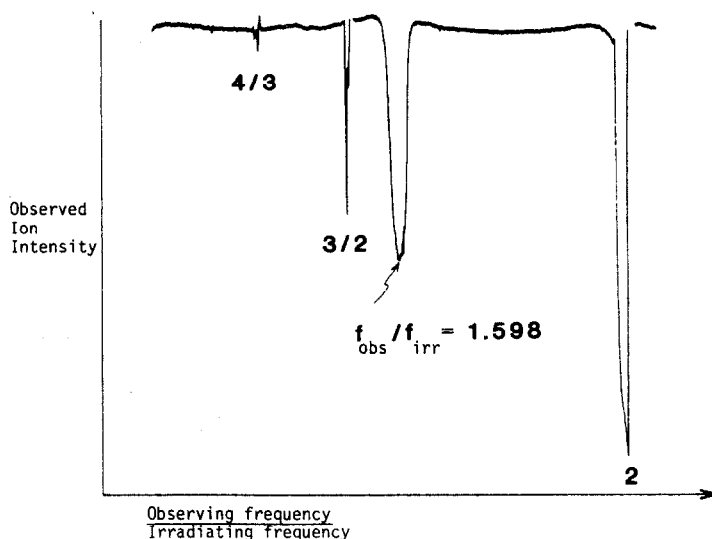
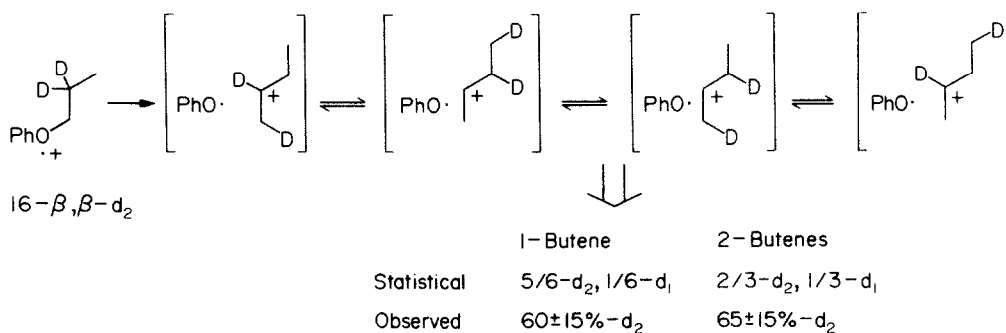


Fig. 17. ICR double resonance spectrum of *n*-butyl phenyl ether molecular ion (m/z 150), with 80 mV/cm irradiating field. Harmonics at frequency ratios 4/3, 3/2 and 2 are included for calibration purposes.

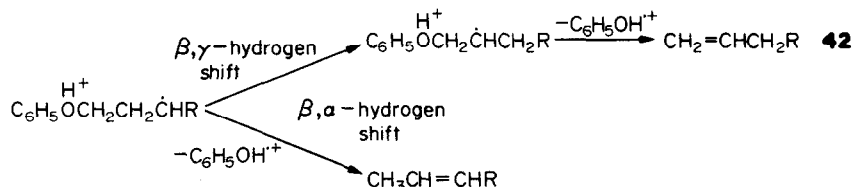
the product ion mass to m/z 94 was measured to be 1.598⁷⁵ (the exact mass ratio of **16** to $\text{C}_6\text{H}_6\text{O}^{++}$ is 1.596). No ion-molecule reaction of **16** with its neutral parent was observed.



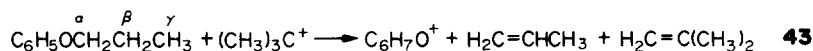
41

Therefore, **16** is the ionic end product that is neutralized at the collector in the EBFlow experiment. Could this neutralization have produced the observed 2-butenes? To probe this we ran a deuterium labelling experiment. From the mass spectrometric studies summarized in reaction 39, we know that **16**- β,β -d₂ ought to give about a 7:3 ratio of dideuterated to monodeuterated butenes (since about 30% of the hydrogen transfer comes from the β -position). Any other source ought to give much more monodeuterated product. The results from 70 eV EBFlow radiolysis of the dideuterated butyl phenyl ether are summarized in reaction 41. There is a large uncertainty in the measured values, since deuterium content was analyzed by GC-MS and since appropriately deuterated butenes were not available for

calibration purposes. The extent of deuteration of *cis* and *trans*-2-butene are the same and are within experimental uncertainty of the expected value. The $d_2:d_1$ ratio for 1-butene is slightly lower; this could be attributed to contamination by as much as 20% 1-butene- d_1 from sources other than reaction 39. Nevertheless, it is clear that at least 90% of the recovered C_4 olefins come from the mass spectrometric expulsion, since the low proportion of β -transfer is a distinctive feature of the unimolecular decomposition of 16.



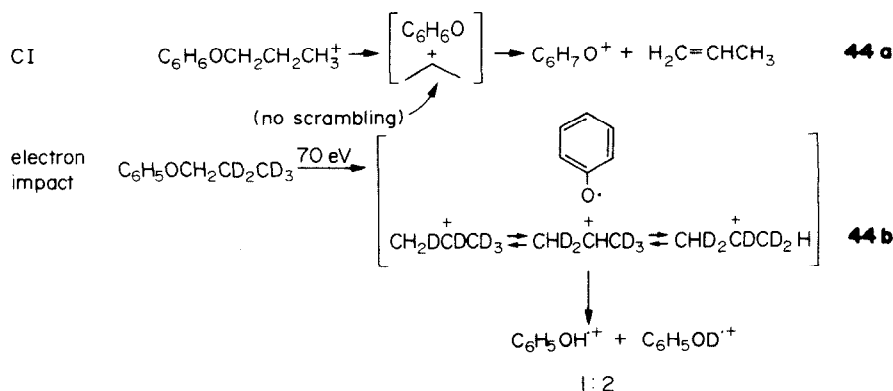
We concluded that the only way a conventional mechanism could be salvaged would be if a 1,3-diradical were expelled in the second step of reaction 40a. This diradical would have needed at least 25 Kcal/mol additional vibrational energy (E^*) to yield so little methylocyclopropane relative to linear butenes (the experimental ratio was 1:100). If E^* were this large, then the translational kinetic energy release ought to have been at least 0.7 Kcal/mol, based on the surmise that $T \geq NE^*/2$ discussed in the previous section. Experimentally, the value of T is reported to be <0.5 Kcal/mol.¹⁰⁹ Moreover, γ -transfer does not fall off with decreasing ionizing energy.¹⁰⁴ Nibbering had proposed 1,2-transpositions of the functional group competitive with vicinal elimination to explain labelling results in phenole.¹⁰⁶ This, and the alternative suggestion of hydrogen shifts such as those depicted in reaction 42, can be excluded on the basis of FIK studies on phenyl *n*-propyl ether ($R = \text{H}$). These shifts would certainly require that fragmentation after β -transfer (for which no shift is required) be faster than the rate of fragmentation after γ -transfer. But the two rates change only slightly with increasing delay times: the ratio of rates at 10^{-11} sec is 0.6 and at 7×10^{-9} sec is 0.5. At the shortest times, the proportions of hydrogen transfer from each chain position are virtually the same as would be expected from complete randomization of the alkyl hydrogens: $\alpha = 2/7$, $\beta = 2/7$, and $\gamma = 3/7$.¹⁰⁸



Proportion of transfer from each chain position $\Delta H = +5$ kcal/mol

	α	β	γ
Statistical (no scrambling)	1/3	1/6	1/2
Observed	0.34	0.17	0.49

We shall not enumerate all the variations on the conventional mechanism that we have ruled out. In our view, the death knell for the conventional mechanism was sounded by Benoit and Harrison, who examined the chemical ionization (CI) of specifically deuterated phenyl *n*-propyl ethers. CI with isobutyl cation is one of the mildest ionization techniques known, especially at the reported pressures of 0.3–0.5 Torr, where ions are collisionally thermalized within a few hundred nanoseconds. Reaction 43 was observed, even though it is endothermic (based on the reported proton affinity of phenol¹¹⁰), so it clearly must have been a thermal decomposition of the protonated ether. Nevertheless, γ -hydrogen transfer is the predominant decomposition, and the experimentally determined proportions are summarized in reaction 43.¹⁰⁹ No aspect of the conventional mechanism suggests that there ought to be any similarity between decompositions of odd electron molecular ions and even electron ions from CI, yet the proportions are much the same.



Once the gas phase solvolytic mechanism was recognized, the unity of the electron impact and CI results became apparent, as represented in reaction 44. The CI experiment is a thermal decomposition of the protonated parent ion and gives an ion-molecule complex of $\text{C}_6\text{H}_5\text{O}$ with an isopropyl cation, as drawn in reaction 44a. The cation moiety has little internal energy, and its isotopic label does not rearrange further (the activation barrier for complete scrambling of the hydrogens of isopropyl cation in solution is 11 Kcal mol,⁶⁸ although that value may not be relevant in the ion-molecule complex). Proton transfer to $\text{C}_6\text{H}_5\text{O}$ (whose proton affinity is ≥ 197 Kcal mol, regardless of its structure)¹¹⁰ gives the observed products with the statistical proportions summarized in reaction 43. Electron impact yields an ion-molecule complex of isopropyl cation and phenoxyl radical (whose proton affinity is 198 Kcal mol).⁷⁸ If formed by 70 eV electron impact, the isopropyl cation in the ion-molecule complex randomizes its label. A statistical product distribution is observed: for the deuterated analogue shown in reaction 44b, the statistical product ratio is 2:5, and the observed 1:2 ratio is attributed to an isotope effect of $k_{\text{H}}/k_{\text{D}} = 1.3$.¹⁰⁹ Note that the results imply that proton transfer occurs so rapidly that there is no preferential contribution from any of the equilibrating isomeric deuterated isopropyl cations. Finally, it should be noted that less energetic electron impact or more exothermic CI yields, for the most part, results intermediates between these two extremes.

The gas phase solvolytic mechanism explains the results for *n*-butyl phenyl ether as well, and a potential energy curve is drawn in Fig. 18.¹¹² This figure has a lot in common with Fig. 6, except that the attractive forces are ion-dipole rather than ion-ion (and the C-O bond dissociation energies of the molecular ion reactants are much less than heterolytic BDE's of neutral reactants). The two dashed curves represent simple C-O bond cleavages for *n*-butyl (upper) and *sec*-butyl (lower) phenyl ether radical cations. The x-axis pertains only to these curves. The abscissa for the solid curve is the reaction coordinate for the gas phase solvolysis. The energy scale of the y-axis considers only the attraction between the ion and an *induced* electric dipole. Therefore the energy wells are really deeper than portrayed, since the neglected ion-permanent dipole attraction is large, especially for the ion-molecule complex between phenoxyl and *s*-Bu⁺. This is the first intermediate along the reaction coordinate, and it corresponds to species 13 (*vide supra* reaction 28) where $\text{M} = \text{C}_6\text{H}_5\text{O}^\cdot$. The energy barrier to proton transfer (which lies between the two intermediate ion-molecule complexes) is at least as high as shown (relative to the final products). The evidence for this is that $\text{C}_6\text{H}_5\text{OD}^{++}$ does not exchange hydrogens with olefins in ion-molecule collisions.⁷⁸ The height of the barrier in front of the first intermediate is based on experiments that the Cambridge group has performed using different leaving groups (*vide infra*). The well depth for the second intermediate on the solid curve is arbitrarily assigned, based on a close approach of $\text{C}_6\text{H}_5\text{OH}^+$ and C_4H_8 .

As the reaction proceeds from the *n*-butyl precursor along the solid curve, a *sec*-butyl cation is formed during dissociation of the C-O bond by migration of a β -hydrogen to form a methyl group. Complete dissociation to phenoxyl radical plus *sec*-C₄H₉⁺ is about 30-35 Kcal mol endothermic, and the first ion-molecule complex is formed. The remaining β -hydrogen scrambles rapidly with the two γ -hydrogens, as is well precededented from solution studies of *sec*-C₄H₉⁺,⁶⁸ and proton transfer provides a much lower exit channel than dissociation. The barriers to complete hydrogen randomization or isomerization to *tert*-butyl are too high for these to be competitive processes in the ion-molecule complex (i.e. with reference to reaction 28, $k_{\text{d}} \gg k_{\text{r}}$). Statistical calculations (based on a 1-butene:2-butene ratio of 1:1) are compared with mass spectrometric results in reaction 39. The small dis-

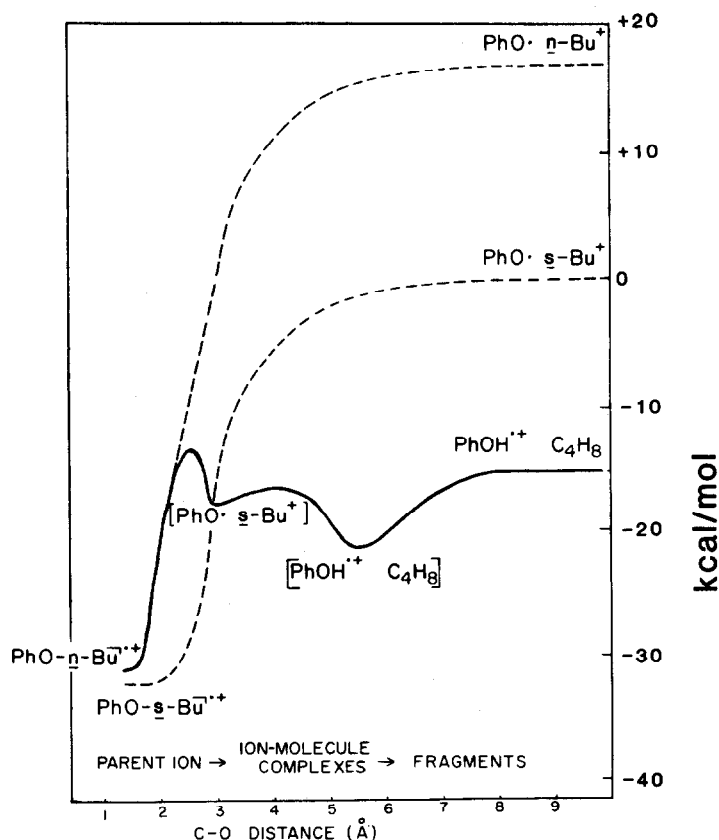


Fig. 18. Qualitative potential energy curve for gas phase solvolytic elimination from the molecular ion of *n*-butyl phenyl ether. The dashed curves represent simple C-O bond cleavages of the molecular ions of the *n*- and *sec*-butyl ethers, using a r^{-4} potential (and $\alpha = 10 \text{ Å}^3$) at distances $\geq 3 \text{ Å}$. The x-axis pertains to distances between centers of charge for the dashed curves. Well depths for ion-molecule complexes neglect the substantial contributions from ion-permanent dipole attraction.

crepancies between the statistical fractions of the observed proportions might be attributed to a contamination of the EBFlow product with 1-butene from nonionic sources (in which case the true isomer ratio from reaction 39 should be <1), incomplete equilibration of label in the complex (e.g. preferential deprotonation of some of the isomeric deuterated cations in the ion-molecule complex in reaction 41), or a low contribution from vicinal elimination from 16. These effects may be combined *ad lib*, and an example is given at the bottom of reaction 39. If 12% of the *sec*-butyl cations do not scramble at all in the complex, and 8% of the molecular ions give vicinal elimination (e.g. deprotonation of $\text{CH}_3\text{CH}_2\text{CH}_2\text{CH}_2^+$ before it isomerizes), the experimental proportions are almost exactly reproduced. The principal remaining question concerns the geometric isomer ratio of the 2-butenes. In the EBFlow study of *n*-butyl phenyl ether, the *cis*:*trans* ratio is essentially unity, while the *trans* isomer prepon-

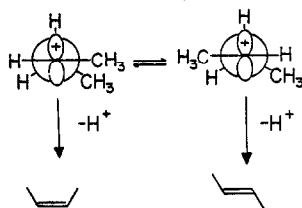
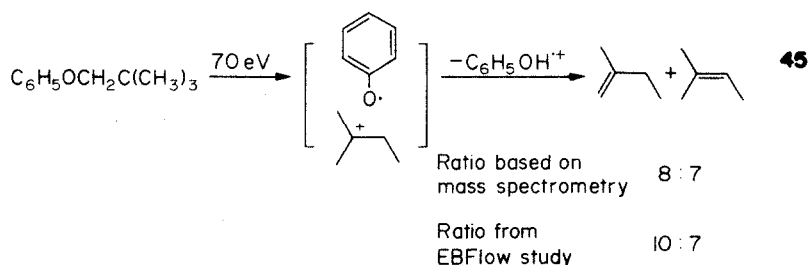


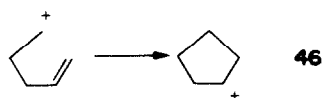
Fig. 19. Two conformers of *sec*-butyl cation (classical structures) and the corresponding olefins from their deprotonation.

derates in deprotonation of free $C_4H_9^+$ by diethyl ether (see Table 2). We offer no definitive explanation for this, but note that *sec*-butyl cation is a mixture of conformers, for which classical structures are drawn in Fig. 19. We speculate that the free cation is quenched in its equilibrium proportions by the gas phase deprotonation and that the equilibrium in the ion-molecule complex is perturbed by the presence of the neutral dipole.

The gas phase solvolytic mechanism explains many other published data. In the case of phenetole, the ethyl cation is so unstable that deprotonation competes with hydrogen randomization. The mechanism explains why the $C_6H_6O^{++}$ from phenyl ethers has the phenolic structure, since phenoxyl radical behaves as a base in what is virtually a bimolecular Brønsted acid-base reaction. Rather than detail further the merits of reaction 37, let us proceed to examine its predictions. An ion-molecule complex of phenoxy with *tert*-amyl cation should lead to a product distribution similar to that of reaction 33 (just as reaction 6 leads to a product distribution like reaction 32). We tested this by 70 eV EBFlow radiolysis of phenyl neopentyl ether and observed the isomer ratio reported in reaction 45, which is within experimental error of our expectation. Once again, we needed to run a control to test for competing reactions that might be contaminating our C_5H_{10} yield. From 70 eV mass spectra of $(CH_3)_3CCD_2OC_6H_5$ and of $(CD_3)_3CCH_2OC_6H_5$ we independently determined the isomer yield, and those data are also summarized in reaction 45. The two sets of results agree and firmly rule out conventional alternatives (which will not be discussed here).⁷⁸

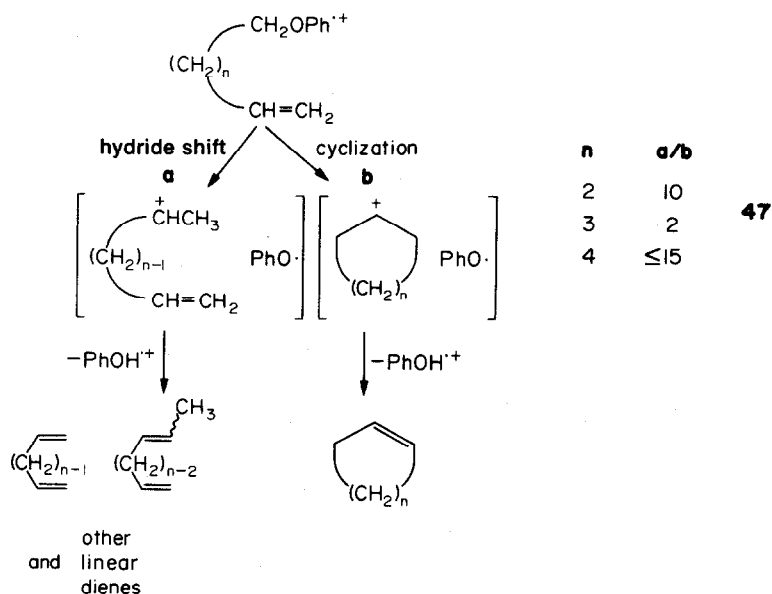


What use is gas phase solvolysis? It provides a regime for examining cations in the absence of solvent. For instance, reaction 46 has been classified as a “disfavoured” reaction because it was not reported for solvolysis conditions under which 6-member rings are easily formed from 5-hexenyl precursors.¹¹³ Gas phase solvolysis permitted us to assess the relative rates of the cyclizations shown in path **b** of reaction 47 as a function of chainlength n . We assumed that the rate of 1,2-hydride transfer, path **a** in the gas phase solvolysis, is the same for all chainlengths. We then measured the ratio of uncyclized products (path **a**) to cyclized products (path **b**) from 70 eV EBFlow radiolysis of the terminal phenoxylkenes. The ratio of path **a** to path **b** products as a function of n is tabulated in reaction 47.¹¹⁴

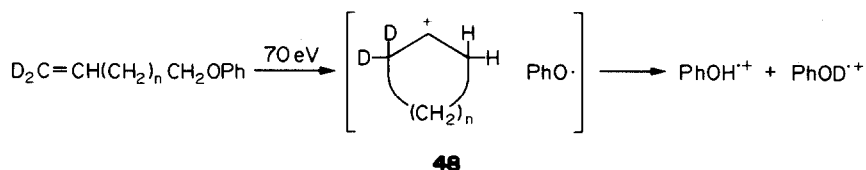


Once again, control studies are required to insure that the EBFlow products truly come from molecular ion decompositions. In this case, we examined the mass spectra of the terminally deuterated analogues shown in reaction 48. Cyclization leads to a cation in which D^+ can be transferred to the phenoxy as well as H^+ . For the reaction that forms a 5-member ring ($n = 2$), the ratio $C_6H_5OH^{++}:C_6H_5OD^{++}$ is about 15:1, as revealed by the high resolution mass spectra in Fig. 20. High resolution was required to distinguish the $C_6H_5OD^{++}$ ion from natural abundance ^{13}C -labelled $C_6H_5OH^{++}$. We need to divide this experimental ratio by the deuterium isotope effect to estimate the ratio of path **b** to path **a**. Estimating the value of k_H/k_D as 4/3 (the value for the gas phase solvolyses in reaction 39, 44 and 45), we get an **a/b** ratio of 11 from the mass spectrometric experiment. This is in close agreement with the ratio of 10 from the EBFlow experiment in reaction 47.

The mass spectrometric experiment for $n = 3$ is much less satisfactory because the cyclohexyl cation is well known to scramble hydrogens in solvolysis studies,¹¹⁵ and the mass spectrometric ratio $C_6H_5OH^{++}:C_6H_6OH^{++}$ is no greater than it is for the $n = 2$ case. However, there is an internal control in the EBFlow experiment for contamination by products of free $C_6H_{11}^+$ or 5-hexenyl radicals. As



discussed in reaction 31, free cyclohexyl cation rearranges to methylcyclopentyl cation which, if deprotonated by a strong enough base, gives methylenecyclopentene as well as 1-methylcyclopentene. Phenoxyl, however, is not as strong a base as methylenecyclopentane; therefore, deprotonation of methylcyclopentyl cation in the ion-molecule complex should yield only 1-methylcyclopentene. This is the result seen in the EBFlow experiment: the ratio of 1-methylcyclopentene to cyclohexene is 2:9, but no methylenecyclopentene is detected. Not only does this rule out free $\text{C}_6\text{H}_{11}^+$ cations (since the parent ether is a strong enough base to form methylenecyclopentane), it also rules out the intermediacy of $\text{H}_2\text{C}=\text{CHCH}_2\text{CH}_2\text{CH}_2\text{CH}_2^\cdot$ radicals, since these cyclize to form cyclopentylmethyl radicals¹¹⁵ and would also yield methylenecyclopentane if they intervened.



The 7-member ring cyclization ($n=4$) is harder to decipher. The $\text{C}_6\text{H}_5\text{OH}^+:\text{C}_6\text{H}_5\text{OH}^+$ ratio in the mass spectrum is about 50:1, but that must reflect hydrogen randomization in the ion-molecule complex, since cycloheptene constitutes a greater proportion than that in the EBFlow products. Path b may have a greater contribution than the value listed in reaction 47, since 1-methylcyclohexene is more than twice as abundant as cycloheptene in the EBFlow products and may represent structural isomerization of the cycloheptyl cation in the ion-molecule complex.

"Onium" ions

Gas phase solvolyses are prevalent in dissociations of oxonium ions, such as those shown in reaction 36. They also occur in hydrogen rearrangements, which were first studied by Djerassi and Fenselau and have been further investigated by the Cambridge group.¹¹⁷ The intermediate is a complex, like species 13 (*vide supra*, reaction 28), and the overall reaction is much the same as reaction 41, but with a different leaving group. As shown in reaction 49, the ion-molecule complex from an n -butyl precursor contains $\text{sec-C}_4\text{H}_9^+$ electrostatically bound to neutral $\text{CH}_3\text{CH}=\text{X}$, and proton transfer yields the observed $\text{CH}_3\text{CH}=\text{XH}^+$ ion. The isomer distribution in the expelled C_4H_8 is unknown, and no EBFlow Study has been performed, since high abundances of interfering ions (e.g. free C_4H_9^+ in the cases $\text{X}=\text{O}$ and $\text{X}=\text{S}$) would make the results difficult to interpret. Nevertheless, we can account for the experimental results if we assume (1) that $k_d \gg k_f$ (see reaction 28), (2) that one β -hydrogen shifts to the α -position and stays there, and (3) the remaining β -hydrogen scrambles with the two γ -hydrogens in the sec -butyl cation. The mass spectrometric results predict the following isomer ratios. If the 1-butene:2-butene ratio is 1:3, the

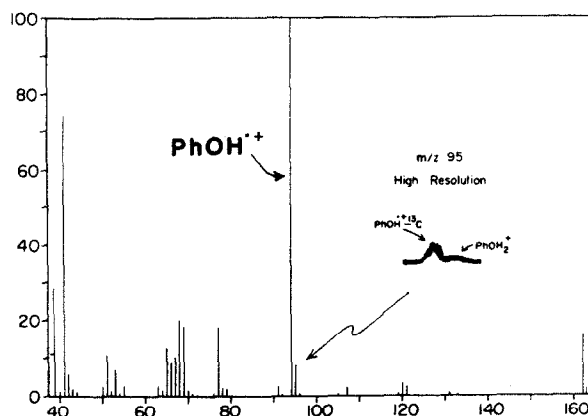
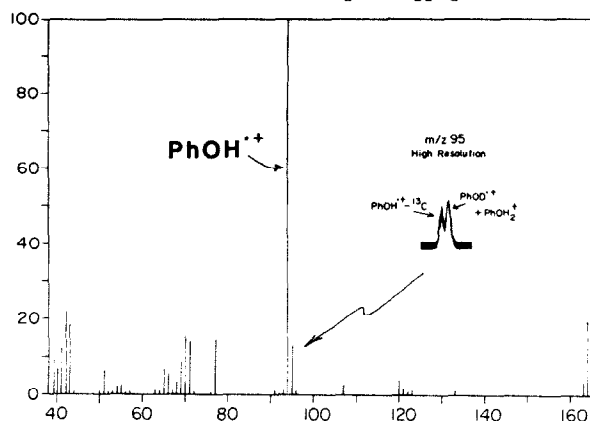
70 eV MASS SPECTRUM OF $\text{H}_2\text{C}=\text{CH}(\text{CH}_2)_2\text{CH}_2\text{OPh}$ 70 eV MASS SPECTRUM OF $\text{D}_2\text{C}=\text{CH}(\text{CH}_2)_2\text{CH}_2\text{OPh}$ 

Fig. 20. Electron impact mass spectra of 5-phenoxy-1-penten-5.

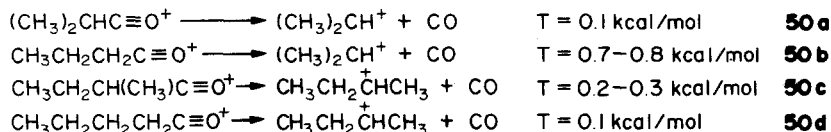
statistical proportions tabulated for $\text{X}=\text{O}$ come very close to the experimental results for nominal 14 eV electron impact. At 70 eV, the mass spectrometric results are virtually the same for $\text{X}=\text{O}$ and $\text{X}=\text{S}$, and the experimental proportions are closely approximated by a statistical calculation based on an isomer ratio of 2:3. Data for $\text{X}=\text{NCH}_3$ (not tabulated here) can be accommodated by supposing that more 1-butene is produced than 2-butene.

The Cambridge group has reported data from which the qualitative shape of the potential energy curve may be deduced, and we have drawn a version of this curve above in Fig. 18. Metastable ion techniques have been used to study appearance potentials and kinetic energy releases of ions that live

$\text{CH}_3\text{CH}=\text{XCH}_2^{\alpha}\text{CH}_2^{\beta}\text{CH}_2^{\gamma}\text{CH}_3^{\delta}$ \longrightarrow $\left[\text{CH}_3\text{CH}=\text{X} \right]$ $\xrightarrow{-\text{C}_4\text{H}_8}$ $\text{CH}_3\text{CH}=\text{XH}^+$	49			
	α	β	γ	δ
Obs'd from 70eV electron impact ($\text{X}=\text{O}$)	0.15	0.29	0.40	0.15
($\text{X}=\text{S}$)	0.16	0.31	0.36	0.15
Obs'd from 14eV electron impact ($\text{X}=\text{O}$)	0.10	0.32	0.50	0.09
Statistical, based on 1-butene:2-butene=1:3	0.08	0.29	0.50	0.12
Statistical, based on 1-butene:2-butene=2:3	0.13	0.27	0.40	0.20

1–100 μsec before decomposing. A comparison of the energetics of reactions 49 and 50 is revealing. From the appearance potential of the $(\text{CH}_3)_2\text{CHC}\equiv\text{O}^+ \rightarrow (\text{CH}_3)_2\text{CH}^+$ dissociation (50a), Williams, Bowen

and Stapleton deduce an activation energy of 29 Kcal mol for CO expulsion. The thermodynamic barrier is about 30 Kcal mol,^{2,8} so it seems reasonable to suppose that there is no reverse activation energy. The kinetic energy release is $T = 0.1$ Kcal mol. Using the estimate $T \geq 2E^*/N$, we conclude that the excess energy of the products (E^*) is no more than 1.5 Kcal mol.



The lower dashed curve in Fig. 21 depicts the potential energy profile for reaction 50a, for which the kinetic barrier is equal to the thermodynamic barrier. The thermodynamic threshold of the dissociation $\text{CH}_3\text{CH}_2\text{CH}_2\text{C}\equiv\text{O}^+ \rightarrow \text{CH}_3\text{CH}_2\text{CH}_2^+ + \text{CO}$ is 50 Kcal mol,^{2,119} as shown by the upper dashed curve in Fig. 21. Experimentally, the activation barrier for appearance of C_3H_7^+ from $\text{CH}_3\text{CH}_2\text{CH}_2\text{C}\equiv\text{O}^+$ is much

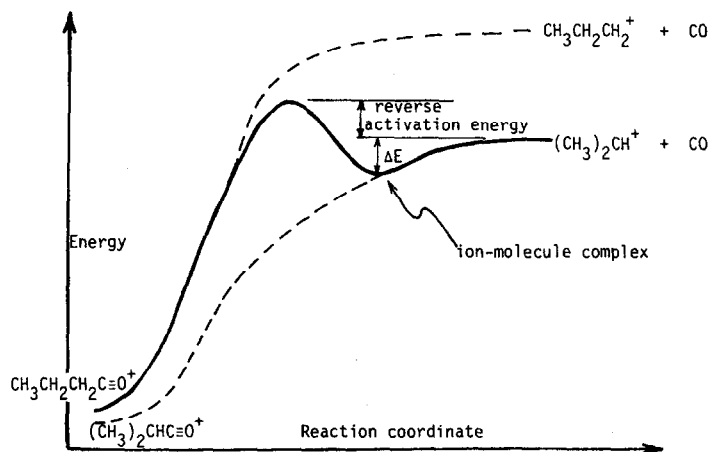
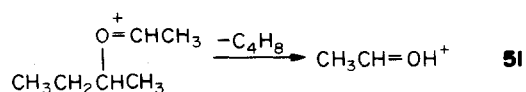


Fig. 21. Potential energy curve for dissociation of *n*-butyryl cation to isopropyl cation plus carbon monoxide. Dashed curves represent simple bond cleavages of the isobutyryl (lower) and *n*-butyryl (upper) cations.

lower, 38 Kcal mol. Clearly, reaction 50b, dissociation with concomitant isomerization, must be taking place. The thermodynamic threshold for 50b ought to be less than for 50a, since the linear acylium ion has a higher heat of formation than its branched isomer.² But the experimental activation energy is greater. Moreover, the kinetic energy release for 50b is $T = 0.7-0.8$ Kcal mol. Evidently, reaction 50b has a reverse activation barrier, and the solid curve in reaction 21 represents the energy along the reaction coordinate. The methylene-carbonyl bond of the linear acylium ion stretches along the thermodynamic curve until its energy exceeds that of free $(\text{CH}_3)_2\text{CH}^+$ plus CO. Then isomerization takes place and products are formed with excess energy.

An alternative interpretation should also be considered. Perhaps the potential energy curves for both reactions are monotonic, and there is no reverse activation energy in either case. Because 50b requires a much more organized transition state, its preexponential (or frequency) factor should be lower than for 50a. The ions decomposing on the 1–100 μsec timescale may need to be much more energetic for 50b than for 50a simply to counterbalance the difference in frequency factors (even though the *potential* energy barrier for 50b could be lower than for 50a). This is a well known phenomenon (called a kinetic shift⁹⁰), and it cannot be completely ruled out. But if it is the preferable explanation, then Fig. 21 still applies, but with *free energy* as the ordinate instead of potential energy. We choose potential energy here, but the same kinetic descriptions, *mutatis mutandis*, pertain even if the data are interpreted in terms of kinetic shifts.



In reactions 50c and 50d, the same difference in kinetic energy releases is reported, and the same explanation is offered. Dissociation of both valeryl cations yields *sec*-C₄H₉⁺ plus CO, and the kinetic energy release is greater for the linear than for the branched isomer. Now, consider reaction 49 (X = O) vs reaction 51. The kinetic energy releases in these two cases are the same (1.0 vs 0.9 Kcal mol) within experimental uncertainty (± 0.15 Kcal mol).¹²⁰ What has happened to the energy difference? Figure 22 depicts a potential energy curve that explains this result: the thermodynamic barrier (ΔH) to separating the products is higher than the kinetic barrier (E_0) for isomerization. This inference is confirmed by cation-molecule reactions described in Part 3: protonated acetaldehyde exchanges hydrogen with neutral C₄H₈ in bimolecular collisions. This exchange reaction (step e in reaction 29) corresponds to reactants entering the solid curve in Fig. 22 from the right hand side.

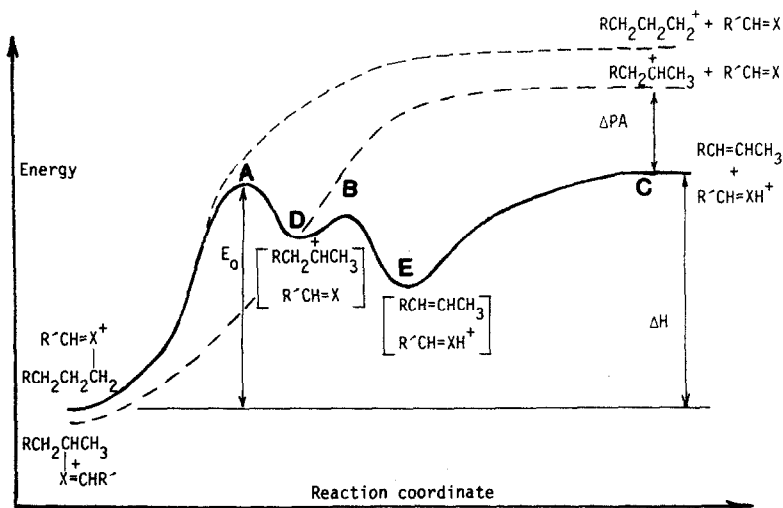


Fig. 22. Potential energy curve for decomposition of *n*-alkyl oxonium ion to a 2-alkene plus an O-protonated aldehyde. Dashed curves represent simple bond cleavages of the *sec*-alkyl (lower) and the *n*-alkyl oxonium ions. The solid curve represents potential energy along the reaction coordinate via ion-molecule complexes D and E.

The experimental evidence (particularly for reaction 50) shows that the ion-molecule complex containing *sec*-C₄H₉⁺ and the neutral leaving group is a *bonafide* intermediate between the *n*-butyl precursor and the dissociation products. In fact, there are *two* intermediate ion molecule complexes, D and E, in reaction 51. The transition state between them, B, corresponds to the barrier to shifting a proton (*vide supra*, Fig. 5), which pertains to ion decompositions as well as to ion-molecule reactions.¹²¹ The presence of this additional barrier (for both reactions 49 and 51) suggests that these reactions will have lower frequency factors than dissociations like reactions 50a-d. The larger values of T are taken, therefore, to represent a kinetic shift rather than any reverse activation barrier.

There are thus three energy barriers in Fig. 22 (labelled A, B and C). When C, the thermodynamic barrier (ΔH) is highest, the value of T should be the same for both precursors (as in reactions 49 and 51, where R = R' = CH₃ and X = O). When A, the barrier for isomerization (E_0) is highest, different values of T are expected for different precursors of a given ion-molecule complex. This situation (where isomerization is the rate-determining step) occurs, for example, when the leaving group is a very strong base. When R' = H and X = NH, the proton affinity of the leaving group (H₂C=NH) is > 200 Kcal mol.

For R = H, the values of T for linear [CH₃CH₂CH₂NH=CH₂] and branched [(CH₃)₂CHNH=CH₂] precursors are 2 and 1.2 Kcal mol, respectively. For R = CH₃, the values for linear (*n*-butyl) and branched (*sec*-butyl) precursors are 3 and 1.7 Kcal mol, respectively.¹²² We surmise that the choice whether A or C corresponds to the rate-determining step is largely a function ΔPA (represented in Fig. 22), the difference between the proton affinity of the leaving group and that of the olefin. As ΔPA decreases, ΔH increases relative to E_0 , and the T values become closer to one another. When the leaving group is acetone (proton affinity = 197 Kcal mol), the T values for (CH₃)₂C=OH⁺ production from linear [CH₃CH₂CH₂Ö=C(CH₃)₂] and branched [(CH₃)₂CHO⁺=C(CH₃)₂] precursors are 0.5 and 0.3 Kcal mol, respectively.¹²³ Here, ΔPA is 12 Kcal mol, and we expect that for smaller values of ΔPA the T values

become virtually the same. In reaction 51, ΔPA is only 4 Kcal mol, and T has the same value as in reaction 49. We note that ΔPA is 13 Kcal mol for reaction 41. Hence, Fig. 18 depicts the isomerization barrier as being higher than the thermodynamic barrier.

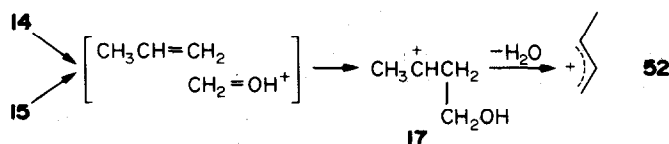


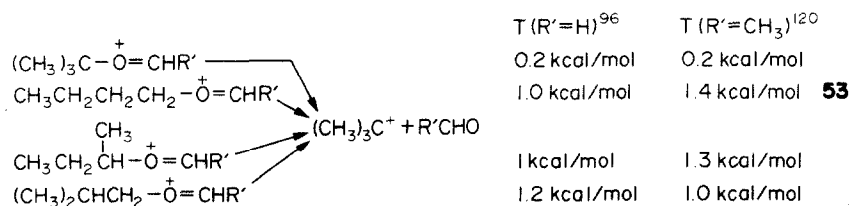
Figure 22 depicts two intermediate ion-molecule complexes, D and E. So far, discussion has focussed on their interconversion (as represented, for example, by the rate constants k_c and k_d in reaction 28) and the simple dissociation of E. There are other reactions that can occur in E, as well. Bowen and Williams have explained the loss of H_2O from ions 14 and 15 ($R = R' = \text{H}$) in terms of the isomerization shown in reaction 52.¹²⁰ The net reaction to form methylallyl cation about 5 times more prevalent than expulsion of CH_2O , and the proportions of these two reactions are the same for both the linear and branched precursors. Formation of a common ion-molecule complex explains this result. Gaseous CH_2O is at least 6 Kcal mol less basic than $\text{CH}_3\text{CH}=\text{CH}_2$, so the ion-molecule complex shown in reaction 52 does not simply dissociate. Electrophilic addition of protonated aldehydes to double bonds is well known (e.g. the Prins reaction), and it occurs in reaction 52 to form ion 17, whose heat of formation is estimated from ΔH_f of the corresponding radical^{7,19} and the ionization potential of *sec*-butyl radical¹²⁷ to be only a few Kcal mol higher than that of 14 or 15. Expulsion of H_2O from 17 is nearly thermoneutral, yet there is a much larger kinetic energy release for H_2O expulsion ($T = 0.8$ Kcal mol for both 14 and 15) than there is for the much more endothermic (yet competitive) expulsion of CH_2O ($T = 0.2$ Kcal mol from both precursors). From appearance potential measurements made by Bowen and Williams, the activation energy for loss of water from 17 is about 15–20 Kcal mol,⁹⁷ and the kinetic energy T is equal (within experimental uncertainty) to $2E^*/N$. It is likely that 17, once formed, expels H_2O via a conventional mechanism through a cyclic transition state, though the geometry is unknown. We note, however, the similarity between a 4-center transition state and transition state B in Fig. 3 above. If ion-dipole forces are included in a Tschuikow-Roux type calculation for thermoneutral expulsion of H_2O from 17,⁹ a 4-center transition state (although formally symmetry-forbidden) does not appear out of line with the experimental results.

Leaving group effects

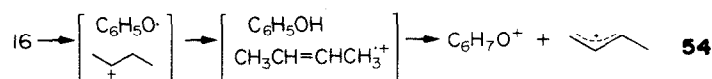
Three important characteristics of the leaving group influence the outcome of a gas phase solvolysis: its proton affinity (as treated in the previous section), its electrical dipole moment, and its chemical reactivity. Effects of a permanent dipole moment have been described in Part 3. In studies of bimolecular gas phase hydrogen exchange, Ausloos and Lias find that deuterated ions, AD^+ , exchange label with a variety of neutrals, BH (C_6H_6 , CH_3OH , AsH_3 , or H_2S), all of which are less basic than A. The net reaction $\text{AD}^+ + \text{BH} \rightarrow \text{A} + \text{BHD}^+$ does not occur, since they are all >3 Kcal mol endothermic. For A = acetaldehyde or for A = acetonitrile, exchange efficiency decreases as the endothermicity of the Brønsted acid-base reaction increases. Since acetonitrile is a stronger base than acetaldehyde, $\text{CD}_3\text{C}\equiv\text{ND}^+$ might be expected to exchange less efficiently with BH than does $\text{CD}_3\text{CD}=\text{OD}^+$. But, to the contrary, it is roughly 2 to 3 times *more* efficient. Why? The larger dipole moment of acetonitrile means that the $[\text{A} \cdots \text{BHD}^+]$ complex is more tightly bound. That is, the increased attraction between the ion and the permanent dipole outweighs the difference in gas phase basicities.

In the same fashion, as mentioned in the discussion of reaction 28, the ratio of rate constants k_d/k_f is strongly influenced by the dipole moment of the leaving group M. A similar effect is to be found in contrasting reactions 50c and d with reactions 53 below. When the leaving group is CO, the well depth represented by ΔE in Fig. 21 is small because of the small permanent dipole moment (0.12D) and molecular polarizability of CO. When the leaving group is CH_2O ($\mu = 2.3\text{D}$), the well is much deeper, $\Delta E \approx 18$ Kcal mol for a point charge 3 Å away from the center of charge of CH_2O .¹²³ An ion-molecule complex of C_4H_9^+ with formaldehyde therefore contains enough energy to surmount the energy barrier for skeletal rearrangement of linear cations to the most stable *tert*-butyl structure. Proof that the ion-molecule complex lives long enough for this to happen is seen in the IKE spectra of the ions in reaction 53. The *tert*-butyl precursor has a small kinetic energy release, while the other three isomers

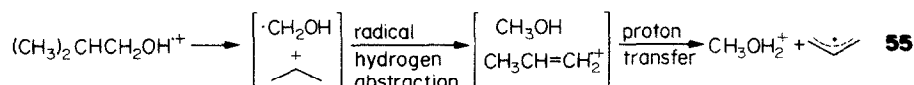
have larger values of T . It is significant that T for the *sec*-butyl precursor is no smaller than for the other two. This implies that the excess energy of the products in all three cases comes from surmounting the energy barrier for isomerization to *tert*-butyl in the ion-molecule complex.



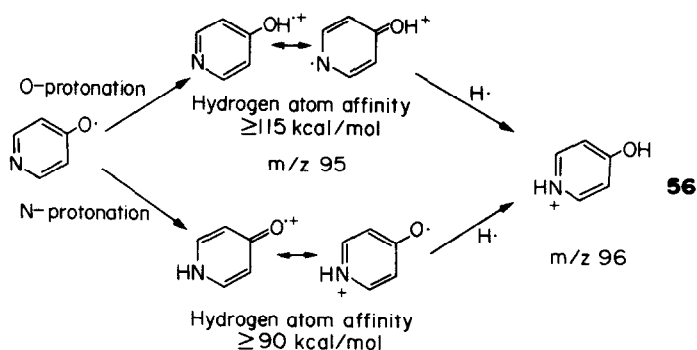
Does skeletal rearrangement compete with deprotonation when the leaving group is both a good base and a strong dipole? When the leaving group is CH_3CHO , *t*-butyl cation should not be deprotonated, since acetaldehyde is a weaker base than isobutene by 7 Kcal mol⁻²⁸ (that is why we infer only linear C_4H_8 products in reaction 49). But metastable peak widths for the dissociation $\text{C}_4\text{H}_9\dot{\text{O}}=\text{CHCH}_3 \rightarrow \text{C}_4\text{H}_9^+$ (reaction 53, where $\text{R}' = \text{CH}_3$) indicate that isomerization does compete with deprotonation on the timescale of microseconds. But when the leaving group is much more basic, there is evidence against isomerization to *tert*-butyl. Both phenoxy radical and $\text{CH}_3\text{CH}=\text{NCH}_3$ are stronger bases than isobutene, yet negligible yields of isobutene are recovered from EBFlow radiolysis of *n*-butyl phenyl ether (linear C_4H_8 : isobutene ≥ 40).⁷³ The low proportion of δ -hydrogen transfer (0.17) in reaction 49 when $\text{X} = \text{NCH}_3$ also argues against extensive skeletal rearrangement, since that would have led to complete hydrogen randomization and a δ -contribution of 1/3.¹¹⁷ Thus, increasing ΔE and increasing ΔPA have opposite effects on the ratio k_d/k_t , just as would have been predicted from the NBS group's study of reactions 28 and 29.^{67,69}



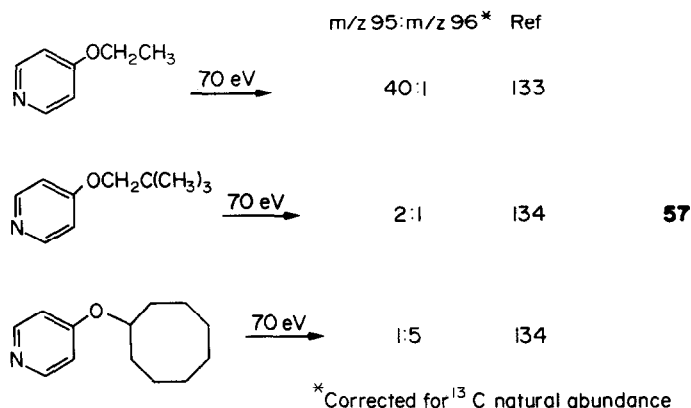
The third characteristic of the leaving group is its chemical reactivity. We shall focus on the consequences of having radical leaving groups in molecular ion decompositions. Hydrogen atom abstraction can occur, though with a much lower likelihood than a competing exothermic proton transfer. This is to be expected, for, as discussed in Part 2, atom transfers generally have higher activation barriers than proton transfers. In decompositions of ion 16, the sequence of steps shown in reaction 54 is possible. The dissociation energy of a methylene C-H bond in *sec*-butyl cation is 80 Kcal mol⁻¹,^{2,67} same as the O-H bond dissociation energy of phenol. Therefore the first step of reaction 54 is thermoneutral. The second step is about 10 Kcal mol exothermic, since the proton affinity of methylallyl radical is 188 Kcal mol.^{2,21} Kwong and Winnik searched for a m/z 95 ion from *n*-butyl phenyl ether and concluded that it occurs, but that the ratio m/z 94: m/z 95 is approximately 100:1.¹²⁵ Their estimate was based on subtracting the theoretical ¹³C contribution to m/z 95 from the observed intensity, and we have confirmed it by examining the high resolution mass spectra of several alkyl phenyl ethers, for instance the upper spectrum shown in Fig. 20.



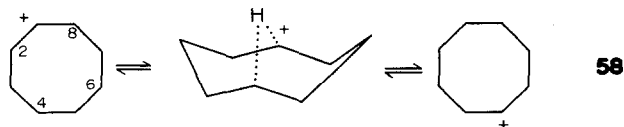
This same pathway has been reported by Bowen and Williams for decomposition of isobutyl alcohol, reaction 55.¹²⁶ Cleavage of a C-O ought to give $\text{CH}_3\dot{\text{C}}\text{HCH}_3$ plus HOCH_2^\cdot , in obedience to Stevenson's rule,³⁰ since the ionization potential of HOCH_2^\cdot is at least 3 Kcal mol greater than that of $(\text{CH}_3)_2\text{C}^\cdot$.^{8,128} If these two fragments do not have enough energy to separate, an ion-molecule complex is formed, in which a methyl hydrogen (BDE = 84 Kcal mol)² of the isopropyl cation is abstracted by the radical. After this exothermic step, subsequent proton transfer from $\text{CH}_3\text{CH}=\text{CH}_2^+$ to CH_3OH (PA = 185 Kcal mol⁻²⁸) yields an allyl radical (PA = 178 Kcal mol⁻²), liberating enough energy to dissociate the ion-molecule complex.



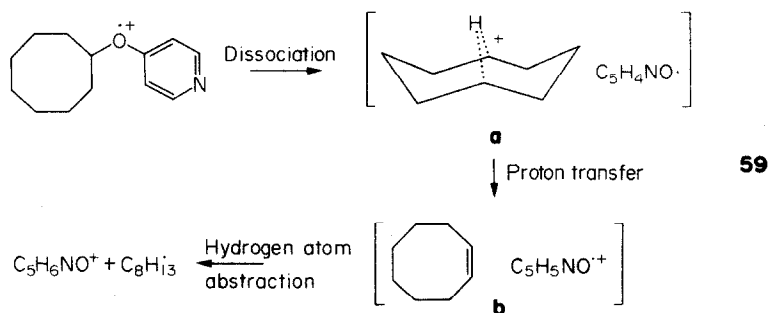
Reactions 54 and 55 are examples of double hydrogen rearrangements, of which there are many other instances in the literature (though they need not proceed via gas phase solvolyses¹²⁶). Radical hydrogen abstraction is followed by proton transfer in the cases above. This must be the order of the steps, especially for reaction 54, since $\text{C}_6\text{H}_5\text{OH}^{+\cdot}$ does not have a hydrogen atom affinity (80 Kcal/mol) large enough to pull hydrogens off of most neutral hydrocarbons. After the proton transfer step, hydrogen abstraction, even when it is thermoneutral, competes poorly with dissociation of the olefin- $\text{C}_6\text{H}_5\text{OH}^{+\cdot}$ complex, as is the case when the olefin is 1,4-pentadiene [the BDE of $(\text{CH}_2=\text{CH})_2\text{CH}-\text{H}$ is 80 Kcal/mol²¹]. Although this hydrocarbon represents 25% of the C_5H_8 yield from 70 eV EBFlow radiolysis of $\text{C}_6\text{H}_5\text{OCH}_2(\text{CH}_2)_2\text{CH}=\text{CH}_2$,¹¹⁴ the abundance of $\text{C}_6\text{H}_7\text{O}^+$ in the mass spectrum at the top of Fig. 20 is no greater (relative to $\text{C}_6\text{H}_5\text{OH}^{+\cdot}$) than it is in the mass spectrum of *n*-butyl phenyl ether.



Many gas phase solvolyses pass through two energy minima, as represented in Figs. 18 and 22. The first ion-molecule complex converts to the second by a proton transfer step, and the second complex then dissociates. Why does this second complex (e.g. **E** in Fig. 22) not react further before dissociating? Two alternative explanations may be offered: (1) the ion-molecule complexes that follow proton transfer steps are too weakly bound to be reactive, or (2) no exothermic reaction channel has been available for the second intermediate in the cases hitherto studied. Let us consider the first explanation. Reactions 54 and 55 pass through sequential, reactive ion-molecule complexes, but proton transfer is not the first step in either case, and in both cases proton transfer is followed by dissociation. Also, all of the ion-molecule complexes drawn contain neutral partners ($\text{C}_6\text{H}_5\text{O}$, $\text{C}_6\text{H}_5\text{OH}$, HOCH_2 , HOCH_3) that have large permanent dipole moments. In Fig. 18, the neutral partner in the second energy minimum is a nonpolar olefin. Perhaps the attraction between an ion and an *induced* dipole is not adequate to hold a complex together long enough for reaction to occur.



We have tested this possibility and find that complexes between ions and neutral olefins are, in fact, strongly enough bound to be reactive. Once an exothermic reaction channel becomes available, proton transfer can be followed by atom abstraction before the ion-molecule complex dissociates. We have demonstrated this by using a leaving group whose hydrogen atom affinity (HA) increases when it is protonated, namely the 4-pyridyloxy radical, shown in reaction 56. We assume that the O-H bond dissociation energy of 4-hydroxypyridine is no greater than that of phenol. But when 4-hydroxypyridine is ionized, the HA of the molecular ion is quite large. Since pertinent data for computing HA's of hydroxypyridines are not available, we shall use estimates for HA's of alkylated analogues. First, let us consider 4-methoxypyridine, whose proton affinity is 226.6 Kcal mol.²⁹ If we assume that its adiabatic ionization potential is no lower than 15 Kcal mol below the reported first *vertical* IP of 4-ethoxypyridine (9.25 eV,¹²⁹ which is already lower than the IP reported from electron impact mass spectrometry¹³⁰), then the HA of 4-alkoxypyridines is >110 Kcal mol. Since the HA of phenol is virtually the same as that of anisole, we choose this value for the O-protonated tautomer in reaction 56, as well. Other tautomers have lower HA's. If the radical is protonated on nitrogen, we estimate its HA as follows: From the measured gas phase basicity of N-methyl-4-pyridone,¹³¹ its proton affinity is 229.6 Kcal mol. If we again assume that the adiabatic IP is no lower than 15 Kcal mol below the reported first vertical IP (8.20 eV,¹²⁹ which is already lower than the IP from electron impact mass spectrometry¹³⁰), then the HA of the molecular ion of N-methyl-4-pyridone is >90 Kcal mol. Regardless of which tautomer is produced by protonation of 4-pyridyloxy radical, the resulting radical cation has a large enough HA to abstract allylic hydrogens exothermically.



In solution, alkyl 4-pyridyl ethers undergo facile elimination when they are N-methylated, and olefin products are recovered.¹³² In gas phase solvolyses of the molecular ions, the olefin is produced in an ion-molecule complex with $\text{C}_5\text{H}_5\text{NO}^+$. If the olefin has no easily abstractable hydrogens (e.g. ethylene), the ion-molecule complex simply dissociates to give m/z 95.¹³³ But if the olefin contains allylic hydrogens, the radical cation abstracts one to yield a protonated hydroxypyridine (m/z 96) and a neutral hydrocarbon radical. The proportions of atom abstraction vs dissociation of this ion-molecule complex are indicated by the ion abundance ratios in reaction 57 for three alkyl 4-pyridyl ethers. In these mass spectra, there are large peaks corresponding to further loss of HCN from the daughter ions. Hence, the m/z 95: m/z 96 ratio is not an accurate measure of the competition between reaction vs dissociation of the second ion-molecule complex. Furthermore, the peak intensity ratio from the neopentyl ether fluctuates with conditions in the AEI-MS 902 on which the 70 eV mass spectra were recorded. We attribute this to a fast second-order ion-molecule reaction, and the value tabulated is the maximum observed, at what we believe to be the lowest accessible pressure.¹³⁴ We decided to study the cyclooctyl ether more carefully using low energy ionization conditions in a photoionization mass spectrometer (PIMS).

The cyclooctyl ether was chosen for scrutiny because the cyclooctyl cation is known to have a non-classical structure, based on solvolysis^{135,136} and NMR¹³⁷ studies. The intervention of this bridged structure, shown in reaction 58, leads to a characteristic interconversion of ring positions. Equivalence of position 2 and 8 with positions 4 and 6 serves as a diagnostic for intermediacy of the ion-molecule complex as shown in reaction 59. The PIMS instrument at UCR was designed to look at low sample pressures (10^{-8} – 10^{-7} Torr), and signal averaging with a multichannel analyzer allows peak intensity ratios to be measured precisely.¹³⁸ An oxygen resonance lamp with calcium fluoride windows provides an intense source of 9.5 eV photons (lines at 1302, 1305 and 1306 Å).¹³⁹ PIMS of several deuterated analogues have been examined, and the most important spectra are shown in Fig. 23. No daughter ions below m/z 96 are

seen for the undeuterated compound, indicating that ion-molecule complex **b** reacts instead of dissociating at this low ionizing energy. Two different tetradeuterio analogues give virtually the same $d_0:d_1:d_2$ ratios (m/z 96: m/z 97: m/z 98) in the protonated hydroxypyridene daughter ions. A kinetic analysis of these data and examination of other deuterated analogues show that these results cannot be rationalized by invoking complete randomization of all the hydrogens in the 8-membered ring. Reaction 59 therefore accurately represents the proper sequence of ion-molecule complexes.¹⁴⁰

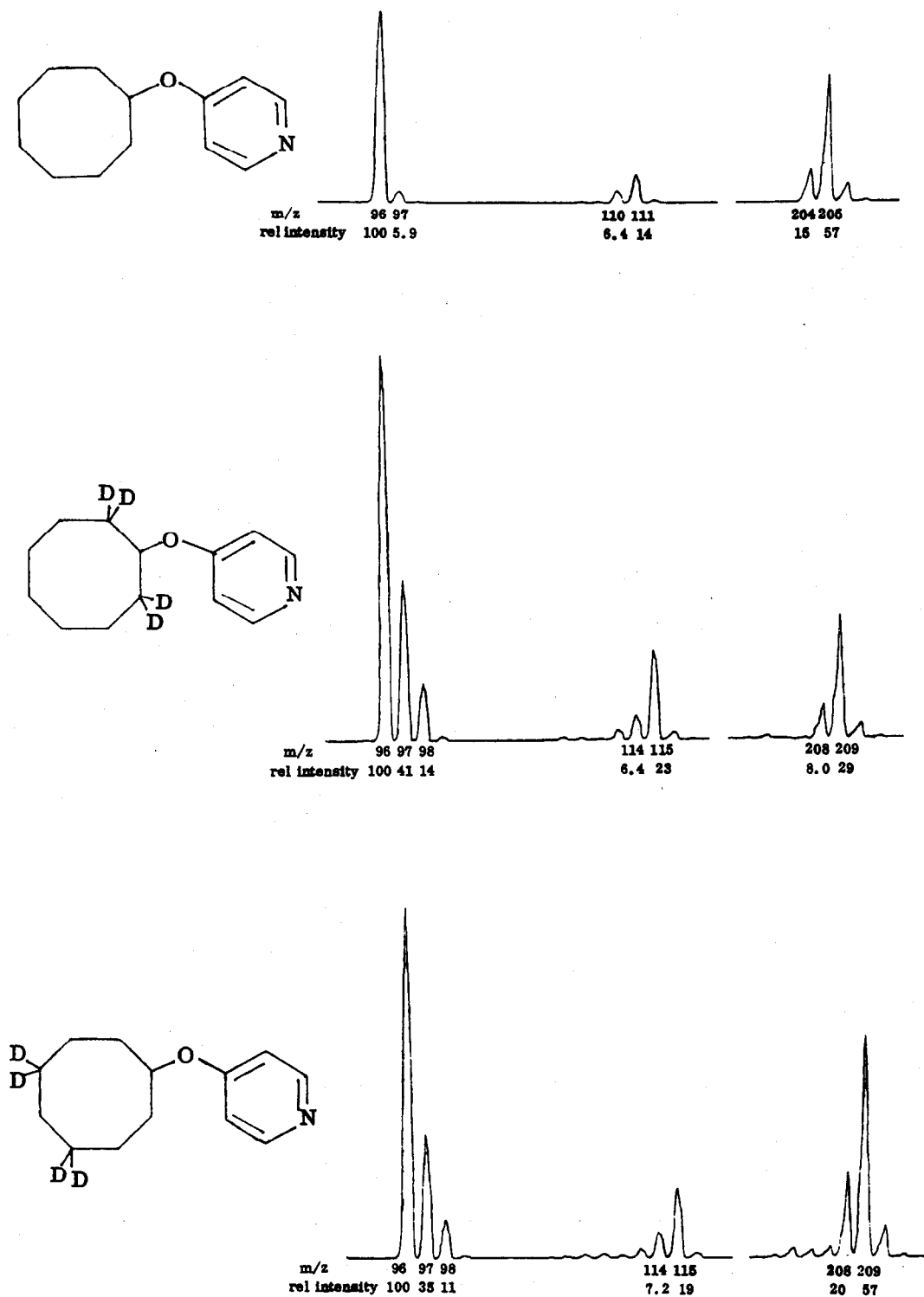
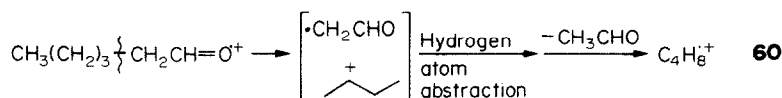


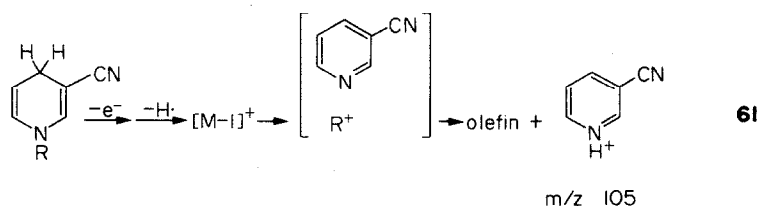
Fig. 23. 130 nm photoionization mass spectra of cyclooctyl 4-pyridyl ether and two tetradeuterated analogues.¹⁴⁰

Prospects

It is now possible to predict the outcome of gas phase reactions from solvolysis experiments. Our study of cyclooctyl 4-pyridyl ether, for instance, represents a test of this, and expectations based on Refs. 135 and 136 are borne out in Fig. 23. The gas phase solvolytic mechanism has also served to unify a large body of seemingly disparate data. The extensive literature on aryl alkyl ether and "onium" ions has been formed into a coherent whole by this mechanism, and some measure of predictability has been achieved.



The basic postulate in predicting gas phase solvolyses is that the weakest bond in the parent ion breaks to form an ion-molecule complex. In determining which bond is weakest, the product ion should be considered to rearrange via low-barrier reactions (e.g. by hydride or methyl shift or by cyclization) to the most stable accessible structure. High barrier isomerizations (e.g. *sec*-butyl \rightarrow *tert*-butyl) cannot, in general, be considered. In this fashion, we interpret the fragmentation shown to the left in reaction 34, which produces the base peak (30% Σ)⁸⁵ at 12 eV. The weakest bond in the hexanal radical cation is the β - γ carbon-carbon bond as represented in reaction 60. The heat of formation of $\cdot\text{CH}_2\text{CHO}$ is 2 Kcal/mol, based on the heat of formation of the enolate anion of acetaldehyde⁵⁴ and the threshold for photodetachment of an electron.¹⁴¹ (Because the heat of formation of $\cdot\text{CHO}$ is at least 5 Kcal/mol greater,¹⁴² the α - β bond is no weaker than the β - γ bond.) After the ion-molecule complex shown in reaction 60 is formed, the $\cdot\text{CH}_2\text{CHO}$ can exothermically abstract a methylene hydrogen from the *sec*-butyl cation. Hence, the neutral products from the deuterated analogue in reaction 34 ought to have the structures shown. The mechanism is dissociative, bearing little resemblance to that of the competing McLafferty rearrangement, and the pathway represented by reaction 35 can be discarded. When hexanal is ionized by nominal 15 eV electron impact, hydrogen transfer from positions 3-6⁸⁵ occurs in nearly the same proportions as from α - δ positions of the oxonium ion (at 14 eV) tabulated in reaction 49. We predict, then, that roughly one-fifth of the C_4H_8^+ is initially formed with the 1-butene structure. This is thermodynamically plausible, since abstraction of a methyl hydrogen from *sec*-butyl cation by $\cdot\text{CH}_2\text{CHO}$ is close to thermoneutral.



Dissociative mechanisms now appear preferable to cyclic transition states that have been inferred in other previously published studies. We shall discuss only one further example here. In 1968, Wang and Thornton reported that the $m/z \ 105$ fragment from the 3-cyanodihydropyridines in reaction 61 does *not* come from expulsion of R^\cdot . Instead, a ring hydrogen atom is lost first, followed by a neutral olefin, as reaction 61 depicts.¹⁴³ This was demonstrated by the production of $m/z \ 106$ in addition to $m/z \ 105$ when $\text{R} = \text{CH}_2(\text{CH}_2)_n\text{CD}_3$ for $n = 0-2$. Our present understanding leads us to suspect that hydrogen transfer from every chain position would have been observed had other deuterated analogues been examined for $\text{R} = n$ -propyl or n -butyl. Olefin loss from the $[\text{M}-1]^+$ ion very probably proceeds via the gas phase solvolytic elimination shown, and quantitative conclusions previously presented (especially isotope effects) should be reassessed in line with our re-interpretation.

Continuing investigations of gas phase ion chemistry can be expected to bring deeper insight into how the presence of solvent affects the course of a reaction. Many of the tools of gas phase chemistry allow a direct comparison (such as in Table 2 above), while others (such as FIK and kinetic energy release studies) allow a more detailed examination of kinetics than is possible in solution. The wealth of quantitative information available from new methods means that we can expect to be able to define

chemical mechanisms more precisely in terms of kinetic parameters. In the past, many organic chemists have viewed mass spectrometry as a separate mechanistic regime, and there has been a tendency to regard molecular ion fragmentations as pertaining only to the chemistry of radical cations. The purpose of this report has been to show a more fundamental connection between chemistry in the mass spectrometer and reactions in solution. Recognition of the mechanistic continuity between liquid and gas phase reactions can serve, in future, to increase our understanding of both realms.

REFERENCES

- ¹A. Mandl, in *Alkali Halide Vapors: Structure, Spectra and Reaction Dynamics* (Edited by Davidovits and D. L. McFadden), p. 389. Academic Press, New York (1979).
- ²Unless otherwise stated, ionization potentials and ion heats of formation are from the NBS compilation of H. M. Rosenstock, K. Draxl, B. W. Steiner and J. T. Herron, *Energetics of Gaseous Ions, J. Phys. Chem. Ref. Data* **6**, Suppl. 1 (1977).
- ³L. H. Jones and R. R. Ryan, *J. Mol. Struct.* **46**, 35 (1978).
- ⁴L. H. Jones, L. B. Asprey and R. R. Ryan, *J. Chem. Phys.* **47**, 3371 (1967).
- ⁵A. Maccoll, *Chem. Rev.* **69**, 33–60 (1969).
- ⁶A. Maccoll, in *Theoretical Organic Chemistry*, p. 230, Butterworths, London (1958).
- ⁷W. von E. Doering, *Proc. Nat. Acad. Sci. U.S.A.* **78**, 5279 (1981).
- ⁸F. A. Houle and J. L. Beauchamp, *J. Am. Chem. Soc.* **101**, 4067 (1979).
- ⁹E. Tschuikow-Roux and K. R. Maltman, *Int. J. Chem. Kinet.* **7**, 363 (1975).
- ¹⁰C. J. Harding, A. Maccoll and R. A. Ross, *J. Chem. Soc. Chem. Comm.* 289 (1967).
- ¹¹H. Kwart and M. T. Waroblak, *J. Am. Chem. Soc.* **89**, 7145 (1967).
- ¹²G. Chuchani, Z. Martin and M. Alonso, *Int. J. Chem. Kinet.* **9**, 819 (1977).
- ¹³A. Maccoll, M. N. Mruzek and M. A. Baldwin, *J. Chem. Soc. Faraday I* **76**, 838 (1980).
- ¹⁴J. Hasse, H.-D. Kamphusmann and W. Zeil, *Z. Phys. Chem. Neue Folge* **55**, 225 (1967).
- ¹⁵K. R. Maltman, E. Tschuikow-Roux and K.-H. Jung, *J. Phys. Chem.* **78**, 1035 (1974).
- ¹⁶G. Chuchani, I. Martin, G. Martin and D. B. Bigley, *Int. J. Chem. Kinet.* **110**, 109 (1979), and Refs. contained therein.
- ¹⁷G. Chuchani, I. Martin, M. E. Alonso and P. Jano, *Ibid.* **13**, 1–6 (1981), and Refs. contained therein.
- ¹⁸S. V. Levanova, R. M. Rodova, A. M. Rozhov and L. A. Shetsova, *Russ. J. Phys. Chem.* **48**, 736–737 (1974).
- ¹⁹Except as otherwise noted, heats of formation and bond dissociation energies are taken from J. C. Cox and G. Pilcher, *Thermochemistry of Organic and Organometallic Compounds*, Academic Press, New York (1970), or are estimated from S. W. Benson, *Thermochemical Kinetics*, 2nd Edn, Wiley, Interscience, New York (1976).
- ²⁰J. H. Davis, W. A. Goddard III and R. G. Bergman, *J. Am. Chem. Soc.* **99**, 2427 (1977).
- ²¹D. M. Golden and S. W. Benson, *Chem. Rev.* **69**, 125 (1969).
- ²²A. B. Trenwith, *Trans. Faraday Soc.* **66**, 2805 (1970).
- ²³R. L. Failes, Y. M. A. Mollah and J. S. Shapiro, *Int. J. Chem. Kinet.* **11**, 1271 (1979); **13**, 7 (1981).
- ²⁴W. J. Marinelli and T. H. Morton, *J. Am. Chem. Soc.* **100**, 3536 (1978); **101**, 1908 (1979).
- ²⁵D. S. Bomse and T. H. Morton, *Tetrahedron Letters* 3481 (1974).
- ²⁶W. J. Chesnavich, T. Su and M. T. Bowers, *J. Am. Chem. Soc.* **100**, 4362 (1978).
- ²⁷J. M. Jasinski and J. I. Brauman, *Ibid.* **102**, 2906 (1980).
- ²⁸D. H. Aue and M. T. Bowers, *Gas Phase Ion Chemistry* (Edited by T. Bowers), Vol. 2, pp. 1–51. Academic Press, New York (1979).
- ²⁹J. R. Hass, M. M. Bursey, D. G. I. Kingston and H. P. Tannenbaum, *J. Am. Chem. Soc.* **94**, 5095–5096 (1972); J. R. Hass, R. G. Cooks, J. F. Elder, Jr., M. M. Bursey and D. G. I. Kingston, *Org. Mass Spectrom.* **11**, 697–711 (1976).
- ³⁰D. P. Stevenson, *Disc. Faraday Soc.* **10**, 35 (1951).
- ³¹P. J. Derrick, A. M. Falick, S. Lewis and A. Burlingame, *J. Phys. Chem.* **83**, 1567–1574 (1979), and Refs. contained therein.
- ³²M. M. Green, *Tetrahedron* (Report number 85) **36**, 2687 (1980).
- ³³J. L. Beauchamp, D. Holtz, S. D. Woodgate and S. L. Patt, *J. Am. Chem. Soc.* **94**, 2798 (1972).
- ³⁴G. Paraskevopoulos and W. S. Nip, *Can. J. Chem.* **58**, 2146 (1980).
- ³⁵F. H. Westheimer, *Chem. Rev.* **61**, 265 (1961).
- ³⁶T. H. Morton and J. L. Beauchamp, *J. Am. Chem. Soc.* **97**, 2355 (1975); **99**, 1288 (1977).
- ³⁷T. H. Morton, K. J. Fishbein, W. Mogilevsky and B. S. Freiser, unpublished results, 1976.
- ³⁸R. Zellner and W. Steinert, *Int. J. Chem. Kinet.* **8**, 397 (1976).
- ³⁹R. B. Cody and B. S. Freiser, private communication.
- ⁴⁰K. L. Busch, W. B. Nixon and M. M. Bursey, *J. Am. Chem. Soc.* **100**, 1621 (1978).
- ⁴¹W. Caminati and E. B. Wilson, *J. Mol. Spectrosc.* **81**, 356 (1980).
- ⁴²T. H. Morton and J. L. Beauchamp, *J. Am. Chem. Soc.* **94**, 3671 (1972).
- ⁴³C. C. Van der Sande and F. W. McLafferty, *Ibid.* **97**, 4617 (1975).
- ⁴⁴M. Sheehan, R. J. Spangler and C. Djerassi, *J. Org. Chem.* **36**, 3526 (1971).
- ⁴⁵H. Schwartz, *Org. Mass Spectrom.* **15**, 491 (1980); *Topics Curr. Chem.* **97**, 1 (1981).
- ⁴⁶H.-F. Grutzmacher and J. Winkler, *Org. Mass Spectrom.* **1**, 295 (1968).
- ⁴⁷K. G. Srinivasan and J. Rocek, *J. Am. Chem. Soc.* **100**, 2789 (1978).
- ⁴⁸P. Kebarle, *Annu. Rev. Phys. Chem.* **28**, 445 (1977).
- ⁴⁹S. A. Sullivan and J. L. Beauchamp, *J. Am. Chem. Soc.* **99**, 5017 (1977).
- ⁵⁰J. H. Stewart, R. H. Shapiro, C. H. DePuy and V. M. Bierbaum, *Ibid.* **99**, 7650–7653 (1977).
- ⁵¹J. M. Riveros, P. W. Tiedmann and A. C. Breda, *Chem. Phys. Lett.* **20**, 345–346 (1973).
- ⁵²P. Kebarle, K. Searles, A. Zolla, J. Scarborough and M. Arshadi, *Adv. Mass Spectrom.* **4**, 621–630 (1968).
- ⁵³R. H. Shapiro, C. H. DePuy, V. M. Bierbaum and J. H. Stewart, presented at the 24th Annual Conference on Mass Spectrometry and Allied Topics, San Diego (1976). Meeting abstracts, pp. 186–188.
- ⁵⁴J. E. Bartmess and R. T. McIver, Jr., *Gas Phase Ion Chemistry*, (Edited by M. T. Bowers), Vol. 2, pp. 88–121. Academic Press, New York (1979).
- ⁵⁵R. R. Squires, C. H. DePuy and V. M. Bierbaum, *J. Am. Chem. Soc.* **103**, 4256 (1981).

- ⁵⁶C. H. DePuy and V. M. Bierbaum, *Acc. Chem. Res.* **14**, 146 (1981).
- ⁵⁷D. F. Hunt and S. K. Sethi, *J. Am. Chem. Soc.* **102**, 6953 (1980); J. R. Lloyd, W. C. Agosta and F. H. Field, *J. Org. Chem.* **45**, 3483 (1980).
- ⁵⁸J. H. J. Dawson, T. A. M. Kaandorp and N. M. M. Nibbering, *Org. Mass Spectrom.* **12**, 330 (1977).
- ⁵⁹A. J. Noest and N. M. M. Nibbering, *J. Am. Chem. Soc.* **102**, 6427 (1981).
- ⁶⁰S. Ingemann, N. M. M. Nibbering, S. A. Sullivan and C. H. DePuy, *ibid.* **104**, in press.
- ⁶¹A. J. Noest and N. M. M. Nibbering, *Adv. Mass Spectrom.* **8**, 227 (1980).
- ⁶²G. K. King, M. M. Maricq, V. M. Bierbaum and C. H. DePuy, *J. Am. Chem. Soc.* **103**, 7133 (1981).
- ⁶³D. Smith, N. G. Adams and M. J. Henchman, *J. Chem. Phys.* **72**, 4951 (1980).
- ⁶⁴J. L. Beauchamp and M. C. Caserio, *J. Am. Chem. Soc.* **94**, 2638 (1972).
- ⁶⁵D. G. Hall, C. Gupta and T. H. Morton, *Ibid.* **103**, 2416 (1981).
- ⁶⁶J. L. Beauchamp, M. C. Caserio and T. B. McMahon, *Ibid.* **96**, 6243 (1974).
- ⁶⁷S. G. Lias, D. M. Shold and P. A. Ausloos, *Ibid.* **102**, 2540 (1980).
- ⁶⁸M. Saunders, P. Vogel, E. L. Hagen and J. Rosenfeld, *Accts. Chem. Res.* **6**, 53 (1973).
- ⁶⁹E. P. Hunter and S. G. Lias, *J. Phys. Chem.* **86**, 2769 (1982).
- ⁷⁰J. E. Liehr, E. A. Brenton, J. H. Bergnon, J. A. McCloskey, W. Blum and W. J. Richter, *Helv. Chim. Acta* **64**, 835 (1981).
- ⁷¹J. C. Person, *J. Chem. Phys.* **43**, 2533 (1965).
- ⁷²J. W. Larson and T. B. McMahon, *J. Am. Chem. Soc.*, in press.
- ⁷³F. B. Burns and T. H. Morton, *J. Am. Chem. Soc.* **98**, 7308 (1976).
- ⁷⁴F. B. Burns, Ph.D. Thesis, Brown University, 1976.
- ⁷⁵T. H. Morton and J. L. Beauchamp, unpublished results, 1973. These experiments were run in a standard Varian series V-5900 ICR under drift conditions. See also P. N. T. van Velzen, W. J. van der Hart, J. van der Greef, N. M. M. Nibbering and M. L. Gross, *J. Am. Chem. Soc.* **104**, 1208 (1982).
- ⁷⁶L. Friedman and J. H. Bayless, *Ibid. Soc.* **91**, 1790 (1969).
- ⁷⁷T. H. Morton, unpublished results, 1976.
- ⁷⁸T. H. Morton, *J. Am. Chem. Soc.* **102**, 1596 (1980). Thermodynamic estimates should be modified if a higher heat of formation of PhO^{\cdot} is used—cf. A. J. Colussi, F. Zabel and S. W. Benson, *Int. J. Chem. Kinet.* **9**, 161 (1979).
- ⁷⁹D. M. Shold and P. A. Ausloos, *Ibid.* **100**, 7915 (1978).
- ⁸⁰B. S. Freiser, *Int. J. Mass Spec. Ion Phys.* **26**, 39 (1978).
- ⁸¹T. H. Morton, *Radiat. Phys. Chem.* **20**, 29 (1982).
- ⁸²H. D. Beckey, *Field Ionization Mass Spectrometry*, Pergamon Press, Oxford (1971).
- ⁸³A. M. Falick, P. J. Derrick and A. L. Burlingame, *Int. J. Mass Spectrom. Ion Phys.* **12**, 101 (1973).
- ⁸⁴H. D. Beckey, K. Levsen and P. J. Derrick, *Org. Mass Spectrom.* **11**, 835 (1976).
- ⁸⁵R. J. Liedtke and C. Djerassi, *J. Am. Chem. Soc.* **91**, 6814 (1969).
- ⁸⁶J. L. Homes and F. P. Lossing, *J. Am. Chem. Soc.* **104**, 2648 (1982).
- ⁸⁷J. L. Holmes and F. P. Lossing, *J. Am. Chem. Soc.* **102**, 1591 (1980).
- ⁸⁸S. Meyerson, C. Fenselau, J. L. Young, W. R. Landis, E. Selke and L. C. Leitch, *Org. Mass Spectrom.* **3**, 689–707 (1969).
- ⁸⁹J. L. Holmes, J. K. Terlouw and F. P. Lossing, *J. Phys. Chem.* **80**, 2860–2862 (1976).
- ⁹⁰R. G. Cooks, J. M. Beynon, R. M. Caprioli and E. R. Lester, *Metastable Ions*, Elsevier, Amsterdam (1973).
- ⁹¹D. H. Williams, *Accts. Chem. Res.* **10**, 280 (1977).
- ⁹²E. L. Spatz, W. A. Seitz and J. L. Franklin, *J. Chem. Phys.* **51**, 5142 (1969).
- ⁹³M. A. Haney and J. L. Franklin, *J. Chem. Phys.* **48**, 4093 (1968); J. L. Franklin, *Science* **193**, 725 (1976).
- ⁹⁴P. F. Bente, III, F. W. McLafferty, D. J. McAdoo and C. Lifshitz, *J. Chem. Phys.* **79**, 713 (1975).
- ⁹⁵J. F. Elder, Jr., J. H. Beynon and R. G. Cooks, *Org. Mass Spectrom.* **10**, 273 (1976).
- ⁹⁶R. D. Bowen, B. J. Stapleton and D. H. Williams, *J. Chem. Soc. Chem. Commun.* **24** (1978).
- ⁹⁷R. D. Bowen and D. H. Williams, *J. Am. Chem. Soc.* **99**, 6822 (1977).
- ⁹⁸P. Longevialle and R. Botter, *J. Chem. Soc., Chem. Commun.* 823 (1980).
- ⁹⁹J. K. MacLeod and C. Djerassi, *J. Am. Chem. Soc.* **88**, 1840 (1966).
- ¹⁰⁰D. H. Williams, R. G. Cooks and I. Howe, *Ibid.* **90**, 6759 (1968).
- ¹⁰¹R. G. Gillis, G. J. Long, A. G. Moritz and J. L. Occolowitz, *Org. Mass Spectrom.* **1**, 527 (1978).
- ¹⁰²F. W. McLafferty and L. J. Schiff, *Ibid.* **2**, 757 (1969).
- ¹⁰³I. Howe and D. H. Williams, *J. Chem. Soc. Chem. Commun.* 1195 (1971).
- ¹⁰⁴P. D. Woodgate and C. Djerassi, *Org. Mass Spectrom.* **3**, 1093 (1970).
- ¹⁰⁵A. N. H. Yeo and C. Djerassi, *J. Am. Chem. Soc.* **94**, 482 (1972).
- ¹⁰⁶N. M. M. Nibbering, *Tetrahedron* **20**, 385 (1973).
- ¹⁰⁷K. B. Tomer and C. Djerassi, *Tetrahedron* **29**, 3491 (1973).
- ¹⁰⁸F. Borchers, K. Levsen and H. D. Beckey, *Int. J. Mass Spectrom. Ion Phys.* **21**, 125 (1976).
- ¹⁰⁹F. M. Benoit and A. G. Harrison, *Org. Mass Spectrom.* **11**, 599 (1976).
- ¹¹⁰D. J. DeFrees, R. T. McIver Jr. and W. J. Hehre, *J. Am. Chem. Soc.* **99**, 3853 (1977).
- ¹¹¹S. Paul and M. H. Back, *Can. J. Chem.* **53**, 3330 (1975).
- ¹¹²T. H. Morton, paper presented at the 2nd Western Regional Ion Chemistry Conf., Lake Arrowhead, CA (1982).
- ¹¹³J. E. Baldwin, *J. Chem. Soc. Chem. Commun.* 734–736 (1976).
- ¹¹⁴D. G. Hall and T. H. Morton, *J. Am. Chem. Soc.* **102**, 5686 (1980).
- ¹¹⁵H.-J. Schneider and R. Busch, *J. Org. Chem.* **47**, 1766 (1982).
- ¹¹⁶A. L. J. Beckwith and G. Moad, *J. Chem. Soc. Chem. Commun.* 472 (1974).
- ¹¹⁷R. D. Bowen and D. H. Williams, *J. Am. Chem. Soc.* **102**, 2752 (1980) and Refs. contained therein.
- ¹¹⁸D. H. Williams, B. J. Stapleton and R. D. Bowen, *Tetrahedron Letters* 2919 (1978).
- ¹¹⁹F. A. Houle, Ph.D. thesis, California Institute of Technology (1979).
- ¹²⁰R. D. Bowen and D. H. Williams, *J. Chem. Soc. Perkin II*, 1411 (1980).
- ¹²¹S. A. McLuckey, D. Cameron and R. G. Cooks, *J. Am. Chem. Soc.* **103**, 1313 (1981).
- ¹²²R. D. Bowen, *J. Chem. Soc. Perkin II* 1210 (1980).
- ¹²³R. D. Bowen and D. H. Williams, *Int. J. Mass Spectrom. Ion Phys.* **29**, 47 (1979).
- ¹²⁴P. A. Ausloos and S. G. Lias, *J. Am. Chem. Soc.* **103**, 3641 (1981).
- ¹²⁵M. A. Winnik, C. R. Lee and P. T. Y. Kwong, *J. Am. Chem. Soc.* **96**, 2901 (1974).

- ¹²⁶R. D. Bowen and D. H. Williams, *J. Chem. Soc. Chem. Commun.* 836 (1981).
- ¹²⁷J. Schultz and J. L. Beauchamp, manuscript in preparation.
- ¹²⁸F. P. Lossing, *J. Am. Chem. Soc.* **99**, 7526 (1977).
- ¹²⁹M. J. Cook, S. El Abbady, A. R. Katritsky, C. Guinon and G. Pfister-Guillozo, *J. Chem. Soc. Perkin II*, 1652 (1977).
- ¹³⁰T. Gronneberg and K. Undheim, *Org. Mass Spectrom.* **6**, 823 (1972).
- ¹³¹D. H. Aue, personal communication. The gas phase basicity of N-methyl-4-pyridone was measured using techniques described in Ref. 121.
- ¹³²G. Schmid and A. W. Wolkoff, *Can. J. Chem.* **50**, 1181 (1972).
- ¹³³A. Maquestiau, Y. van Haverbeke, C. de Meyer, A. R. Katritsky, M. J. Cook and A. D. Page, *Can. J. Chem.* **53**, 490 (1975).
- ¹³⁴A. Rodriguez, W. P. Freeman, and T. H. Morton, unpublished results, 1981.
- ¹³⁵A. C. Cope and D. M. Gale, *J. Am. Chem. Soc.* **85**, 3747 (1963).
- ¹³⁶W. Parker and C. I. F. Watt, *J. Chem. Soc. Perkin II*, 1647 (1975).
- ¹³⁷R. P. Kirchen and T. S. Sorenson, *J. Am. Chem. Soc.* **101**, 3240 (1979); R. P. Kirchen, N. Okazawa, N. Ranganayakalu, A. Rauk and T. S. Sorenson, *J. Am. Chem. Soc.* **103**, 597 (1981).
- ¹³⁸H. W. Biermann, G. W. Harris and J. N. Pitts, Jr., *J. Phys. Chem.* **86**, 2958 (1982).
- ¹³⁹D. Davis and W. Braun, *Appl. Optics* **7**, 2071 (1968).
- ¹⁴⁰H. W. Biermann, W. P. Freeman and T. H. Morton, *J. Am. Chem. Soc.* **104**, 2307 (1982).
- ¹⁴¹A. H. Zimmerman, K. J. Reed and J. I. Brauman, *Ibid.* **99**, 7203 (1977); cf. M. Rossi and D. M. Golden, *Int. J. Chem. Kinet.* **11**, 715 (1979).
- ¹⁴²J. M. Dyke, N. B. H. Jonathan, A. Morris and M. J. Winter, *Mol. Phys.* **39**, 629 (1980).
- ¹⁴³B. J. S. Wang and E. R. Thornton, *J. Am. Chem. Soc.* **90**, 1216 (1968).